ДОКЛАДЫ
АКАДЕМИИ НАУК СССР

SOVIET PHYSICS

"Doklady"

VOLUME 1 NUMBER 4

A Translation
of the
"Physics Section"
of the

Proceedings of the Academy of Sciences of the USSR

(RUSSIAN ORIGINAL VOL. 109, NOS. 1-6)

Published by the
AMERICAN INSTITUTE OF PHYSICS
INCORPORATED

SOVIET PHYSICS

"Doklady"

A translation of the "Physics Section" of the Proceedings of the Academy of Sciences of the USSR.

A publication of the

AMERICAN INSTITUTE OF PHYSICS

Governing Board

Allen V. Astin
Robert F. Bacher
W. S. Baird
H. A. Bethe
R. T. Birge
Frank D. Dexter
I. C. Gardner
S. A. Goudsmit
Charles Kittel
Hugh S. Knowles
R. B. Lindsay
William F. Meggers
Harry F. Olson
R. R. Palmer
R. F. Paton
Eric Rodgers
Ralph A. Sawyer
Frederick Seitz
H. D. Smyth
Mark W. Zemansky

Officers and Staff

Frederick Seitz
Chairman, Governing Board
Henry A. Barton
Director
Wallace Waterfall
Executive Secretary
Mark W. Zemansky
Treasurer
Theodore Vorburger
Advertising Manager
Ruth F. Bryans
Publication Manager
Kathryn Setze
Assistant Treasurer
Alice Mastropietro
Circulation Manager
Eugene H. Kone
Director of Public Relations

American Institute of Physics Advisory Board on Russian Translations

Elmer Hutchisson, *Chairman*
Dwight Gray, Morton Hamermesh, Vladimir Rojansky,
Victor Weisskopf

Soviet Physics—"Doklady" is a bi-monthly journal published by the American Institute of Physics for the purpose of making available in English reports of current Soviet research in physics as contained in the "Physics Section" of the Proceedings of the Academy of Sciences of the USSR. The Proceedings appears thirty-six times per year and the "Physics Sections" are accumulated and English translations of them are published in six issues per year.

Transliteration of the names of Russian authors follows the system employed by the Library of Congress.

This translating and publishing project was undertaken by the Institute in the conviction that dissemination of the results of research everywhere in the world is invaluable to the advancement of science. The National Science Foundation of the United States encouraged the project initially and is supporting it in large part by a grant. Translation and printing are being handled by Consultants Bureau, Inc.

The American Institute of Physics and its translators propose to translate faithfully all of the scientific material in the "Physics Section" of the Proceedings of the Academy of Sciences of the USSR appearing after January 1, 1956. The views expressed in the translated material, therefore, are intended to be those expressed by the original authors, and not those of the translators nor of the American Institute of Physics.

One volume is published annually. Volume 1 will consist of six issues and will contain all scientific material published in the "Physics Section" of the original Russian journal during the 1956 calendar year.

Subscription Prices:

Per year (6 issues)	
United States and Canada	$25.00
Elsewhere	27.50
Back Numbers	
Single copies	$ 6.00

Subscriptions should be addressed to the American Institute of Physics, 57 East 55th Street, New York 22, N. Y.

Copyright by American Institute of Physics 1957

SOVIET PHYSICS
"Doklady"

A translation of the "Physics Section" of the Proceedings of the Academy of Sciences of the USSR.

VOLUME 1, NUMBER 4 JULY-AUGUST, 1956

THE CALCULATION OF π-ELECTRONIC POLARIZABILITY OF POLYENES AND BENZENE BY THE "METALLIC" MOLECULAR MODEL

M. N. Adamov and I. S. Milevskaia

(Presented by Academician A. N. Terenin January 27, 1956)

I. This paper is concerned with the quantum mechanical calculation of the π-electronic polarizability of molecules with conjugated bonds – $C_{2m}H_{2m+2}$ polyene chains and benzene – by the use of the simplest "metallic" model. It should be noted that a similar calculation recently appeared in an article by Bolton [1]. The latter unnecessarily resorted to approximation whereas it is easy to calculate the polarizability exactly. An exact calculation enables us to judge the approximation methods and can serve as a criterion of the suitability of the model.

The simplest "metallic" model which can be used for an approximate description of the motion of π-electrons in aromatic molecules or in molecules with conjugated bonds can be characterized as follows. It is assumed that in the absence of an external field the electrons move freely along certain curves and that outside of these paths the potential energy of the electrons becomes infinite. Because electron interactions are neglected the variables in the Schroedinger equation are separable. The total energy E of the model is the sum of the energies in single electron orbits populated in accordance with the Pauli exclusion principle.

Similar additivity is also valid with respect to the polarizability $\alpha = -(\partial^2E/\partial F^2)_{F=0}$. Here F is the external electric field strength. Therefore these assumptions reduce the calculation of polarizability of a many-electron system to the calculation of polarizabilities for the different single-electron orbits.

When the effect of an external electric field F on an electron is considered we shall use an upper index (k) with quantities which are proportional to F^k. The perturbed wave function can be written as

$$\psi = \psi^{(0)} + \psi^{(1)} + \psi^{(2)} + \ldots, \tag{1}$$

and the corresponding energy as

$$E = E^{(0)} + E^{(1)} + E^{(2)} + \ldots \tag{2}$$

The polarizability α can be determined from

$$E^{(2)} = -{}^1/_2\alpha F^2 = {}^1/_2\left[\int \overline{\psi}^{(0)} W\psi^{(1)}d\tau + \int \overline{\psi}^{(1)} W\psi^{(0)}d\tau\right], \tag{3}$$

where W is the perturbation energy operator.

The correction function $\psi^{(1)}$ must satisfy the differential equation

$$(H^{(0)} - E^{(0)})\, \psi^{(1)} = (E^{(1)} - W)\, \psi^{(0)}; \tag{4}$$

$H^{(0)}$ is the unperturbed Hamiltonian and $\psi^{(1)}$ is subject to the same boundary conditions as $\psi^{(0)}$.

From the normalization requirement for ψ there follows the condition:

$$\int \overline{\psi}^{(1)} \psi^{(0)}\, dl + \int \overline{\psi}^{(0)} \psi^{(1)}\, d\tau = 0. \tag{5}$$

$\psi^{(1)}$ is expanded in the usual series of unperturbed eigenfunctions and the correction $E^{(2)}$ to the degenerate level $E_k^{(0)}$ is

$$E^{(2)} = \sum_n{}' \frac{|W_{nk}|^2}{E_k^{(0)} - E_n^{(0)}}{}^{*}; \qquad W_{nk} = \int \bar{\psi}_n^{(0)} W \psi_k^{(0)}\, d\tau. \tag{6}$$

$E^{(2)}$ can also be calculated by the variational principle:

$$\begin{aligned} E_2 = \int \bar{\psi}^{(0)} (W - E^{(1)})\, \psi^{(1)} d\tau + \int \bar{\psi}^{(1)} (W - E^{(1)})\, \psi^{(0)}\, d\tau + \\ + \int \bar{\psi}^{(1)} (H^{(0)} - E^{(0)})\, \psi^{(1)}\, d\tau = \min \end{aligned} \tag{7}$$

by the Ritz method. Different trial functions with variable parameters can be used as $\psi^{(1)}$. Assuming $\psi^{(1)} = \lambda W \psi^{(0)}$ (λ is a variable parameter) we obtain the well-known Kirkwood equation for the polarizability [2].

Reference [1] gives within the framework of the "metallic" model an approximate evaluation of the longitudinal polarizability of polyene chains and of benzene from Kirkwood's equation and also from (6) with only one term ($n = k + 1$) of the infinite sum. Moreover, polarizabilities of polyenes by the "metallic" model have been calculated approximately in [3,4]. However, when this model is used it is easy to obtain a rigorous solution of Eq. (4) for $\psi^{(1)}$ in finite form and to calculate the polarizability exactly.

II. We shall calculate the polarizability of an electron moving along a straight line of length L ($0 \leq x \leq L$) in a square potential well with infinitely high walls. If we express all quantities in atomic units we have

$$\begin{gathered} H^{(0)} = -\frac{1}{2}\frac{d^2}{dx^2}; \quad W = Fx; \quad \psi^{(0)} = \sqrt{\frac{2}{L}} \sin \omega_k x; \\ \omega_k = \frac{k\pi}{L}, \quad k = 1, 2, \ldots; \quad E^{(0)} = {}^1/_2\, \omega_k^2; \quad E^{(1)} = {}^1/_2\, FL. \end{gathered} \tag{8}$$

Solving (4) we have

$$\psi^{(1)} = \frac{1}{2} F \sqrt{\frac{2}{L}} \left[\frac{x - {}^1/_2 L}{\omega_k^2} \sin \omega_k x + \frac{Lx - x^2}{\omega_k} \cos \omega_k x \right]. \tag{9}$$

From (3) we obtain an expression for the polarizability of the k-th orbit:

$$\alpha_k = \frac{L^4}{4k^2\pi^2} \left(\frac{5}{k^2\pi^2} - \frac{1}{3} \right). \tag{10}$$

A similar expression for the polarizability was obtained by Gibbs [5] by finding the limit of the infinite sum in (6). For all excited electron states ($k > 1$) the polarizability was negative.

It is clear from (3) and (6) that in the general case the polarizability only cannot be negative for the electron ground state.

In calculating the polarizability of polyenes we use a model in which the electrons move freely along a plane broken line of length $2ma$; each section of the broken line forms the angle 30° with the polyene axis ($a = 2.6$ atom.units – is the length of the carbon-carbon bond).

If the coordinate along the broken line is denoted by s the calculation of the longitudinal polarizability gives $W = Fs \cos 30°$. As a result we obtain $\alpha_{\parallel} = {}^3/_4\, \alpha$, where $\alpha = 2 \sum_{k=1}^{m} \alpha_k$; α_k is calculated by (10) with $L = 2ma$.

---

*In this case, for a continuous as well as discrete energy spectrum, an integral must be added to the summation in (6).

TABLF 1

$2m$	$\alpha_\parallel$	α_p	α_v
4	54	—	—
6	204	300	286
8	513	664	607
10	1032	1228	1100

Table 1 gives the calculated values of $\alpha_\parallel$ for a number of polyenes. For comparison we give the results of approximate calculations of the longitudinal polarizability obtained by Bolton from (6) (α_p) and from Kirkwood's equation (α_v). Unlike our model for polyene it is assumed in Bolton's calculations that the bent polyene chain is replaced by a rectilinear segment of length L = = (2m + 1) a cos 30°, directed along the axis of the molecule.

III. In the model of the benzene molecule the region of free electronic motion is a circle of radius R. Denoting the angular coordinate by φ we have:

$$H^{(0)} = -\frac{1}{2R^2}\frac{d^2}{d\varphi^2}; \quad W = FR\cos\varphi; \quad E^{(0)} = \frac{k^2}{2R^2}; \quad k = 0, 1, 2, \ldots$$

For k = 0

$$\psi^{(0)} = \frac{1}{\sqrt{2\pi}}; \quad E^{(1)} = 0; \tag{11}$$

$$\psi^{(1)} = -\frac{2R^3F}{\sqrt{2\pi}}\cos\varphi; \tag{12}$$

$$\alpha = 2R^4. \tag{13}$$

For k ≠ 0

$$\psi^{(0)} = C_1e^{ik\varphi} + C_2e^{-ik\varphi}; \quad 2\pi(|C_1|^2 + |C_2|^2) = 1: \quad E^{(1)} = 0. \tag{14}$$

The unperturbed energy levels are doubly degenerate (without including spin degeneracy).

Due to the invariance of the perturbed Hamiltonian with respect to the substitution $\varphi \to -\varphi$, $H(\varphi) = H(-\varphi)$ the correct zeroth order eigenfunctions, which make a continuous transition into the exact eigenfunctions, will be:

$$\psi_0 = \frac{1}{\sqrt{\pi}}\cos k\varphi, \tag{15}$$

$$\psi_0 = \frac{1}{\sqrt{\pi}}\sin k\varphi. \tag{16}$$

For (15) we obtain

$$\psi^{(1)} = \frac{R^3F}{\sqrt{\pi}}\left[\frac{\cos(k-1)\varphi}{2k-1} - \frac{\cos(k+1)\varphi}{2k+1}\right]. \tag{17}$$

When k > 1

$$\alpha = -\frac{2R^4}{4k^2-1}. \tag{18}$$

When k = 1

$$\alpha = -{}^5/_3R^4. \tag{19}$$

For (16) we obtain

$$\psi^{(1)} = \frac{R^3F}{\sqrt{\pi}}\left[\frac{\sin(1-k)\varphi}{2k-1} - \frac{\sin(k+1)\varphi}{2k+1}\right]. \tag{20}$$

When k > 1

$$\alpha = -\frac{2R^4}{2k^2-1}. \tag{18'}$$

When k = 1

$$\alpha = {}^{1}/_{3}R^{4}. \tag{21}$$

Thus the calculated polarizability is positive only for the ground state and one of the first two excited states. By summing the polarizabilities of the six π-electrons we obtain the π-electron polarizability of benzene in the plane of the ring from Eqs. (13), (19) and (21), $\alpha = {}^{4}/_{3}R^{4}$ instead of Bolton's $\alpha = {}^{2}/_{3}R^{4}$).

Equating the perimeters of the model circle and of the six-member cycle $2\pi R = 6a$, we obtain $\alpha = 50.7$.

The polarizability of benzene in the plane of the ring is obtained experimentally as $\alpha = 55.3$ [6].

In Bolton's calculations the contribution of the π-electrons is approximately half of the total polarizability of benzene. From our calculation almost all of the polarizability of benzene is determined by the π-electrons. However, the value which we have calculated for the polarizability is probably a little high since the π-electrons in our model have too great mobility.

LITERATURE CITED

[1] H. Bolton, Trans. Faraday Soc. 50, 1265 (1954).

[2] J.G. Kirkwood, Physik. Z. 33, 57 (1932).

[3] M.V. Vol'kenshtein and S.M. Iazykova, Doklady Akad. Nauk SSSR 104, 834 (1955).

[4] E. Haugh and J. Hirschfelder, J. Chem. Phys. 23, 10, 1779 (1955).

[5] J.H. Gibbs, Phys. Rev. 94, 292 (1954).

[6] K.C. Denbigh, Trans. Faraday Soc. 36, 936 (1940).

Received January 11, 1956

A.A. Zhdanov Leningrad State University

ON NONIONOSPHERIC FLUCTUATIONS OF THE INTENSITY OF RADIO WAVES FROM NEBULAE

V. L. Ginzburg, Corresponding Member of the Academy of Sciences USSR

It is usually assumed at the present time that the intensity fluctuations (flickering or twinkling) of discrete sources of cosmic radio waves are caused entirely by the earth's ionosphere. This opinion is based first of all on experimental data which show that in many cases flickering due to the ionosphere really occurs and secondly, on the fact that the observed intensity fluctuations, which last for seconds or minutes, cannot be associated with actual changes in the intensity of radio emission from nebulae (radio nebulae), with which discrete sources have been identified in all known cases. This is sufficiently shown by the fact that the time required for the passage of light through a nebula is at least many days (for example, in the case of the Crab Nebula this time is of the order of 3 years), so that the intensity of the radio emission cannot noticeably change in minutes. Therefore when it was recently suggested [1] that there exist intensity fluctuations from a certain source which are not due to the ionosphere, this source was assumed to be of stellar size. But, as we have more than once emphasized, the existence of such "radio stars" is extremely unlikely. Thus in the absence of fluctuations the current from the source observed in [1] is $F = 10^{-22}$ erg/cm^2 sec · cps for the wave length $\lambda = 124$ cm. But for a source of radius r at distance R from the earth with the effective temperature T_{ef}:

$$F = \frac{2\pi k T_{ef}}{\lambda^2}\left(\frac{r}{R}\right)^2 = \frac{8.65\cdot 10^{-16}\, T_{ef}}{\lambda^2}\left(\frac{r}{R}\right)^2 \frac{\text{erg}}{\text{cm}^2\cdot\text{sec}\cdot\text{cps}}. \qquad (1)$$

Assuming $r = r_{\odot} = 7\cdot 10^{10}$ cm, $R \sim 10^{19}$, which corresponds to the nearest stars, for the object of [1] we obtain the average effective temperature $T_{ef} \sim 4\cdot 10^{13}$ degrees, whereas for the sun the same wavelength gives on the average $T_{ef} \sim 10^6$ degrees. In addition this estimate is probably too low since a radio star probably has a smaller radius (a red dwarf) and can be located at a greater distance. Thus, the hypothetical radio star must have a radio emitting power which is at least 10^7 to 10^8 times greater than that of the sun, and we are discussing an average level of radiation which is approximately constant in time (during the fluctuations noted in [1], which lasted 2-3 minutes, the intensity increased by a factor of about 6).

The data in [1] are still entirely too meager to establish firmly the nonionospheric character of the observed fluctuations, for which there are only a few indications. It is in order, however, to ask what necessary conclusions would result if it were firmly established that nonionospheric flickering of discrete sources does exist. In this connection we also wish to point out that such nonionospheric oscillations must not necessarily be attributed to the source itself, which leads to the assumption of its stellar character *, but can in theory depend on the conditions for the propagation of the radio waves in interstellar and interplanetary space in the path from the source to the earth. We are referring to diffraction from a phase screen such as exists in the case of diffraction by ionospheric inhomogeneities or by the inhomogeneities in the solar corona [2].

Considering emission from radio nebulae and assuming that the "screen" is sufficiently distant, we can neglect the temporal change of the diffraction pattern in the coordinate system associated with the screen (for inhomogeneities in the solar system it may not be permissible to do this). In this case the intensity fluctuations of the source observed on the earth (with characteristic period τ) will be associated with the relative motion of the earth and the screen of velocity v, which is generally of the order of the velocity of the earth in its orbit: $v_{\oplus} = 3\cdot 10^6$ cm/sec

---

* We ignore the possibility of the existence of unknown radiating objects within or near the solar system, which is very unlikely.

and changes in time due to change of the vector $\mathbf{v}_{\perp}$. It is thus clear that $\tau \sim x_0/v \sim 3 \cdot 10^{-7}\, x_0$, where x_0 is the characteristic size of the diffraction pattern near the earth. For $\tau \sim 10 - 10^3$ sec, $x_0 \sim 3 \cdot 10^7 - 3 \cdot 10^9$ cm. This distance is such that at different points of the earth's surface the pattern must be temporally shifted by $\Delta t \lesssim \tau$ (the time Δt depends on the orientation of the observation points and the distances between them). If the diffraction pattern is nearly the result of diffraction at the edge of the screen, then

$$x_0 \sim \sqrt{\frac{\lambda b\,(a+b)}{\pi a}}\,, \tag{2}$$

where b and a are, respectively, the distance of the screen from the earth and from the source. We may assume a point source, so that its radius is $r \ll a x_0/b$; the edge of the screen can be assumed to be sharp if the refractive index on the edge changes at distances L which are smaller than the first Fresnel zone $\rho = \sqrt{\lambda ab/(a+b)}$. On the other hand it is reasonable to require the fulfillment of the inequality $L \gg \ell \sim 10^{15}/N_m$, where ℓ is the mean free path in a gas with the concentration of particles N_m. Since in the cases which interest us $\gtrsim 10^{12} - 10^{13}$ even the condition $\rho \gtrsim L \gtrsim \ell$ is very stringent – it becomes $ab/(a+b) \gtrsim (10^{24} - 10^{26})\, \lambda^{-1} \sim 10^{22} - 10^{24}$, which can occur only in unusual cases. However, for consideration of the effect of the magnetic field and especially for corpuscular currents of solar origin the condition $L \gg \ell$ is not necessary and the possibility of observing diffraction of the discussed type is more real. For $a \gg b$ and $\lambda \sim 3 \cdot 10^2$ according to (1) $x_0 \sim \sqrt{\frac{\lambda}{\pi} b} \sim 3 \cdot 10^7 - 3 \cdot 10^9$ for $b \sim 10^{13} - 10^{17}$.

In the case $a \gg b$ and diffraction from a screen with smooth inhomogeneities[*] with the characteristic period d (it is assumed that the phase modulation is $|\Delta\varphi| \lesssim 1$):

$$x_0 \sim b\theta \sim \frac{b\lambda}{d}\,, \tag{3}$$

and $x_0 \sim 3 \cdot 10^7 - 3 \cdot 10^9$ for $b/d \sim 10^5 - 10^7$; for $d > \ell \gtrsim 10^{12}$ this means that $b > 10^{17} - 10^{19}$.

For sufficiently strong phase modulation the condition $|\Delta\varphi| = \frac{2\pi}{\lambda} |\Delta n|\, z \gtrsim 1$, must be observed, where Δn is the change of the refractive index in the path z. For a rarefied ionized gas this condition becomes $\lambda \Delta N z \gtrsim 3 \cdot 10^{12}$, since

$$\Delta n = -\frac{2\pi e^2\, \Delta N}{m\omega^2} = -4.5 \cdot 10^{-14}\, \Delta N \lambda^2, \tag{4}$$

where ΔN is the corresponding change of electron concentration. It is easily seen that fulfillment of the condition $|\Delta\varphi| \gtrsim 1$ is easily attained both in interstellar space and for the different conceivable inhomogeneities in the solar system.[**] Because of the phase character of the modulation the observed diffraction pattern can appreciably depend on λ and also on the band width of the receiver. We also note that wave diffraction in the path from the source to the earth can result in an appreciable increase of the angular size of the source as observed from the earth, just as occurs in a number of similar cases.

The existence of inhomogeneities in the interstellar medium and interplanetary medium also results in refraction which will usually be insignificant but in exceptional cases may amount to angular minutes.

The above discussion is intended only to indicate the possibility of nonionospheric flickering of radio nebulae. A more detailed theoretical analysis of this question is quite premature because of the complete absence of the experimental information required for a concrete analysis. On the experimental side the first problem is the answer to the question as to the very existence of nonionospheric fluctuations of discrete sources, principally by simultaneous observations from a few widely separated points. If the existence of such flickering is firmly established the course of further study is quite clear, at least on the theoretical side.

---

[*] Inhomogeneities in interstellar or interplanetary space can be associated with different particle currents or be due to the same causes which result in the formation of ionospheric inhomogeneities [3,4].

[**] It is also entirely possible that $|\Delta\varphi| \gg 1$; in this case in (3) $d \sim \pi d_1/\Delta\varphi$, where d_1 is the characteristic diameter of the inhomogeneities [2]. For $d_1 > \ell \gtrsim 10^{12}$ and for the other parameters above we have $b > (10^{17} - 10^{19})\, \pi/\Delta\varphi$.

LITERATURE CITED

[1] J.D. Kraus, H.C. Ko and D.V. Stoutenburg, Nature 176, 304 (1955).

[2] V.L. Ginzburg and V.V. Pisareva, Trans. 5th Conference on Problems of Cosmogony (Acad. Sci. USSR Press, 1956), p. 229.

[3] B.N. Gershman and V.L. Ginzburg, Doklady Akad. Nauk SSSR 100, 647 (1955).

[4] V.L. Ginzburg, Trans. 5th Conference on Problems of Cosmogony (Acad. Sci. USSR Press, 1956), p. 512.

[5] O.B. Slee, Australian J. Phys. 8, 498 (1955).

[6] A.W.L. Carter, Australian J. Phys. 8, 594 (1955).

Received January 16, 1956

P.N. Lebedev Physics Institute, Academy of Sciences, U.S.S.R.

Note added in proof: In recently published articles [5,6] it is pointed out that there are true fluctuations of intensity from the source Hydra A. It was established that the source is of diameter 1.6' and is thus not a star. If it is not assumed [5,6] that this source is 2 – 3 parsecs distant from the sun the only explanation of the observed fluctuations appears to be the one which is discussed in the present article.

THE ANOMALOUS SCATTERING OF LIGHT IN GLASS

A. I. Koliadin

(Presented by Academician A. N. Terenin January 7, 1956)

The Rayleigh scattering of light in glass has been studied less than in other transparent and cloudy media although it is of interest not only in connection with the nature of the vitreous state but as having an entirely unusual character. D.I. Levin [1] first noted that opalescent sodium borosilicate glass shows an anomalously high dependence of scattering on the wave length of the primary beam. M.M. Gurevich [2], who performed quantitative measurement of the integral scattering coefficient of this glass in all directions, found that it is proportional to λ^{-8}. We have obtained the scattering curves of different wave lengths in the visible spectrum for opalescent specimens of sodium borosilicate glass which differ by a factor of more than 1000.

A beam of polarized light from an incandescent lamp or from a monochromator illuminated by a SVDSH-250 mercury lamp was sent along the diameter of a sample in the shape of a spherical film. A visual photometer turning around the sample measured the ratio of the scattered beam brightness per unit thickness of the beam in the viewing direction to the brightness of a mat white screen illuminated by the same beam perpendicular to the screen's surface. In the most strongly opalescent samples the scattering could be measured only in green, yellow and red light; when violet light was used the entire sample shone because of multiple scattering and was almost opaque to the primary beam. In a less opalescent sample, on the other hand, because of its smallness the scattering of red light could not be determined and the scattering curves of yellow, green and violet light were obtained. The curves were extrapolated to 0 and 180° allowing for the fact that in these directions the scattering coefficient should not depend on the direction of polarization of the initial beam and should show a maximum or minimum.

All the curves obtained were of the same character, showing that by far the larger part of the energy is scattered in the backward hemisphere. When the primary beam was polarized in the scattering plane the curves rose monotonically from 0 to 180°. When the beam was polarized perpendicular to the scattering plane the curves passed through a minimum which in all cases was at the scattering angle $\varphi = 90°$. In weakly opalescent samples the brightness at the minimum fell to almost zero; in these cases, where the total scattering intensity was sufficiently high, at 90° the primary beam could no longer be distinguished against the background of overall illumination due to multiple scattering. When the brightness of the background is subtracted from the measured brightnesses of the beam and for each sample for each orientation of the polarizer, curves are plotted showing the angular dependence of the ratios of the differences for any two wave lengths, no systematic trend can be observed in these graphs. It therefore follows that, just as in Rayleigh's equation the scattering function in our glass can be represented as the product of an expression containing the wave length and all quantities which characterize the medium, and an angular factor. This indicates that the scattering curves for different wave lengths in any sample can be superposed by multiplying all ordinates by factors which are independent of the angle; this was done. Fig. 1,A shows a typical pair of curves (a and b) obtained with a sample of average opalescence. The points of the curves are averages of the measured scattering brightnesses for the green mercury line combined in the best possible manner with the scattered brightnesses of yellow and violet lines. The scale of the ordinates on the left is given for the green line. The scattering curves of the violet and yellow beams are obtained through multiplication of the ordinates in Fig. 1,A by 10.2 and 0.6, respectively. The initial curves at the minimum do not drop to zero but only to the background level, which for the yellow line was about $^1/_5$, for the green line $^1/_3$ and for the violet line 1.0 of the beam brightness in the direction $\varphi = 10°$.

Fig. 1,B gives the scattering curves of another sample, obtained by the use of a tungsten lamp and interference filter ($\lambda_{max} = 562$ mμ).

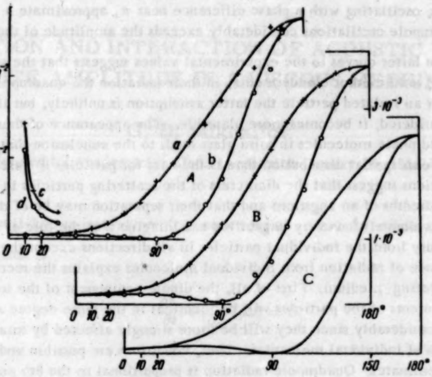

Fig. 1

The differences in the scattering curves of different wave lengths in the investigated samples with different degrees of opalescence are as follows:

1. The scattering intensity as evaluated from the ordinates of the upper curve at $\varphi = 90°$, changed by a factor of 1300.

2. The ratio of backward and forward scattered brightnesses changed from 5.5 to 55, reaching the highest value in samples with an average amount of opalescence.

3. In the two least opalescent samples at small angles a relative scattering increase was observed which was all the more pronounced when the total scattering was small (depending on the wave length and the transparency of the sample). Fig. 1,A (c and d) shows in a tenfold enlarged scale the initial portion of the curves for the mercury green line in the most transparent sample. The last property is not typical for the phenomenon; it may be intrinsic but can also be a systematic error resulting from the fact that the photometer set for small angles may receive light scattered from the surface of the sample, by the polaroid and other optical parts in the path of the initial beam. This error disappears in the light beam scattered by strongly opalescent glass but seriously distorts the result with a weakly opalescent sample.

Our results are in contradiction with the well-known theory of classical (non-Raman) scattering which includes both the phenomena in cloudy turbid media and scattering induced by molecular fluctuations. This theory states that, as a rule, the characteristic curve is symmetrical or extended in the forward direction. A curve that is stretched in the backward direction is possible in two cases: either when the particles are small and their refractive index is very large (absorbing and totally reflecting particles), or when the refractive index, the wave length and the particle size satisfy certain resonance conditions [3]. In glass only oxides and salts with relative refractive index close to unity can be precipitated: the resonance conditions cannot be fulfilled simultaneously in the entire visible spectrum. Moreover, neither the asymmetry of our curves nor the angle of maximum polarization agrees with the theory. In [4] the possibility is considered that backward scattering is predominant and that the spectral dependence is of the form λ^{-m}, where $m < 4$, but the equations derived are also in disagreement with our results.

We consider the interference of emission from two dipoles separated by the distance a, which is small compared with λ, along the primary beam, and oscillating with equal amplitudes and phase difference δ perpendicular to the primary beam. When both dipoles oscillate perpendicular to the scattering plane the radiation intensity depends on the angle as $\cos^2(\pi a/\lambda \cos\varphi + \delta/2)$. For oscillations in the scattering plane the factor $\cos^2\varphi$ is added because of the transversality of the light waves. By using some value for the ratio a/λ it is easy to obtain δ giving any desired ratio of the intensities for $\varphi = 0$ and $\varphi = \pi$. Fig. 1,B gives curves of these functions for $a/\lambda = 0.01$ and

$\delta = 0.973\,\pi$. Two dipoles, oscillating with a phase difference near π, approximate a system of charges in which the amplitude of the quadrupole oscillations considerably exceeds the amplitude of the dipole oscillations.

The similarity of the latter curves to the experimental values suggests that the scattering particles in glass act as quadrupoles, or that, unlike other cloudy media, in their radiation the quadrupole component prevails over the dipole component. For an isolated particle the latter assumption is unlikely, but if interference of radiation from many particles is considered, it becomes more plausible. The appearance of these particles as a result of diffusion of the precipitated phase molecules in solid glass leads to the conclusion that they must be of more uniform size and of more uniform spatial distribution than is the case for particles in gaseous and liquid scattering media. Certain considerations suggest that the diameters of the scattering particles in sodium borosilicate glass may be from tenths to hundredths of an angstrom and that their separation may be of the same order, so that the number of particles in the volume λ^3 is very large. We can imagine that the role of interference is that of reducing the radiation intensity from the individual particles in all directions except the direction of the primary beam, just as the interference of radiation from individual molecules explains the rectilinear propagation of light in a homogeneous nonscattering medium. First of all, the dipole component of the scattered beam will be eliminated, since the dipole moments of the particles will be identical in the same degree as their volumes; the quadripole moments can differ considerably since they will be more strongly affected by small differences of volume and by the individual properties of individual molecules. Thus, conditions are possible under which the quadrupole scattering component predominates. Quadrupole radiation is proportional to the 8th power of the frequency; this explains the spectral form of scattering in sodium borosilicate glass.

The above discussion is the first attempt to explain the observed anomaly qualitatively. Other explanations are possible, such as an attempt to relate it to radiation from a magnetic dipole. But in this case, it is necessary to assume attenuation resulting from interference by the component corresponding to the electric dipole.

An anomalous scattering curve is observed in some other glasses, specifically in those in which scattering can be attributed to the precipitation of a second phase. On the other hand, heavy flint, which consists almost entirely of silica and lead oxide, scatters almost equally in the forward and backward directions. This indicates that scattering here is caused not by the separation of the glass into two phases but by statistical fluctuations of the concentration of lead oxide such as are assumed in the molecular theory of scattering.

If calculations and further experiments confirm our hypotheses regarding the role of interference, then anomalous scattering, which is characterized by a high degree of dependence on the wavelength and by a scattering curve which is stretched in the backward direction, can be expected in other cloudy media, particularly in those which because of the smallness, uniform size and uniform distribution of the scattering particles, approximate continuous and optically homogeneous bodies.

LITERATURE CITED

[1] D. I. Levin, Symposium, The Structure of Glass, Trans. Conference on the Theory of Glass Structure, November 23-27, 11, 1953 (Leningrad, 1955).

[2] M. M. Gurevich, J. Tech. Phys. (USSR) 23, 986 (1953).

[3] K. S. Shifrin, Scattering of Light in a Cloudy Medium (1951)

[4] H. Mueller, Proc. Roy. Soc. 166, 425 (1938).

Received December 21, 1955

THE DISTORTION AND INTERACTION OF ACOUSTIC WAVES OF FINITE AMPLITUDE IN A VISCOUS MEDIUM

G. D. Mikhailov

(Presented by Academician M. L. Leontovich January 16, 1956)

We shall write the well-known hydrodynamical equations of a viscous fluid for the one-dimensional problem.

The continuity equation is

$$\frac{\partial \rho}{\partial t} + \frac{\partial}{\partial x}(\rho u) = 0; \tag{1}$$

the equation of motion is

$$\frac{\partial}{\partial t}(\rho u) + \frac{\partial}{\partial x}\left(\rho u^2 + p - \mu \frac{\partial u}{\partial x}\right) = 0, \tag{2}$$

where $\mu = (^4/_3\ \eta + \xi)$; η is the coefficient of sheer viscosity; and ξ is the coefficient of volume viscosity.

The equation of state is taken in the isoentropic form

$$\frac{\partial p}{\partial x} = c^2(\rho)\frac{\partial \rho}{\partial x}, \tag{3}$$

where $c^2(\rho)$ is a function of the density ρ.

In order to obtain acoustical equations in the first and second approximations we use the series expansions of the following variables in powers of a small parameter:

$$\begin{gathered} \rho = \rho_0 + s\rho_1 + s^2\rho_2 + \ldots; \quad p = p_0 + sp_1 + s^2p_2 + \ldots; \\ u = u_1 + su_2 + s^2u_3 + \ldots; \\ c^2(\rho) = c_0^2 + 2c_0\left(\frac{\partial c_0}{\partial \rho_0}\right)\rho_1 s + \left[h_1^2\rho_1^2 + 2c_0\left(h_1\rho_2 + \frac{h_2\rho_1}{2}\right)\right]s^2 + \cdots \end{gathered} \tag{4}$$

Here $h_1 = \left(\frac{\partial c_0}{\partial \rho_0}\right)$, $h_2 = \left(\frac{\partial^2 c_0}{\partial \rho^2{}_0}\right)$.

After suitable transformations [1] we obtain the familiar acoustical equations of the first approximation:

$$\frac{\partial \rho_1}{\partial t} + \rho_0\frac{\partial u_1}{\partial x} = 0; \qquad \rho_0\frac{\partial u_1}{\partial t} = -c_0^2\frac{\partial \rho_1}{\partial x} + b\nu_0\rho_0\frac{\partial^2 u_1}{\partial x^2}, \tag{5}$$

where $b = (^4/_3 + \nu'_0/\nu_0)$; $\nu_0 = \eta/\rho_0$; $\nu'_0 = \xi/\rho_0$.

The equations of the second approximation will be

$$\frac{\partial \rho_2}{\partial t} + \rho_0 \frac{\partial u_2}{\partial x} + \frac{\partial}{\partial x}(\rho_1 u_1) = 0;$$

$$\rho_0 \frac{\partial u_2}{\partial t} + \frac{\partial}{\partial t}(\rho_1 u_1) + \rho_0 \frac{\partial u_1^2}{\partial x} = -c_0\left(\frac{\partial c_0}{\partial \rho_0}\right)\frac{\partial \rho_1^2}{\partial x} - c_0^2 \frac{\partial \rho_2}{\partial x} + b\nu_0\rho_0 \frac{\partial^2 u_2}{\partial x^2}. \tag{6}$$

Assuming furthermore that

$$\rho_2 = \rho_{11} + \frac{1}{2}\left(\frac{c_0^2 \rho_1^2}{\rho_0} + \rho_0 u_1^2\right) \tag{7}$$

and performing the proper exclusions and substitutions of terms in (5) we obtain

$$\frac{\partial^2 u_1}{\partial t^2} - c_0^2 \frac{\partial^2 u_1}{\partial x^2} - b\nu_0 \frac{\partial^3 u_1}{\partial x^2 \partial t} = 0; \quad \frac{\partial^2 \rho_1}{\partial t^2} - c_0^2 \frac{\partial^2 \rho_1}{\partial x^2} - b\nu_0 \frac{\partial^3 \rho_1}{\partial x^2 \partial t} = 0. \tag{8}$$

Performing the same operations on (6) we obtain

$$L_0\rho_{11} = -m_1 \frac{\partial}{\partial t}\left(u_1 \frac{\partial^2 u_1}{\partial x^2}\right) + g\rho_0 \frac{\partial^2 \rho_1}{\partial x^2} + \rho_0 \frac{\partial^2 u_1^2}{\partial x^2} +$$

$$+ m_2 \frac{\partial^2}{\partial x^2}\left(u_1 \frac{\partial^2 u_1}{\partial x^2}\right) - b\nu_0 \frac{\partial}{\partial x}\left(\rho_1 \frac{\partial^2 u_1}{\partial x^2}\right). \tag{9}$$

Here for brevity L_0 denotes the linear differential operator

$$L_0 = \frac{\partial^2}{\partial t^2} - c_0^2 \frac{\partial}{\partial x^2} - b\nu_0 \frac{\partial^3}{\partial x^2 \partial t}, \quad m_1 = \frac{b\nu_0}{c_n^2}\rho_0; \; g = \frac{c_0}{\rho_0}\left(\frac{\partial c_0}{\partial \rho_0}\right); \quad m_2 = \frac{b^2\nu^2\rho_0}{c_0^2}.$$

We further evaluate the terms on the right-hand side of (9) as they apply to acoustical conditions. We know that (8) has solutions for a monochromatic wave propagated in a viscous medium:

$$u_1 = A_1 e^{-\alpha_1 x} \cos \omega_1\left(t - \frac{x}{c_0}\right), \quad \rho_1 = B_1 e^{-\alpha_1 x} \cos \omega_1\left(t - \frac{x}{c_0}\right), \tag{10}$$

where A_1 and B_1 are, respectively, the amplitude of displacement velocity and the density amplitude.

Evaluating the relative magnitude of each term on the right-hand side of Equation (9) with the aid of (10) we obtain for a viscous liquid

$$L_0 u_2 = -\frac{\partial^2}{\partial x \partial t}(g\rho_1^2 + u_1^2), \tag{11}$$

$$L_0 \rho_{11} = \rho_0 \frac{\partial^2}{\partial x^2}(g\rho_1^2 + u_1^2), \tag{12}$$

or, in consideration of (5) and (10), we obtain a relationship between the displacement of velocity amplitude and the density amplitude in the form

$$A_1 = B_1(c_0/\rho_0). \tag{13}$$

We now undertake to obtain the acoustical pressure in the second approximation for the two cases: 1) when in a viscous medium a harmonic source of sound is excited at the coordinate origin with the single frequency ω_1; 2) when the same source of sound is excited with two different frequencies ω_1 and ω_2.

We now proceed to solve the first problem. Using (3) and (4) we obtain an expression for the second approximation of the pressure:

$$\frac{\partial p_2}{\partial x} = c_0^2 \frac{\partial \rho_2}{\partial x} + c_0 \left(\frac{\partial c_0}{\partial \rho_0}\right) \frac{\partial \rho_1^2}{\partial x} \tag{14}$$

or

$$p = c_0^2 \rho_{11} + S_0 \rho_1^2. \tag{15}$$

We shall obtain an expression for ρ_{11}. For this purpose we use Equations (12), (10) and (13). Then

$$L_0 \rho_{11} = k_0 e^{-2\alpha_1 x} \cos 2\omega_1 \left(t - \frac{x}{c_0}\right), \tag{16}$$

where $k_0 = b v_0 / \rho_0$. The solution of (16) gives

$$\rho_{11} = (C_* e^{-4\alpha_1 x} + M_0 e^{-2\alpha_1 x}) \sin\left[2\omega_1 \left(t - \frac{x}{c_0}\right) + \pi\right].$$

We use the arbitrary constant $C = + iC_*$, where C_* is the real value. Then

$$\rho_{11} = Ce^{-4\alpha_1 x} \cos 2\omega_1 \left(t - \frac{x}{c_0}\right) - M_0 e^{-2\alpha_1 x} \sin 2\omega_1 \left(t - \frac{x}{c_0}\right). \tag{17}$$

Substituting (17) and ρ_1 of (10) in (15) and considering that S_0 can be neglected, we obtain

$$p_2 = c_0^2 (M_0 e^{-2\alpha_1 x} + C_* e^{-4\alpha_1 x}) \sin\left[2\omega_1 \left(t - \frac{x}{c_0}\right) + \pi\right].$$

To determine C_* we use the boundary condition: for $x = 0$, $p_2 = 0$ (i.e., at the coordinate origin the source oscillates harmonically). Then for the additional pressure in the second harmonic traveling wave we have:

$$p_2 = p_{02} (e^{-2\alpha_1 x} - e^{-4\alpha_1 x}) \sin\left[2\omega_1 \left(t - \frac{x}{c_0}\right) + \pi\right], \tag{18}$$

where

$$p_{02} = \frac{B_1 B_2}{4\alpha_1} \left[\left(\frac{\partial c_0}{\partial \rho_0}\right) + \frac{c_0}{\rho_0}\right].$$

We now reach the second part of the problem. Let the source of sound at the coordinate origin oscillate with the two frequencies ω_1 and ω_2 ($\omega_1 < \omega_2$). Then the solution of the first approximation wave equations (8) can be represented as the sum of two waves:

$$u_1 = u_1' + u_1'' = A_1 e^{-\alpha_1 x} \cos \omega_1 \left(t - \frac{x}{c_0}\right) + A_2 e^{-\alpha_2 x} \cos \omega_2 \left(t - \frac{x}{c_0}\right);$$
$$\rho_1 = \rho_1' + \rho_1'' = B_1 e^{-\alpha_1 x} \cos \omega_1 \left(t - \frac{x}{c_0}\right) + B_2 e^{-\alpha_2 x} \cos \omega_2 \left(t - \frac{x}{c_0}\right). \tag{19}$$

Substituting (19) in, (12\` and retaining only the cross terms, we obtain

$$L_0 \rho_{11} = 2\pi_0 \frac{\partial^2 \rho_1' \rho_1''}{\partial x^2} = N_1 e^{-\alpha x} \cos (\omega_1 - \omega_2)\left(t - \frac{x}{c_0}\right) +$$
$$+ N_2 e^{-\alpha x} \cos (\omega_1 + \omega_2)\left(t - \frac{x}{c_0}\right) \tag{20}$$

Here

$$N_1 = -\frac{B_1 B_2 (\omega_1 - \omega_2)^2}{c_0}\left[\left(\frac{\partial c_0}{\partial \rho_0}\right) + \frac{c_0}{\rho_0}\right]; \quad N_2 = -\frac{B_1 B_2 (\omega_1 + \omega_2)^2}{c_0}\left[\left(\frac{\partial c_0}{\rho_0}\right) + \frac{c_0}{\rho_0}\right].$$

Solving (20), we obtain for the density of the difference wave and the sum wave the expressions

$$\rho_{11}^{(2)} = \pi_1 e^{-\alpha_r x} \cos (\omega_1 - \omega_2)\left(t - \frac{x}{c_0}\right) - N_1^0 e^{-\alpha x} \sin (\omega_1 - \omega_2)\left(t - \frac{x}{c_0}\right),$$
$$\rho_{11}^{(2)} = \pi_2 e^{-\alpha_s x} \cos (\omega_1 + \omega_2)\left(t - \frac{x}{c_0}\right) - N_2^0 e^{-\alpha x} \sin (\omega_1 + \omega_2)\left(t - \frac{\dot{x}}{c_0}\right), \tag{21}$$

where

$$\alpha = \alpha_1 + \alpha_2 = \alpha_1 (1 + n^2); \quad \alpha_r = \alpha_1 (1 - n)^2; \quad \alpha_s = \alpha_1 (1 + n)^2; \quad \alpha_1 = b\nu_0 \omega_1^2 / 2c_0^3;$$
$$n = \omega_2 / \omega_1.$$

Substituting (21) in (15) we obtain*

$$p_r = c_0^2 \left[\pi_1 e^{-\alpha_r x} \cos (\omega_1 - \omega_2)\left(t - \frac{x}{c_0}\right) - N_1^0 e^{-\alpha x} \sin (\omega_1 - \omega_2)\left(t - \frac{x}{c_0}\right)\right].$$
$$p_s = c_0^2 \left[\pi_2 e^{-\alpha_s x} \cos (\omega_1 + \omega_2)\left(t - \frac{x}{c_0}\right) - N_2^0 e^{-\alpha x} \sin (\omega_1 - \omega_2)\left(t - \frac{x}{c_0}\right)\right].$$

With the arbitrary constants $\pi_1 = -iN_1^0$ and $\pi_2 = -iN_2^0$, we obtain the expression for the extra pressure in running waves which represent combinations (the difference and sum) of the frequencies:

$$p_r = p_{0r} \left(e^{-\alpha_r x} - e^{-\alpha x}\right) \sin (\omega_1 - \omega_2)\left(t - \frac{x}{c_0}\right),$$
$$p_s = p_{0s} \left(e^{-\alpha x} - e^{-\alpha_s x}\right) \sin \left[(\omega_1 + \omega_2)\left(t - \frac{x}{c_0}\right) + \pi\right], \tag{22}$$

---

[*] Consider that $N_1^0 \gg S_0 B_1 B_2$ and $N_2^0 \gg S_0 B_1 B_2$.

where

$$p_{0r} = \frac{B_1B_2(\omega_1-\omega_2)}{2\alpha_r}\left[\left(\frac{\partial c_0}{\partial \rho_0}\right)+\frac{c_0}{\rho_0}\right]; \quad p_{0s} = \frac{B_1B_2(\omega_1+\omega_2)}{2\alpha_s}\left[\left(\frac{\partial c_0}{\partial \rho_0}\right)+\frac{c_0}{\rho_0}\right]. \tag{23}$$

The terms in square brackets in (23) and (18) show the causes of the appearance of harmonics and combination waves in the medium.

Performing suitable operations on (18) and (22) we determine that the pressure amplitude in the second approximation has a maximum in space. The position of the maximum is associated with the absorption coefficient of the fundamental wave as follows for the second harmonic, frequency difference and frequency sum, respectively:

$$x_2 = \frac{\ln 2}{2\alpha_1}; \quad x_r = \frac{\ln[(1+n^2)/(1-n)^2]}{2n\alpha_1}; \quad x_s = \frac{\ln[(1+n)^2/(1+n^2)]}{2n\alpha_1}.$$

A comparison shows that $x_r > x_s$, that is, the maximum for the frequency sum is situated close to the radiator.

The following conclusions follow from the analysis.

1. The phenomenological treatment of the propagation and interaction of the waves predicts the spatial intensity maximum both for the harmonics and the combination waves.

2. The positions of the maxima for a given frequency are determined by the viscosity of the medium.

3. By the use of (18), for example, it is easily shown that for low viscosity or at small distances from the source ($\alpha_1 x \ll 1$) a familiar expression is obtained for the second approximation [2]. When the expression in round brackets is expanded in terms of $\alpha_1 x$, we obtain $p_2 = k_0 x \sin[2\omega_1(t - x/c_0) + \pi]$.

4. On the other hand, for very high viscosity or far from the source ($\alpha_1 x \gg 1$) a solution is obtained in the form $p_2 = k_0 e^{-2\alpha_1 x} \sin[2\omega_1(t - x/c_0) + \pi]$.

5. If in the initial equations the viscosity is considered to be a second order quantity it is easy to obtain an expression for the pressure of the second harmonic in the form $p_2 = p_{02}(1 - e^{-4\alpha_1 x}) \sin 2\omega_1(t - x/c_0)$.

The above considerations are easily extended to combination waves.

6. A comparison shows qualitative agreement with experiment [3].

LITERATURE CITED

[1] C. Eckart, Phys. Rev. 73, 1 (1948).

[2] H. Lamb, Dynamical Theory of Sound (1931) p. 183.

[3] G. D. Mikhailov, J. Exptl.-Theoret. Phys. (USSR) 30, 1142 (1956) [Soviet Physics – J.E.T.P., p. 970].

Received January 10, 1956

A GAUGE-INVARIANT ANALOGUE OF THE WIGNER DISTRIBUTION

R. L. Stratonovich

(Presented by Academician N. N. Bogoliubov January 17, 1956)

The well-known Wigner distribution [1-3] is given by

$$w_1(p, q) = (2\pi)^{-n} \int e^{-i\tau p} \rho\left(q + \frac{\tau}{2},\ q - \frac{\tau}{2}\right) d\tau, \tag{1}$$

where $\rho(x,x')$ is the density matrix: $\rho(x,x') = \overline{\psi(x)\psi^*(x')}$; $\underline{p}$ and $\underline{q}$ can designate both the spatial vector ($n = 3$) and the relativistic 4-vector ($n = 4$); and the system of units is used in which $\hbar = 1$ and $c = 1$. The distribution (1) can be used formally when an external electromagnetic field is present, in which the momentum $\underline{p}$ is characterized not only by the velocity $\underline{v}$ and mass $\underline{m}$ of a particle but also by the electromagnetic potentials:

$$p = P + eA(q) \quad (P = mv). \tag{2}$$

The velocity $\underline{v}$ and momentum P, which have a specific physical meaning, are gauge-invariant concepts; however, it follows from (2) that this does not apply to the momentum $\underline{p}$. It is therefore expedient to replace (1) by the distribution $w_2(P, q) = w_1(P + eA, q)$ for gauge-invariant quantities. It would be natural to require that the distribution $w_2(P, q)$ be gauge-invariant. However, this is not the case since

$$\int \exp\left\{-i\tau\left[p + \frac{\partial}{\partial q} f(q)\right] + i\left[f\left(q + \frac{\tau}{2}\right) - f\left(q - \frac{\tau}{2}\right)\right]\right\} \rho\, d\tau \neq \int e^{-i\tau p} \rho\, d\tau. \tag{3}$$

Consequently, in order to obtain the gauge-invariant distribution $w(P, q)$ we must change the basic equation (1). This equation is equivalent to the following definition of the local moments of the momentum $\underline{p}$:

$$\begin{aligned}\langle p_{k_1} \cdots p_{k_s} \rangle_q &\equiv \int p_{k_1} \cdots p_{k_s} w_1(p, q)\, dp = \\ &= \left[\frac{\partial}{\partial i\tau_{k_1}} \cdots \frac{\partial}{\partial i\tau_{k_s}} \rho\left(q + \frac{\tau}{2},\ q - \frac{\tau}{2}\right)\right]_{\tau=0}.\end{aligned} \tag{4}$$

Analogously, seeking an invariant function $w(P,q)$ is equivalent to seeking an invariant method of determining the local moments

$$\langle P_k \ldots P_{k_s} \rangle_q \equiv \int P_{k_1} \ldots P_{k_s} w(P, q)\, dP. \tag{5}$$

We shall investigate the effect of a gauge transformation on (4):

$$A \to A + \frac{1}{e}\left[\frac{\partial}{\partial q} f\right]; \quad \rho(x, x') \to e^{if(x) - if(x')} \rho(x, x'). \tag{6}$$

From the equality

$$\frac{\partial}{\partial i\tau} e^{if(q+\tau/2)-if(q-\tau/2)} =$$

$$= e^{if(q+\tau/2)-if(q-\tau/2)} \left\{\frac{\partial}{\partial i\tau} + \frac{1}{2}\left[\frac{\partial}{\partial q}\left(f\left(q+\frac{\tau}{2}\right)+f\left(q-\frac{\tau}{2}\right)\right)\right]\right\}, \tag{7}$$

we see that in order to obtain invariance of the moments it is sufficient to replace the operator $\partial/\partial i\tau$ by the operator $\partial/\partial i\tau - \frac{e}{2} A\left(q+\frac{\tau}{2}\right) - \frac{e}{2} A\left(q-\frac{\tau}{2}\right)$. We therefore postulate the following gauge-invariant method of determining the local moments of (5):

$$\langle P_{k_1}\ldots P_{k_s}\rangle_q = \left[\left(\frac{\partial}{\partial i\tau_{k_1}} - \frac{e}{2} A_{k_1}\left(q+\frac{\tau}{2}\right) - \frac{e}{2} A_{k_1}\left(q-\frac{\tau}{2}\right)\right)\ldots\right.$$

$$\left.\ldots\left(\frac{\partial}{\partial i\tau_{k_s}} - \frac{e}{2} A_{k_s}\left(q+\frac{\tau}{2}\right) - \frac{e}{2} A_{k_s}\left(q-\frac{\tau}{2}\right)\right)\rho\left(q+\frac{\tau}{2},\ q-\frac{\tau}{q}\right)\right]_{\tau=0}. \tag{8}$$

From the summation of the resulting expressions we obtain the characteristic function of the local distribution:

$$\theta_q(t) = \sum_{s=0}^{\infty}\frac{1}{s!}\sum_{k_1\ldots k_s=1}^{n} it_{k_1}\ldots it_{k_s}\langle P_{k_1}\ldots P_{k_s}\rangle_q = [\theta(t,\tau)]_{\tau=0}, \tag{9}$$

where

$$\theta(t,\tau) = \exp\left\{it\left[\frac{\partial}{\partial i\tau} - \frac{e}{2} A\left(q+\frac{\tau}{2}\right) - \frac{e}{2} A\left(q-\frac{\tau}{2}\right)\right]\right\}\times$$

$$\times\,\rho\left(q+\frac{\tau}{2},\ q-\frac{\tau}{2}\right). \tag{10}$$

In order to obtain the explicit form of (10) we introduce the differential equation which it obeys. We vary the vector $\underline{t}$ with respect to its length but not its direction: $\delta t = \epsilon t |t|^{-1} = \epsilon n$. Then the operator in the exponential of (10) commutes with its variation. We thus obtain

$$n\frac{\partial}{\partial t}\theta = \left\{n\frac{\partial}{\partial\tau} - \frac{ie}{2} n\left[A\left(q+\frac{\tau}{2}\right) + A\left(q-\frac{\tau}{2}\right)\right]\right\}\theta. \tag{11}$$

This differential equation must be solved subject to the boundary condition

$$|\theta(t,\tau)|_{t=0} = \rho\left(q+\frac{\tau}{2},\ q-\frac{\tau}{2}\right). \tag{12}$$

By the usual method of solving a linear equation in first order partial derivatives we obtain

$$\theta(t,\tau) = \exp\left\{-\frac{ie}{2}\int_0^{|t|}\left[A\left(q+\frac{t+\tau-n\xi}{2}\right) + A\left(q-\frac{t+\tau-n\xi}{2}\right)\right]d\xi\right\}\rho\left(q+\frac{t+\tau}{2},\ q-\frac{t+\tau}{2}\right). \tag{13}$$

Special interest attaches to the boundary value of (9), which in accordance with (13) is

$$\theta_q(t) = \exp\left\{-\frac{ie}{2}t\int_{-1}^{1} A\left(q+\frac{\eta t}{2}\right)d\eta\right\}\rho\left(q+\frac{t}{2},\ q-\frac{t}{2}\right). \tag{14}$$

Hence by inversion we obtain the distribution density

$$w(P, q) = $$

$$= (2\pi)^{-n}\int \exp\left\{-it\left[P+\frac{e}{2}\int_{-1}^{1} A\left(q+\frac{\eta t}{2}\right)d\eta\right]\right\}\rho\left(q+\frac{t}{2},\ q-\frac{t}{2}\right)dt. \tag{15}$$

Gauge invariance of this distribution is also confirmed by direct examination.

If we introduce the "gauge-invariant density matrix"

$$\rho_{in}(x, x') = e^{-i\Phi(x,x')}\rho(x, x');$$

$$\Phi(x, x') = \frac{e}{2}(x-x')\int_{-1}^{1} A\left(\frac{x+x'+\eta(x-x')}{2}\right)d\eta = e\int_{x'}^{x} A_\mu(dx)^\mu, \tag{16}$$

it will be associated with w (P, q) by the usual Wigner transformation [1].

We shall now determine what equation for w (P, q) is derived from the wave equation

$$\hat{F}\rho = 0; \quad \hat{F} = F\left(\frac{\partial}{\partial ix} - eA(x)\right) \equiv F\left(\frac{\partial}{\partial ix_\mu} - eA_\mu(x)\right). \tag{17}$$

Considering the form of the function $\Phi(x, x')$, after a number of transformations we obtain

$$\left(\frac{\partial}{\partial ix_\mu} - eA_\mu(x)\right)e^{i\Phi(x,x')} = e^{i\Phi(x,x')}\left(\frac{\partial}{\partial ix_\mu} - \frac{e}{2}(x_\lambda - x'_\lambda)\int_{-1}^{1} H_{\lambda\mu}\frac{1+\eta}{2}d\eta\right) \tag{18}$$

$$(H_{\lambda\mu} = \partial_\lambda A_\mu - \partial_\mu A_\lambda),$$

from which it follows that

$$F\left(\frac{\partial}{\partial ix_\mu} - eA_\mu\right)\rho = e^{i\Phi}F\left(\frac{\partial}{\partial ix_\mu} - \frac{e}{2}(x_\lambda - x'_\lambda)\int_{-1}^{1} H_{\lambda\mu}\frac{1+\eta}{2}d\eta\right)\rho_{in} = 0. \tag{19}$$

Using the variables t = x − x' and q = (x + x')/2, as well as w (P, q), this equation can be written as

$$F\left(\frac{\partial}{\partial it_\mu} + \frac{1}{2}\frac{\partial}{\partial iq_\mu} - \right.$$

$$\left. - \frac{e}{2}t_\lambda\int_{-1}^{1} H_{\lambda\mu}\left(q+\frac{t\eta}{2}\right)\frac{1+\eta}{2}d\eta\right)\rho_{in}\left(q+\frac{t}{2},\ q-\frac{t}{2}\right) = 0; \tag{20}$$

$$F\left(P_\mu + \frac{\hbar}{2i}\frac{\partial}{\partial q_\mu} - \frac{e}{2} i\hbar \frac{\partial}{\partial P_\lambda}\int_{-1}^{1} H_{\lambda\mu}\left(q + \frac{i\hbar\eta}{2}\frac{\partial}{\partial P}\right)\frac{1+\eta}{2}d\eta\right) w(P, q) = 0. \tag{21}$$

For clarity the constant $\hbar$, which characterizes quantum effects, is written out in the last equation.

Let us consider as an example the relativistic case of particles with zero spin, where $F(P_\mu) = P^2 - m^2$. The imaginary part of Equation (21) gives the equation of motion which, when the first terms of the expansion in $\hbar$ are retained, becomes

$$\begin{gathered}\Big\{P_\lambda \frac{\partial}{\partial q_\lambda} + eP_\lambda H_{\mu\lambda}(q)\frac{\partial}{\partial P_\mu} + \frac{e\hbar^2}{48}\left[\frac{\partial H_{\mu\lambda}(q)}{\partial q_\rho \partial q_\lambda}\right]\frac{\partial^2}{\partial P_\mu \partial P_\rho} + \\ + \frac{e\hbar^2}{8}\left[\frac{\partial H_{\mu\lambda}(q)}{\partial q_\rho}\right]\frac{\partial^2}{\partial P_\mu \partial P_\rho}\frac{\partial}{\partial q_\lambda} + \frac{e^2\hbar^2}{8}\left[\frac{\partial H_{\mu\lambda}(q)}{\partial q_\rho}\right] H_{\nu\lambda}\frac{\partial^3}{\partial P_\mu \partial P_\rho \partial P_\nu} - \\ - \frac{e\hbar^2}{24} P_\lambda \left[\frac{\partial^2 H_{\mu\lambda}(q)}{\partial q_\rho \partial q_\nu}\right]\frac{\partial^3}{\partial P_\nu \partial P_\rho \partial P_\nu} + O(\hbar^4)\Big\} w(P, q) = 0.\end{gathered} \tag{22}$$

For $\hbar \rightarrow 0$ this equation becomes the nonquantum relativistic kinetic equation containing the Lorentz force. The real part of (21) gives the additional equation

$$\begin{gathered}\Big\{P_\lambda^2 - m^2 - \frac{e\hbar^2}{16}\left[\frac{\partial H_{\mu\lambda}(q)}{\partial q_\lambda}\right]\frac{\partial}{\partial P_\mu} - \frac{\hbar^2}{4}\frac{\partial^2}{\partial q_\lambda^2} - \\ - \frac{\hbar^2}{4} e^2 H_{\mu\lambda} H_{\nu\lambda}\frac{\partial^2}{\partial P_\mu \partial P_\nu} + O(\hbar^4)\Big\} w(P, q) = 0,\end{gathered} \tag{23}$$

which concerns the relations between the four momentum components and which is converted in the nonquantum case to the trivial relation $P^2 - m^2 = 0$. The more complicated quantum case results from the Heisenberg uncertainty principle.

The present results enable us to determine not only the local average values but also the averages for a given time – in other words, the average values for a selected space-like hypersurface σ:

$$\begin{gathered}\langle f(P, q)\rangle_\sigma = m^{-1}\int_\sigma w(P, q) f(P, q) P\nu d^3\sigma\, d^4P = \\ = m^{-1}\int_\sigma w(P, q) f(P, q)\delta(G(q)) P \frac{\partial}{\partial q} G(q) d^4q\, d^4P,\end{gathered} \tag{24}$$

where ν is the vector which is normal to σ; $G(q)$ is chosen so that $G(q) = 0$ is the equation of the surface σ. Substituting in (24) the equality (15) as well as suitable expressions for the operator $f(x, x')$:

$$f(P, q) = \int e^{-i(x-x')P - i\Phi(x, x')}\delta\left(\frac{x+x'}{2} - q\right) f(x, x') d^4x\, d^4x', \tag{25}$$

we obtain

$$\begin{aligned}\langle f(x, x')\rangle_\sigma = \int \Big\{ &\frac{1}{2}\rho(x, x')\left(\frac{\partial}{\partial i x'_\mu} - eA_\mu(x')\right) f(x', x) + \\ &+ \frac{1}{2} f(x', x)\left(\frac{\partial}{\partial i x_\mu} - eA_\mu(x)\right)\rho(x, x') + \\ &+ \frac{e}{2}(x_\lambda - x'_\lambda)\int_{-1}^{1} H_{\lambda\mu}\left(\frac{x + x' + \eta(x - x')}{2}\right)\frac{\eta}{2}\, d\eta\, \rho(x, x')\, f(x', x)\Big\} \times \qquad (26) \\ &\times \delta\left(G\left(\frac{x + x'}{2}\right)\right) G_\mu\left(\frac{x + x'}{2}\right) d^4x\, d^4x'\end{aligned}$$

$$\left(G_\mu(q) = \frac{\partial}{\partial q_\mu} G(q); \quad 2f\,\frac{\partial}{\partial x}\rho = f\frac{\partial \rho}{\partial x} - \frac{\partial f}{\partial x}\,\rho\right).$$

The first two terms in (26) appear naturally and are to a certain extent trivial; the same cannot be said of the third term.

LITERATURE CITED

[1] E. Wigner, Phys. Rev. 40, 749 (1932).

[2] J. E. Moyal, Proc. Cambridge Phil. Soc. 45, 99 (1949).

[3] Iu. L. Klimontovich, Doklady Akad. Nauk SSSR 87, 927 (1952).

Received December 26, 1955

THE NUCLEAR QUADRUPOLE MOMENT OF U^{233}

A. G. Zimin and N. M. Iashin

(Presented by Academician M. A. Leontovich February 10, 1955)

We used optical atomic spectroscopy to investigate the hyperfine structure of the lines of neutral and ionized U^{233} About 50 lines were observed with six-component hyperfine structure, thus confirming the previously established value of the nuclear spin of U^{233} as $I = {}^5/_2$ [1-3].

We studied in detail the hyperfine structure of spark lines whose lower levels belong to the configuration $5f^3\ 6d\ 7s$. These lines are given in Table 1, with the intervals between the components of the hyperfine structure. The hyperfine structure of these spark lines was caused by the splitting of both the lower and upper levels, with greater splitting of the lower levels. This conclusion is based on a study of the relative intensities of the hyperfine structure and of the magnitudes of the intervals.

TABLE 1

Wavelength in A	Classification	Intervals between hyperfine components* in 10^{-3} cm^{-1}
4188.07	${}^6L_{11/2} - 242_{11/2}$	110; 112; 116; 102; 105
4297.11	${}^6L_{11/2} - 235_{11/2}$	98; 116; 135; 133; 116
4515.28	${}^6L_{11/2} - 224_{9/2}$	127; 143; 146; 126; 115
4666.86	${}^6L_{11/2} - 217_{13/2}$	102; 105; 101; 94; 79
4171.59	${}^6L_{13/2} - 257_{13/2}$	77; 93; 115; 138; 161
4538.19	${}^6L_{13/2} - 237_{11/2}$	66; 86; 128; 152; 194
4567.69	${}^6L_{13/2} - 236_{13/2}$	90; 107; 142; 169; 215
5008.22	${}^6L_{13/2} - 217_{13/2}$	53; 73; 92; 108; 135
4477.71	${}^6K_{9/2} - 232_{11/2}$	154; 138; 106; 75; 62
4543.13	${}^6K_{9/2} - 229_{11/2}$	137; 119; 100; 78; 60
4646.60	${}^6K_{9/2} - 224_{9/2}$	177; 152; 124; 103; 69

---

* The intervals are given in the order of diminishing frequency. The intervals are determined with an accuracy of ± .0002 cm^{-1}.

The coefficients of the magnetic (A) and quadrupole (B) interactions of the electron shells with the nucleus were calculated from the equation:

$$\Delta\nu = a_0 + \frac{A}{2}C + \frac{A'}{2}C' + BC(C+1),$$

where $\Delta\nu$ is the interval (in cm^{-1}) between the components of the hyperfine structure; a_0 is a constant and $C = F(F+1) - I(I+1) - J(J+1)$. The term $\frac{A'}{2}C'$ is the magnetic interaction of the upper level – we neglect the quadrupole interaction of the upper level because of its smallness. The coefficients of the magnetic and quadrupole interactions were calculated for the three deepest levels $^6L_{11/2}$, $^6L_{13/2}$ and $^6K_{9/2}$ by the method of least squares. The coefficients of the quadrupole interaction were obtained by averaging the values of the coefficients calculated for different lines with a common level. For the $^6K_{9/2}$ level the values of the coefficient that were calculated for different lines differ both in magnitude and in sign, since in this case the average value has no meaning. For the $^6L_{11/2}$ and $^6L_{13/2}$ levels the average values of the coefficients are as follows: $B(^6L_{11/2}) = -(5.5 \pm 1.5) \cdot 10^{-5}$ cm^{-1} and $B(^6L_{13/2}) = -(1.7 \pm 0.7) \cdot 10^{-5}$ cm^{-1}. The large inaccuracy in the determination of the constants is clearly associated with interaction of the levels.

The optical quadrupole moment Q_{op} is defined in terms of the coefficient B by Casimir's equation:

$$Q_{op} = -\,{}^8/_3\,\frac{hc}{e^2}\,B\,\frac{IJ\,(2I-1)(2J-1)}{\sum \langle 3\cos^2\theta_i - 1\rangle\langle r_i^{-3}\rangle}$$

into which there enter states with $m = J$ which are averaged over the electronic wave function. In order to determine the sign of the quadrupole moment $3\cos^2\vartheta - 1$ is averaged over the angular part of the wave functions of the levels $(f^3ds)^6L_{11/2}$ and $^6L_{13/2}$. These wave functions are constructed for intermediate coupling $(J'j)$ where J' is the moment of the electronic core f^3d in which the electrons are subject to LS coupling and $\underline{j}$ is the moment of the s-electron which is bound to the core by jj-coupling. Averaging over the wave functions with $m_L = 4.5$ which enter into the wave function of the core is difficult because the functions include a complicated linear combination of the wave functions of the individual electrons. However, the statistical weights of these functions are small compared with the weights of the functions with $5 < m_L \leq 8$ and they can be neglected with an accuracy up to 10%. This is entirely acceptable since the accuracy of the experiment is ~ ± 40%. According to the calculations $\langle 3\cos^2\vartheta - 1\rangle$ has a positive sign, from which it follows that $Q_{op}(U^{233}) > 0$.

In order to evaluate the quadrupole moment we used the value of $\langle r^{-3}\rangle$ given by Sternheimer for the $5f^3$ configuration [4]. The value obtained is $Q_{op} \approx 13 \cdot 10^{-24}$ cm^2. A more exact evaluation of $\langle r^{-3}\rangle$ for the $5f^36d7s$ configuration can be made by Fermi's method [5], into which, however, there enters the magnitude of the multiplet splitting, which we do not know.

In conclusion we wish to thank Doctor of Physico-Mathematical Sciences, A. R. Striganov, for suggesting the present work and Professor Ia. A. Smorodinskii for his interest.

LITERATURE CITED

[1] L. A. Korostyleva, A. R. Striganov and N. M. Iashin, J. Exptl.-Theoret. Phys. (USSR) 28, 471 (1955).

[2] N. I. Kaliteevskii and M. P. Chaika, Doklady Akad. Nauk SSSR 103, 49 (1955).

[3] K. L. V. Sluis and J. R. McNally, J. Opt. Soc. Amer. 44, 87 (1954).

[4] R. Sternheimer, Phys. Rev. 84, 244 (1951).

[5] E. Fermi, Z. Physik 82, 729 (1933).

Received December 17, 1955

REGROUPING OF THE LATENT IMAGE IN THE PHOTOGRAPHIC ACTION OF IONIZING PARTICLES

A. L. Kartuzhanskii

(Presented by Academician A. F. Ioffe February 6, 1955)

When photographic film is illuminated for a period which does not exceed the duration of the ionic stage of formation of the latent image (10^{-5} sec for AgBr at room temperature) each center of the latent image formed in the crystals of the emulsion consists of one atom [1]. But for development of the image the centers must be of greater than atomic size. It has therefore been suggested that after illumination a regrouping of the latent image takes place, that is, some centers grow in size at the expense of others. This process in emulsions was subsequently detected experimentally [2] and was found to be identical in its mechanism with the relaxation of photoconductivity in large single crystals of AgHal [3]. The process is essentially as follows: after illumination there takes place an emptying of shallow levels in which photoelectrons had temporarily been trapped and filling of deep levels, that is, photolytically formed Ag atoms collect at sensitivity centers.

Since there exists extensive similarity of the photographic effect of brief illumination and of ionizing particles [4] it can be assumed that the regrouping of the latent image also occurs after the action of ionizing particles on the crystal has been completed. This hypothesis is all the more reasonable since the transit time through the crystal (10^{-13} sec) is considerably shorter than the duration of the ionic stage (10^{-5} sec). But direct verification of this hypothesis by the same method which was used for the effect of light [2] requires an extremely strong source of particles ($\gtrsim 10^{14}$ particles per cm^2 per second). It is therefore more convenient to use certain indirect information which is the direct result of regrouping, that is, the ability or inability of a crystal of the emulsion to record particles of a given type and energy; as will be shown, this property is determined entirely by the regrouping of the latent image.

Let a crystal have N sensitivity centers with the same energetic relationship to the conduction band. In order to convert any one of these centers into a development center it is required that there be formed in it a group of not less than n_0 Ag atoms, n_0 being identical for all centers. Furthermore, let all n conduction electrons which appear in the crystal as a result of passage of the particle be used for the formation of Ag atoms, that is, there is no recombination. Then 10^{-5} sec after the passage of the particle n separate Ag atoms are formed in the crystal, of which N atoms occupy sensitivity centers and the remaining $n - N$ are formed near random disturbances of the crystal structure. If we ascribe to the sensitivity centers only acceptor properties and to the remaining traps only donor properties it can be expected that after regrouping there remain only N centers, each consisting of a few atoms. It makes no difference which atoms go to any particular center; only their distribution over the centers is of importance. Then the question as to whether among these centers there will be at least one which contains not less than n_0 Ag atoms is equivalent to the problem of finding the probability of the distribution of n indistinguishable balls in N identical boxes, where at least one of the boxes contains not less than n_0 balls; Bose statistics cannot be applied to this problem.

The probability that not less than n_0 balls will be found simultaneously in some boxes is expressed by the equation*

$$W = \sum_{k=1}^{n=n/n_0} (-1)^{k-1} \frac{\binom{N}{k} \cdot \binom{N+n-n_0k-1}{n-n_0k}}{\binom{N+n-1}{n}}, \qquad (1)$$

---

* At our request this equation was derived by G.I. Zel'tser, to whom the author is very grateful.

where the symbol$\binom{a}{b}$ denotes the binomial coefficient $C_b^a = \left(\frac{a!}{b!(ab)!}\right)$. The upper limit of summation, if n is not a multiple of n_0, is the nearest whole number without a remainder.

We note the following properties of the function W (n). Firstly, $W(n) \equiv 0$ for $n < n_0$. Secondly, the largest values of n for which no box contains n_0 balls is $N(n_0 - 1)$ and therefore $W(n) \equiv 1$ for $n > N(n_0 - 1)$; in particular, when $N = 1$, $W(n) \equiv 1$ beginning with $n = n_0$. The presumable existence in the crystal of a center containing not less than n_0 atoms is thus expressed by the inequality

$$n \geqslant N(n_0 - 1) + 1. \qquad (2)$$

Thirdly, the region of values of n in which $0 < W(n) < 1$ for a given n_0 is determined by the magnitude of N, and as N increases the extent of the range increases. Since the beginning of this region is always given by $n^{-1} = n_0$ the increase of the range takes place through its terminal value, i.e. the value of $n'' = N(n_0 - 1) + 1$. Therefore for a given value of n, W (n) decreases as N increases. Physically this denotes a decreased probability for the formation of a development center through regrouping accompanied by an increase of the number of sensitivity centers; this is quite understandable since the centers compete with each other.

We shall now show how to obtain the values of n, n_0 and N for comparison of (1) and (2) with experiment. It is easiest to obtain n, for which purpose it is necessary to know only the size of a crystal and the ionizing power of the particle passing through the crystal; the latter quantity, which is calculated by the Bethe-Livingston equation, is known quite accurately [5]. In order to determine n_0, effective use is made of the analysis of the curves which reveal noninterchangeability under the action of prolonged low-intensity illumination [6,7]. In particular, it was shown by this method that in the most highly sensitive crystals $n_0 = 8$, and for a longer development time [6] n_0 can be even smaller. An analysis of a large number of experimental curves, by the present author, suggests that n_0 does not exceed 50 even in the least sensitive crystals. The values of N are least well known; here we can use only individual data from electron-microscopical studies of emulsion crystals. Thus, according to some data, during the period of chemical aging in highly sensitive crystals, on the average 4-5 sensitive centers are formed, and variation of the conditions for aging for the purpose of obtaining the highest sensitivity does not affect the number of centers formed although it materially affects the depth of the corresponding levels. On the other hand [8], in crystals of low sensitivity after irradiation with α-particles it is possible to find 100-200 and more centers per crystal.* The majority of these are probably not sensitivity centers; it is evident that the sensitivity centers in this case had small energy depth which deprived them of any material advantage in their competition with other random electron traps.

We shall verify (1) and (2) in the two limiting cases of small and large values of n. The smallest values of n are obtained when a singly-charged relativistic particle passes through a crystal with the smallest possible ionizing power ($dE/dx \cong 700$ ev per 1 μ of path in AgHal), which is therefore the most difficult to record photographically. The crystals of emulsions used for this purpose have a diameter of about 0.3μ [9], i.e. $dE/dx \cong 200$ ev per crystal when traversed for a maximum distance by the particle. The low grain density in the tracks of such particles indicates that traversal of the crystals along their periphery is insufficient to lead to their development, so that 200 ev must be considered the threshold value. Since the production of one photoelectron in AgHal requires, according to different data [10,11] from 5.8 to 7.6 ev, n is from 26 to 35. Since the recording of such particles requires the highest crystal sensitivity we shall use the smallest value 8 for n_0. Then the condition for development (2) leads to the values $N \leq 4$-5, which is in excellent agreement with the above-mentioned experimental data.

Large values of n are obtained, for example, when highly-ionizing α-particles emitted by naturally radioactive elements pass through the crystals. Their energy does not exceed 8 to 9 Mev, and for a crystal of 0.3μ thickness, n is of the order 10^4 and greater. The high grain density in the tracks of such particles indicates that dE/dx in this case is much above the threshold value, so that almost all crystals including those traversed along their periphery can be developed. Even when an excessively high value of n_0 is used knowingly in the computations, by setting it equal to 50 (which corresponds to extremely insensitive crystals), according to (2) all crystals with $N \lesssim 200$ will be developed. As has already been shown experimentally [8],N is of just this order of magnitude. If it is considered that the crystals have a diameter of the order $\sim 0.75\mu$ and the particles have the energy 5.3 Mev, i.e. $dE/dx = 360$ kev per crystal ($n = 5\text{-}6 \cdot 10^4$), then Condition (2) would then be satisfied by a factor of 5 to 6, and even crystals with $N \sim 10^3$ could be developed. The ease with which the Inequality (2) is satisfied and the broad diversity of the conditions which satisfy it suggest the reason why photographic recording of natural alpha radiation is so easy that it was accomplished almost half a century ago. Thus the consequences of the proposed scheme of latent image regrouping is confirmed by experiment both for small and large values of n.

---

* Although the authors assumed [8] that the crystals which they were investigating were of high sensitivity, they were considering only their sensitivity to light, which was the result of the large size of the crystals and the broadening of the spectral region of sensitivity through the addition of AgI, which methods cannot be used for increasing sensitivity to particles.

It follows from (2), in accordance with practice, that for the recording of weakly ionizing particles one should not use an emulsion containing large crystals. Although the increase of the diameter d is accompanied by a proportional increase of n, N increases at the same time proportionally to the surface (d^2). Consequently, for a given n_0 as d increases it becomes more difficult to satisfy (2) since n/N decreases as 1/d.

The agreement of (1) and (2) with experiment in the limiting cases suggests that intermediate cases can also be described by these expressions. The fact that for nuclear emulsions it is customary to determine the threshold energy E of a given kind of particle already recorded by an emulsion makes it easy to obtain the threshold value of dE/dx and thus n. In (2) for the threshold value of n there remains only the sign of equality, which enables us to obtain any value of n_0 of of N when the other can be determined independently. When n_0 and N are both known, a verification of the fulfillment of (2), for which purpose it is possible to use data on gaps in the track, enables us to estimate the loss associated with recombination which is neglected in the derivation of (1).

LITERATURE CITED

[1] A. L. Kartuzhanskii, Progr. Phys. Sci. (USSR) 51, 161 (1953).

[2] A. L. Kartuzhanskii, Progr. Sci. Photogr. (USSR) 3, 76 (1955).

[3] P. V. Meikliar, J. Exptl.-Theoret. Phys. (USSR) 21, 42 (1951).

[4] A. L. Kartuzhanskii, Progr. Phys. Sci. (USSR) 52, 341 (1954).

[5] J. Webb, Progr. Phys. Sci. (USSR) 38, 77 (1949).

[6] P. V. Meikliar, J. Exptl.-Theoret. Phys. (USSR) 23, 217 (1952).

[7] J. H. Webb, J. Opt. Soc. Amer. 40, 3 (1950).

[8] H. Hoerlin and F. A. Hamm, J. Appl. Phys. 24, 1514 (1953).

[9] E. Pickup, Can. J. Phys. 31, 898 (1953).

[10] K. A. Yamakawa, Phys. Rev. 82, 522 (1951).

[11] P. J. van Heerden, Dissertation (Utrecht, 1945).

Leningrad Agricultural Institute

Received December 28, 1955

SUBLIMATION OF A CRYSTAL LATTICE BY A STRONG SHOCK WAVE

Iu. N. Riabinin

(Presented by Academician N. N. Semenov February 6, 1956)

In matter which is subjected to very strong compression we can expect to find considerable changes in the properties which depend on the structure of the outer electron shells. From Bridgman's experiments [1] it is known how the volume of a substance changes as well as its compressibility up to 100,000 kg/cm^2. It is possible to calculate [2] what changes in the atomic volumes and in the compressibilities of elements may be expected above 100,000 kg/cm^2.

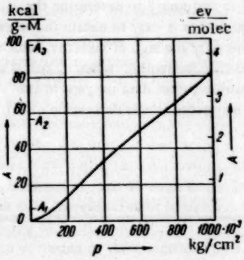

Fig. 1. Dependence of the energy A on pressure.
A_1 = heat of fusion – 7.22 kcal/g-M; A_2 = heat of sublimation at 18° = 57.1 kcal/g-M; A_3 heat of formation of Na (solid) + $^1/_2$ Cl_2 (gas), A_3 = 98.33 kcal/g-M.

When a crystal lattice is compressed isothermically, work is done to overcome the ionic repulsive forces. The greater the total compressibility of the substance, the greater the energy which it acquires under pressure, since the work of isothermal compression is $A = \int p dv$. At very-high pressure the atoms themselves must begin to undergo compression due to the deformation of their electron shells. It can be assumed that under such compression matter will accumulate a large amount of elastic energy. The state of matter depends on its internal energy. It is therefore of interest to learn what energy matter can possess under compression up to various ultrasonic pressures.

By using the equation of state of highly compressed matter [10], we can calculate the energy A (work of isothermal compression) as a function of pressure. The author has carried through such calculations for rock salt.

From data on the compressibility of NaCl [3,4] the following equation of state was obtained:

$$V = \frac{0.962}{\left(\frac{p + 78000}{88000}\right)^{\frac{1}{3.6}}}$$

The values of the volumes V (cm^3) calculated by this equation for the pressure range p = 10,000-100,000 kg/cm^2 are in good agreement with Bridgman's experimental measurements in this range. This equation was used to calculate the energy A as a function of pressure in the range of 10,000-1,000,000 kg/cm^2. The results are given in Fig. 1. As can be seen from this figure, for isothermal compression of 1 g-M (58.46 g) of NaCl crystals at room temperature from 1 to 1,000,000 kg/cm^2, 81 kcal must be expended, almost entirely to overcome repulsive forces. In matter which is compressed up to such a high pressure the large amount of 3.5 ev per molecule of elastic energy will be stored up. To give an idea of how large this amount of energy is we need only point out that the heat of sublimation of crystals at 18° is 57.1 kcal/g-M.

It should be noted that when the compression takes place not along an isotherm but along a Hugoniot adiabat the energy stored up in the matter for the same volume change will be greater than would follow from the curve of Fig. 1. In this case the energy is determined by elastic repulsive forces and by the thermal motion of the atoms since for such adiabatic compression the temperature of the compressed matter will be very much elevated.

We know that when a strong shock wave passes through matter the compression at the front follows a Hugoniot adiabat and the expansion follows a Poisson adiabat. Thus the energy of the substance during expansion will be greater than during compression. The more strongly compressed the matter at the front of the wave is or, correspondingly, the higher its energy in this state, the greater will be the energy difference upon expansion. When matter is compressed by this means to very high pressures it can be expected that it will possess quite high energy when expanded. It is not impossible that this energy will be sufficient to overcome the lattice binding force, as a result of which sublimation of a portion of the lattice molecules can take place.

In order to verify the validity of this hypothesis and show that during expansion after strong compression by the indicated method a sufficiently large quantity of energy can be accumulated, it was necessary to create a shock compression experimentally and investigate the changes which resulted. For this purpose it was required that a method be developed for compressing matter to hundreds of thousands of atmospheres, followed by very rapid expansion.

In order to satisfy the indicated compression conditions the usual static method of obtaining very high pressures is unsatisfactory because of the slowness of the processes of both compression and expansion as well as because of the impossibility of obtaining high enough pressures by this means. A dynamical method is required for very rapid compression and expansion. It is possible to use the high pressure resulting from the detonation of explosive materials and the pressure rise in a convergent cylindrical shock wave [5].

After compression by such a shock wave the tested material, which is contained within an ampoule placed in a metal cylinder, begins to expand rapidly as the convergent wave begins to diverge after passing through the middle of the cylinder. The pressure exerted by the shock wave on the surface of the compressed material can be estimated from the equations of gas dynamics [6-9].

After a dynamical compression method was developed and preservation of the substance in the ampoule after compression and expansion was insured, a few experiments were performed on the compression of rock salt.

White fine-grained salt was used. It was easily pressed into an ampoule with an outside diameter of 3 mm. The pressure was calculated at the radial distance corresponding to the outer surface of the sample. After compression to the order of 110,000 atmos the ampoule contained white strongly compressed salt with no noticeable external changes. When the pressure reached the order of 200,000-260,000 atmos the pressed salt was of a light gray color. After compression up to the order of 300,000 atmos followed by rapid expansion the salt was gray. In order to determine what changes during compression and expansion brought about the conversion of the color from white to gray the salt was studied after being removed from the ampoule.

The structure of the salt was studied by x-ray analysis. Powder patterns of the salt before and after the experiment showed no change of the crystal structure. Consequently, the change in color is not associated with any change of the crystal structure of the sample.

The gray salt was then analyzed chemically. To determine the alkali content it was dissolved in water and 0.1 N hydrochloric acid was titrated in the presence of phenolphthalein. The solution gave the pink coloring that is characteristic of an alkaline reaction. The alkali in this case could be formed only in the presence of free sodium. There is thus reason to believe that during the strong compression and subsequent expansion of the sample there took place a partial decomposition of the sample: $2NaCl \rightarrow 2Na + Cl_2$. It is evident that a certain amount of very finely dispersed metallic sodium in the pressed salt gave it the gray color.

After compression to about 470,000 atmos, followed by expansion, the portion of the ampoule which contained the salt was very much stretched. The ampoule contained a small amount of dark gray powder. The small amount of powder prevented its analysis. In this instance the larger portion of the salt had evidently been sublimated during expansion and had escaped from the ampoule through fine cracks. The cylindrical vessel was undamaged.

After compression to the order of 610,000 atmos, followed by expansion, the ampoule was broken and empty, and the cylinder was also damaged on the inside.

The above results suggest that under the given conditions of compression and expansion, a very large amount of energy is stored up in matter. This energy is evidently sufficient not only to sublimate a portion of the NaCl molecules, but also to dissociate some of them into $2Na + Cl_2$. It is therefore possible that in these experiments such an effect can actually occur. It can be assumed that this takes place as a result of possible redistribution of the energy among the separate particles during the course of the expansion.

The author wishes to thank M. A. Sadovskii, Corresponding Member of the Academy of Sciences of the U.S.S.R., for his interest and assistance.

LITERATURE CITED

[1] P. W. Bridgman, Recent Work in High Pressures (Foreign Lit. Press, 1948).

[2] Iu. N. Riabinin, Doklady Akad. Nauk SSSR 104, 5, 721 (1955).

[3] P. W. Bridgman, Proc. Am. Acad. Arts Sci. 76, 1, 1 (1945).

[4] R. W. Goranson and E. A. Johnson, Phys. Rev. 57, 845 (1940).

[5] W. S. Kolski, F. A. Lucy, R. G. Shreffler and F. J. Willig, J. Appl. Phys. 23, 1300 (1952).

[6] Ia. B. Zel'dovich, Theory of Shock Waves and Application to Gas Dynamics (1946).

[7] K. P. Staniukovich, Theory of Unstable Motion in Gases (1948).

[8] L. D. Landau and E. M. Lifshits, Mechanics of Continuous Media (1953).

[9] J. M. Walsh and R. H. Christian, Phys. Rev. 97, 6, 1544 (1955).

[10] Iu. N. Riabinin, Physics of Metals and Metallography (USSR) 2, 225 (1956).

Institute of Chemical Physics,
Academy of Sciences, U.S.S.R.
and
High Pressure Physics Laboratory,
Academy of Sciences, U.S.S.R.

Received February 3, 1956

DURATION OF FLUORESCENCE IN MESODERIVATIVES OF ANTHRACENE

A. S. Cherkasov, V. A. Molchanov, T. M. Vember and K. G. Voldaikina

(Presented by Academician A. N. Terenin January 18, 1956)

At the present time the average fluorescence duration τ of organic compounds can be determined both by indirect methods (such as absorption, polarization and quenching by added quenchers) and by direct measurements. Because of experimental difficulties the latter method has been used for only a small number of substances.

In order to calculate the mean persistence of fluorescence from the area of the long wave absorption band it is customary to use the equation [1]

$$\frac{1}{\tau} = 8\pi c \nu_A^2 n^2 \frac{1000 \cdot 2.3}{N} \int \varepsilon \, d\nu, \tag{1}$$

where c is the velocity of light in cm/sec; ν_A is the average frequency in cm^{-1}; n is the refractive index; and ϵ is the molar extinction coefficient.

Forster [2] used a few substances to show that the calculated values of τ agree better with indirect measurements (allowing for the absolute quantum yield of fluorescence) if the calculations are made with the somewhat different equation:

$$\frac{1}{\tau} = 8\pi c n^2 \frac{1000 \cdot 2.3}{N} \int \frac{(2\nu_0 - \nu)^3}{\nu} \varepsilon \, d\nu, \tag{2}$$

where ν_0 is the frequency at the axis of symmetry of the fluorescence and absorption spectra.

Equations (1) and (2) give the "limiting" value of τ for the ideal case of complete absence of quenching, that is, when the fluorescence quantum yield is unity, this value of τ should theoretically be obtained (with absence of quenching which is not associated with change of τ) by dividing the experimentally obtained average value of τ_e by the quantum yield B:

$$\tau_f = \frac{\tau_e}{B}. \tag{3}$$

For the purpose of learning the effect of different substitutes on the average persistence of fluorescence we performed direct measurements on alcohol solutions of a number of mesoderivatives of anthracene on the phase fluorometer of A. M. Bonch-Bruevich, V. A. Molchanov and V. I. Shirokov [3]. We also calculated the "limiting" average value for all of these compounds from Equations (1), (2) and (3).

In the measurement of τ_e the fluorescence was excited by the group of mercury lines at ~365 mμ separated out by a filter. It was established by preliminary experiments that under our conditions for the measurement of τ_e (concentration 10^{-5}–10^{-6} M/l, small thickness of absorbing layer) the effect of reabsorption [4] did not exceed the accuracy of the measurement.

TABLE 1

Absolute Quantum Yield and Mean Fluorescence Persistence of Anthracene Mesoderivatives

Substance	Absolute quantum yield	$\tau_a \cdot 10^9$ sec*	$\tau'_a \cdot 10^9$ sec**	$\tau_e \cdot 10^9$ sec	$\tau_f \cdot 10^9$ sec
Anthracene	0.22***	10.3	15.6	4.5	20.5
9-Methylanthracene	0.29	10.0	15.5	5.2	18.3
9-Ethylanthracene	0.30	9.3	14.4	5.1	17.0
9-n-Propylanthracene	0.31	9.6	14.9	5.5	17.7
9-n-Butylanthracene	0.35	9.9	15.3	5.7	16.3
9-Isobutylanthracene	0.39	9.5	14.7	5.9	15.1
9,10-Dimethylanthracene	0.63	9.5	14.3	11.0	17.5
9-Methyl-10-ethylanthracene	0.53	8.6	13.0	10.1	19.0
10-Di-n-propylanthracene	0.76	8.5	12.5	10.5	13.8
9-Phenylanthracene	0.45	7.4	11.5	5.1	11.3
9-n-Tolylanthracene	0.44	7.6	11.8	5.9	13.4
9-n-Bromophenylanthracene	0.27	7.3	11.5	4.2	15.5
9,10-Diphenylanthracene	0.84	6.2	9.0	6.8	8.1
9,10-Di-o-tolylanthracene	0.57	6.9	10.9	7.6	13.3
9,10-Di-m-tolylanthracene	0.64	5.5	8.7	6.8	10.6
9,10-Di-n-tolylanthracene	0.73	5.9	9.3	6.6	9.0
9,10-Di-n-bromophenylanthracene	0.55	6.2	9.8	6.3	11.5
9-Phenyl-10-α-naphthylanthracene	0.66	6.5	10.5	6.1	9.2
9,10-Di-α-naphthylanthracene	0.49	5.3	8.0	5.2	10.6
9-Chloroanthracene	0.11	9.5	14.6	2.8	25.4
9-Bromoanthracene	0.017	8.9	13.8	1.1	65.0
9,10-Dichloroanthracene	0.48	8.8	13.3	7.2	15.0
9,10-Dibromoanthracene	0.095	8.3	12.5	1.9	20.0
9-Methyl-10-bromoanthracene	0.10	8.1	12.1	2.1	21.0
9-Ethyl-10-bromoanthracene	0.11	8.5	12.8	2.1	19.1
9-n-Propyl-10-bromoanthracene	0.12	7.8	11.8	2.3	19.2
9-Bromo-10-bromomethylanthracene	–	7.6	11.6	1.9	–
9-Phenyl-10-bromoanthracene	0.16	7.4	11.0	2.1	13.1
9-Aminoanthracene	0.29	5.3	17.9	10.0	34.5
9-Monoacetylaminoanthracene	0.44	8.9	14.0	5.5	12.5
9-Diacetylaminoanthracene	0.35	9.0	14.2	5.7	16.3
9-Benzoylaminoanthracene	0	–	–	–	–
9-Nitroanthracene	0	–	–	–	–
9-Methoxyanthracene	0.17	10.4	16.1	3.9	23.0
9,10-Dimethoxyanthracene	0.41	8.4	12.6	9.2	22.4
9-Methyl-10-methoxyanthracene	0.24	9.3	12.9	5.1	21.2
9-Methoxy-10-chloroanthracene	0.05	9.0	12.3	1.0	20.0
9-Methoxy-10-bromoanthracene	0.06	8.7	12.0	2.2	36.8
9-Acetoxyanthracene	0.15	9.8	15.4	3.0	20.0
9,10-Diacetoxyanthracene	0.44	8.5	13.2	9.4	21.4
9-Benzoxyanthracene	small	9.2	14.3	11.7	–
9,10-Dibenzoxyanthracene	0	–	–	–	–
9-Anthracenecarboxylic acid	0.04	8.3	13.0	4.1	102
9-Chloro-10-anthracene-carboxylic acid	0.33	7.7	12.5	6.3	19.0
9-Bromo-10-anthracene-carboxylic acid	0.11	6.7	10.2	3.0	27.2
9-Acetylanthracene	0	–	–	–	–
9-Benzoylanthracene	0	–	–	–	–

---

* τ_a – average duration of excited state calculated from (1).

** τ'_a – average duration of excited state calculated from (2).

*** Absolute quantum yield of anthracene fluorescence in alcohol according to Bowen.

The results are given in Table 1, which shows that the values of τ calculated from (1), τ_a and (2), τ'_a differ very much from each other. The values of τ'_a calculated from (2) for many compounds are in agreement with the values determined from the experimental values τ_e and the fluorescence quantum yields, and are evidently more reliable. Therefore the data obtained from Equation (1) will hereafter not be considered. A comparison of the "limiting" mean fluorescence persistences as calculated from the areas of the long-wave absorption bands of various anthracene mesoderivatives shows that the introduction of various substitutes into anthracene has little effect on the persistence: the values of τ'_a for all of the compounds investigated lies within the narrow limits $8 \cdot 10^{-9}$–$18 \cdot 10^{-9}$ sec. For some substitutions the general rule is observed that the limiting mean fluorescence persistence of doubly substituted anthracene is always shorter than the fluorescence persistence of the corresponding singly substituted forms. The value of τ'_a for the majority of the doubly substituted compounds is $12 \cdot 10^{-9}$–$13 \cdot 10^{-9}$ sec, while for the majority of the singly substituted compounds it is $14 \cdot 10^{-9}$–$16 \cdot 10^{-9}$ sec. Arylated anthracene derivatives are an exception for which τ'_a is shorter, being approximately $11.5 \cdot 10^{-9}$ sec for singly substituted and $8 \cdot 10^{-9}$–$11 \cdot 10^{-9}$ sec for doubly substituted compounds.

An examination of the directly measured mean fluorescence persistence τ_e for anthracene derivatives with the corresponding calculated values of τ'_a shows that its value changes in the same direction as the fluorescence yield; for a number of compounds the changes show complete parallelism (within the limits of accuracy of the determination of these quantities).

Let us compare τ'_a and $\tau_f = \frac{\tau_e}{B}$ for various anthracene derivatives. Table 1 shows that they practically coincide for monoalkyl and dialkyl derivatives, for monoaryl and diaryl derivatives, for monoacetylaminoanthracene and diacetylaminoanthracene, i.e. for those derivatives of anthracene in which substitutions into the nucleus increase the fluorescence yield. For substitutions which decrease the yield the ratio of τ_e to the quantum yield is greater than that calculated for τ'_a. The greatest difference in the values of τ'_a and τ_f is observed for 9-bromoanthracene ($\tau'_a = 13.8$; $\tau_f = 65$) and for 9-anthracene-carboxylic acid ($\tau'_a = 13.0$; $\tau_f = 102$), i.e. for the compounds whose quantum yield is smallest. The introduction of a bromine atom into 9-bromoanthracene or anthracene-carboxylic acid increases the yield and considerably decreases the difference between τ'_a and τ_f.

The introduction of bromine into monoalkylated and monoarylated anthracene decreases both the fluorescence yield and the measured value of τ_e, with the latter decreasing to a lesser extent while τ_f for 9-alkyl-10-bromoanthracene is 1.5-2 times greater than τ'_a.

Thus on the basis of our investigation of the quantum yield and mean fluorescence persistence of anthracene mesoderivatives we are able to conclude that when substitutions are introduced into the anthracene nucleus which lower the fluorescence yield, the quenching does not take place in only one way. In addition to the quenching which decreases the mean persistence there is also quenching during a period which is considerably shorter than the duration of the excited state and thus does not affect τ. The nature of this quenching is not understood.

LITERATURE CITED

[1] T. P. Kravets, Absorption of Dye Solutions (Moscow, 1912); A. Einstein, Physik.Z. 18, 121 (1917); R. Ladenburg, Z. Physik 4, 451 (1921).

[2] T. Forster, Fluoreszenz organischer Verbindungen (Göttingen, 1951), p. 158.

[3] A. M. Bonch-Bruevich, V. A. Molchanova and V. I. Shirokov, Bull. Acad. Sci. USSR, Phys. Ser. 20, 5 (1956).

[4] M. D. Galanin, Trans. Phys. Inst., Acad. Sci. USSR 5, 341 (1950); A. Schmillen, Z. Physik 135, 294 (1953).

Received January 13, 1956

AN EXPERIMENTAL VERIFICATION THAT THE VELOCITY OF LIGHT IS INDEPENDENT OF THE VELOCITY OF THE SOURCE WITH RESPECT TO AN OBSERVER

A. M. Bonch-Bruevich

(Presented by Academician A. A. Lebedev February 15, 1956)

1. The hypothesis that the velocity of light in free space is independent of the motion of the source of radiation with respect to an observer is in agreement with the concept of light propagation in a motionless ether, and its coordination with the principle of relativity of motion is the nucleus of Einstein's special theory of relativity. The alternative assumption – that the velocity of light is the vector sum of the velocity of the source with respect to the observer and the velocity of light from a fixed source was the basis of the ballistic theory ([1-4] and others).

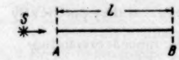

Fig. 1. Scheme of the experiment. S is the moving source of light.

Comstock was the first to point out that any dependence of the velocity of light on the motion of the source must be revealed directly in certain motions of double stars [5]. Examining this question quantitatively de Sitter concluded that the velocity of light is independent of the motion of the source [6]. This paper resulted in a lively controversy [7-9], which was renewed more than ten years later [10-13]. Finally, in 1953, it was shown that with an assumed metric for astronomical space (which, moreover, requires basic justification) observations of double stars will not lead to a definite result [14]. It can be assumed that the formulation of a trustworthy direct experiment to show that the velocity of light is independent of the motion of the source is meaningful because of the fundamental importance of this hypothesis.

This is all the more desirable because until the present, attempts have been made to circumvent the theory of relativity, even where its applicability is obvious. Thus Ives, who in 1938 succeeded in observing the transverse Doppler effect predicted by Einstein, attempts to treat this effect on the basis of pre-Einsteinian concepts [15].

2. The scheme of our direct experiment, which was suggested by S. I. Vavilov, is clear from Fig. 1. The experiment is a comparison of the time required by light to traverse a fixed distance L for two different values of the velocity of the source. The performance of such an experiment, despite all its apparent simplicity, encounters such great difficulties that until the present it has not been attempted.

In order to measure the difference in the transit time of light along the base line L for two different velocities of the source, we used a phase method of measuring small time intervals. Before being sent along the base line the light was modulated in intensity with the frequency F = 12 Mc by a diffractive modulator with standing ultrasonic waves in a liquid (Fig. 2,A). Originally a modulator with one radiator [16] was used, but later a modulator, designed by Iu. V. Popov, with two emitters of ultrasonic vibrations was used [17]. The modulation phase at the point B (Fig. 1) lags behind the modulation phase of the light, leaving the modulator by a quantity which is proportional to the time required to send a signal along L. Therefore the change of velocity of the source of radiation in the direction AB by the amount $\underline{v}$ results, according to the ballistic theory, in a shift of the modulation phase at the point B by the quantity

$$\Delta\varphi_b = \frac{2\pi L}{\lambda}\left(\frac{v}{c}\right), \qquad (1)$$

where λ is the light-modulating wavelength. From relativistic theory

$$\Delta\varphi_r = 0. \tag{2}$$

As has been pointed out by G. S. Landsberg, the edges of the sun can serve as moving light sources. The equatorial velocity of rotation of the sun is well known from observations of the Doppler shift of spectral lines and has the value 1.95 ± 0.01 km/sec [18]. Having estimated the accuracy of the projection of an image of the sun's edge on the entrance slit of our modulator, we concluded that the consistent use in our experiment of light from the right and left equatorial edges of the sun is equivalent to a change of velocity of the source of not less than 3.5 km/sec.

L was given a length of 2000 m (the apparatus was set up on the grounds of the Main Astronomical Observatory of the Academy of Sciences of the U.S.S.R. at Pulkova). Thus, as follows from (1), $\Delta\varphi_b = 25'$, which corresponds to a difference in the time for traversal of the base line by light from the two different equatorial edges of the sun given by $\Delta t_b = 75 \cdot 10^{-12}$ sec.

In order to detect such small phase shifts we used the phase-measuring portion of a high resolution fluorometer [19,20]. In the phasemeter steps were taken to eliminate the specific errors of phase measurements, the causes of which were revealed by a preliminary special study [21]. To one of the leads of the phasemeter a potential was applied which was taken from the load of the photomultiplier whose photocathode received light traversing the base line (Fig. 2,B). The reference signal was the second harmonic of the potential supplied to the optical modulator.

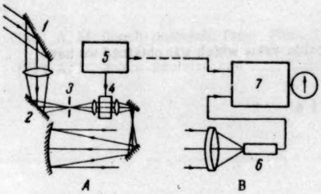

Fig. 2. Scheme of the apparatus at the beginning and end of the base line.
1 and 2) Mirrors of the coelostat; 3) entrance slit of the modulator; 4) vessel with standing ultrasonic waves; 5) generator which feeds ultrasonic emitter; 6) photomultiplier; 7) phasemeter.

Mirrors were used in the experimental apparatus (a mirror in the coelostat and a revolving mirror on the base). The use of these in our experiment requires special justification since the adherents of the ballistic theories maintained that when light from a moving source is reflected, its velocity can change [1-4]. Such justification comes from an analysis of Tolman's interference experiment involving the sun [3,4] and of the observations of the rotational velocity of the sun obtained with a spectrograph, diffraction grating and coelostat with mirror.

3. The measurements were observations of the difference in instrumental readings at the output of the phasemeter when light was directed along the base line from the two different equatorial edges of the sun, for which purpose the position of the coelostat mirror was changed. The orientation of the solar equator for a given time of the day was established by preliminary observations.

It was found that the passage of light along the 2000 m line is accompanied by considerable random fluctuation of the reading by the output instrument when the position of the coelostat mirror is unchanged. These are presumably associated with thermal inhomogeneities in the atmosphere, as well as with oscillations of the mirrors and differences in the phase modulation at different points in the cross section of the light beam [16]. Therefore, in order to obtain a definitive result more than 1700 measurements of phase differences were made involving the two sides of the sun. In order to avoid systematic errors we measured alternately the values of $\Delta\varphi$ going from left to right and vice versa. Fig. 3 illustrates the distribution of the number of readings obtained from deviations at the phasemeter output (readings which corresponded to the transition from the left to the right side of the sun were taken with reversed sign).

A statistical treatment of the measurements gives for the most probable value of the measured quantity:

$$\Delta\varphi_0 = \frac{\Sigma n\Delta\varphi}{\Sigma n} = 0.37',$$

which corresponds to the most probable difference in transit time of light along the base line $\Delta t_0 = 1.4 \cdot 10^{-12}$ sec.

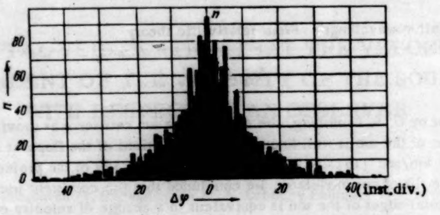

Fig. 3. Distribution of readings n from observed deviations $\Delta\varphi$ of the phasemeter output going from the right to the left end of the solar equator. Instrumental division 4.4'.

For the root mean square difference $\Delta\varphi$ from the most probable value which was obtained we have

$$\sigma_{\Delta\varphi_0} = \frac{1}{\sqrt{\Sigma n}} \sqrt{\frac{\Sigma n \Delta\varphi^2}{\Sigma n}} = 1.4'$$

and, correspondingly, $\sigma_{\Delta t_0} = 5.1 \cdot 10^{-12}$ sec.

It is easily seen that the value found satisfies the hypothesis of relativistic theory, while the result predicted by ballistic theory lies far outside the limits of experimental error. Thus we have for the first time (to our knowledge) performed a direct experiment to compare the velocity of light from sources moving with different velocities with respect to an observer, and this is a direct confirmation of the second postulate of the special theory of relativity.

A great deal of the work of the experiment was performed by V. I. Shirokov and V. A. Molchanov, to whom I am very grateful. I also take this opportunity to thank A. A. Mikhailov, Corresponding Member of the Academy of Sciences of the U.S.S.R., Professor V. A. Krat and Professor O. A. Mel'nikov for their collaboration in setting up the experiment on the grounds of the Main Astronomical Observatory of the Academy of Sciences of the U.S.S.R., and Iu. V. Popov for information regarding an optical modulator which he had constructed.

LITERATURE CITED

[1] W. Ritz, Ann. chim. et phys. 13, 145 (1908).

[2] J. Thomson, Phil. Mag. 19, 301 (1910).

[3] O. Stewart, Phys. Rev. 32, 418 (1911).

[4] C. Tolman, Phys. Rev. 35, 136 (1912).

[5] D. Comstock, Phys. Rev. 80, 267 (1910).

[6] W. de Sitter, Physik. Z. 14, 429,1267 (1913).

[7] P. Gutnik, Astr. Nachr. 195, 4670 (1913).

[8] E. Freundlich, Physik. Z. 14, 835 (1913).

[9] W. Zurhellen, Astr. Nachr. 198, 1 (1914).

[10] W. de Sitter, Bull. Astr. Inst. Netherlands 2, 121, 163 (1924).

[11] M. La Rosa, Z. Physik 21, 333 (1924); 34, 698 (1925).

[12] W. Bernheimer, Z. Physik 36, 302 (1926).

[13] H. Thirring, Z. Physik 31, 133 (1925).

[14] P. Moon and D. Spenser, J. Opt. Soc. Amer. 43, 635 (1953).

[15] H. Ives and G. Stilwell, J. Opt. Soc. Amer. 28, 215 (1938).

[16] A. M. Bonch-Bruevich and V. A. Molchanov, J. Tech. Phys. (USSR) 25, 1653 (1955).

[17] Iu. M. Popov, Abstract of Dissertation, Exact Measurement of Distances by the Velocity of Light Propagation, State Optical Inst., Leningrad (1955).

[18] A. A. Belopol'skii, Bull. Comm. for Solar Study, 1934, No. 9, 5.

[19] A. M. Bonch-Bruevich, V. I. Shirokov and V. A. Molchanov, Bull. Acad. Sci. USSR, Phys. Ser. 20, 5 (1956).

[20] A. M. Bonch-Bruevich, Progr. Phys. Sci. (USSR) 1956, No. 1.

[21] A. M. Bonch-Bruevich and V. I. Shirokov, J. Tech. Phys. (USSR) 25, 1825 (1955).

Received February 8, 1956

THE DISTORTION OF ULTRASONIC WAVES OF FINITE AMPLITUDE IN LIQUIDS

L. K. Zarembo, V. A. Krasil'nikov and V. V. Shklovskaia-Kordi

(Presented by Academician M. A. Leontovich March 2, 1956)

1. Some nonlinear effects in liquids, such as cavitation, sound streaming and radiation pressure, have been well studied. A few articles have appeared recently on certain new nonlinear acoustic-effects in liquids. G. D. Mikhailov [1] "mixed" two ultrasonic waves and observed sum and difference frequencies. Fox and Wallace [2] suggested the possibility of explaining the increased absorption observed for higher ultrasonic intensities by nonlinearity of the equation of motion and of the relation between density and pressure in a wave of finite amplitude, and by the associated harmonics. A. G. Gorelik and V. A. Zverev [3] observed the amplitude and phase modulation of ultrasound by sound in water.

Since the appearance of harmonics determines to some extent the higher absorption coefficient of a wave of finite amplitude in a liquid and, so far as we knew, harmonics had not been observed in liquids, we became interested in observing them directly. The present paper concerns the experimental study of the behavior of harmonics in a finite-amplitude wave propagated in a liquid.

2. The amplitudes of the second and third harmonic were measured in tap water and the amplitude of the second harmonic was also measured in transformer oil.* The second harmonic was also observed qualitatively in methyl alcohol and glycerin. The liquids were contained in a plexiglas tank measuring 68 × 10 × 11 cm with a 5 cm layer of glass wool at its end; the side walls and bottom of the tank were covered with sheets of white vacuum rubber. The radiator was a round quartz plate with an air cushion on its inactive side; the diameter of the plate was 2.5 cm; the diameter of the silver coating produced through vacuum evaporation was 2.3 cm. The quartz was coupled inductively with the output of an oscillator whose high frequency output is 350 w. The plate was excited by a fundamental frequency of 1.5 Mc. The oscillator frequency was stabilized by a quartz stabilizer in the driver stage. The ultrasonic receivers of the fundamental and harmonic frequencies were resonant quartz plates for 1.5, 3.0 and 4.5 Mc with a 3.7 cm silvered diameter. The voltage from the receivers was amplified by resonance amplifiers. The pass bands of the amplifiers were not wider than ± 50 kc; the amplification factors were: 20 at 1.5 Mc; 50 at 3.0 Mc; and 100 at 4.5 Mc; linear amplification was used in the measurements. The amplifier output voltage was applied to a cathode-ray oscilloscope and voltmeter.

The quartz plates whose fundamental frequencies were equal to the harmonic frequencies were "opaque" to the fundamental frequency, and standing waves were formed. The reflection of the fundamental wave by the receiver and radiator makes it impossible to determine the dependence of a harmonic amplitude on the path traversed by the wave.

Two methods were used to eliminate the standing waves. a) Between the radiator and receiver an acoustical filter was placed which was partially "transparent" to the measured frequency and which reflected other frequencies at some angle. For this purpose a 9 × 9 cm copper plate of 0.45 mm thickness was used, which was placed in the ultrasonic beam at the angle of maximum observed "transparency" of pressure for the measured harmonic. This system, consisting of an acoustical filter, a resonant receiver and a resonant amplifier, constituted a spectral analyzer for fixed lines of the "acoustic spectrum". The radiator and receiver were kept at fixed positions and the filter was moved. The amplitudes of harmonics at the filter were calculated from the receiver readings. In this conversion the absorption coefficient for a small-amplitude wave was used since the

---

* It is also possible to measure higher harmonics.

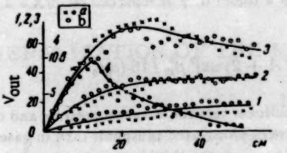

Fig. 1. Acoustic pressure amplitude of the second harmonic as a function of distance from the radiator. 1-3) In water: 1) V = 500 v/(I_{10} = 0.5 w/cm², p_{10} = = 1.25 atmos); 2) V = 1 kv (I_{10} = 2 w/cm², p_{10} = 2.45 atmos); 3) V = 2 kv (I_{10} = 7.8 w/cm², p_{10} = 4.9 atmos); 4) in transformer oil, V = 2 kv (I_{10} = 7.8 w/cm², p_{10} ≃ ≃ 4.9 atmos). a) measured with a filter; b) measured with the receiver covered with rubber.

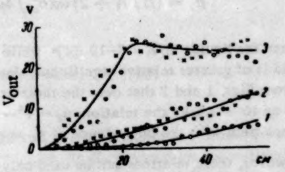

Fig. 2. Acoustic pressure amplitude of the third harmonic in water as function of distance from the radiator.
1) V = 500 v; 2) V = 1 kv; 3) V = 2 kv.

maximum intensity of the harmonics beyond the filter did not exceed a few tenths w/cm². b) In the second method the receiver was covered with a sheet of white vacuum rubber. Although this lowered the sensitivity of the receiver it also greatly attenuated the reflected wave. The results from the two methods were in good agreement.

It should be noted that during the measurements special attention was paid to keeping the receiver strictly parallel to the ultrasonic wave front. In addition, in water the amplitude of the received signal was considerably affected by air bubbles which appeared on the surfaces of the receiver, filter and radiator and on the side walls of the tank. During the measurements the bubbles were removed regularly.

The amplitude of the second harmonic, at different voltages V on the quartz, as a function of distance from the radiator in water and transformer oil is shown in Fig. 1. Fig. 2 gives the third harmonic as a function of distance in water. The vertical axis in Figs. 1 and 2 gives the cathode-ray voltmeter readings, which are proportional to the acoustical pressure. The relative error of these measurements did not exceed ± 5% with ~1 kv applied to the quartz and ± 10% for higher voltages.

Absolute measurements of harmonic intensities were made in water by a radiometer with 2 kv applied to the quartz (the intensity near the quartz was I_{10} = 7.8 w/cm²) and using the copper filter. The harmonic intensities were: at 40 cm from the radiator I_1 = 3 w/cm², I_2 = 0.33 w/cm², I_3 = 0.19 w/cm²; at 20 cm I_1 = 5 w/cm², I_2 = 0.30 w/cm², I_3 = 0.19 w/cm². These measurements took into consideration the incomplete "transparency" of the filter to the measured harmonic as well as a certain amount of passage of the fundamental frequency and of other harmonics through the filter. The relative error of the absolute measurements was ±20%.

In methyl alcohol and glycerin the second harmonic was observed only qualitatively since the amplitude of the received signal changed irregularly, especially with ~ 1 kv and higher voltages on the quartz. The cause of this effect is not known.

3. Harmonics can appear in a liquid either because of a nonlinear equation of motion or because of a nonlinear relation between pressure and density in an adiabatic process. If we follow [2] in comparing the equation of a gas adiabatic curve:

$$p = p_0(\rho/\rho_0)^\gamma \simeq p_0 + p_0\gamma(\rho - \rho_0)/\rho_0 + \gamma(\gamma - 1)\,p_0(\rho - \rho_0)^2/2\rho_0^2$$

with the equation for a liquid:

$$p = p_0 + A(\rho - \rho_0)/\rho_0 + B(\rho - \rho_0)^2/2\rho_0^2,$$

we reach the conclusion that the solution of the nonlinear equations for a gas in the case of a finite-amplitude plane wave propagated without losses in the medium can be used for a liquid if γ is replaced by $B/A + 1$. Then the amplitudes of the second and third harmonics will be:

$$p_2 = (B/A + 2)\,\omega x p_{10}^2 / 4\rho_0 c_0^3; \qquad p_3 = 3\,[(B/A + 2)\,\omega x]^2\, p_{10}^3 / 16\,(\rho_0 c_0^3)^2.$$

Since for liquids $B/A = 6-10$ [4]• while $\gamma = 1.3-1.6$ the nonlinear relation between pressure and density in a liquid is of greater relative significance for the distortion of a wave propagated in liquids than in gases. It follows from Figs. 1 and 2 that near the radiator the second harmonic is $\sim x$; the third harmonic is $\sim x^2$; for $x = \text{const}$ up to ~ 1.5 kv the relation $p_2 \sim V^2 \sim p_{10}^2$ is well satisfied for the second harmonic, which is in qualitative agreement with the dependence of p_2 on p_{10}.

However, these relations can be used only at short distances from the radiator, where energy losses through absorption can be neglected. In a dissipative medium, as was shown in [5,2] it is possible to stabilize the harmonics if absorption is compensated by increased energy of the harmonics at the expense of the fundamental wave. At distances which are close to the experimentally established stabilizing distance the above relations give highly excessive values of the harmonic pressure amplitudes. Certain qualitative relations for a dissipative medium can be obtained by introducing absorption into the solutions of equations for a nondissipative medium as in [6]. The stabilization distance of the nth harmonic, x_n', is determined from the condition $dp_n/dx\,|_{x=x_n'} = 0$. The stabilization distance of the second harmonic which is obtained in this manner is $x_2' = {}^1\!/_6\,\alpha_1$, where α_1 is the absorption coefficient (for pressure) for a small-amplitude fundamental frequency (assuming that the absorption coefficient of the second harmonic is given by $\alpha_2 = 4\alpha_1$). From this relation it follows that: 1) at higher fundamental frequencies the stabilization distance is smaller; 2) in more viscous liquids the stabilization distance is smaller, as is confirmed qualitatively by the comparison of measurements in transformer oil and in water; 3) the stabilization distance is independent of intensity. However, the values of the stabilization distance in water which were obtained from $x_2' = {}^1\!/_6\,\alpha_1$, using $\alpha_1 = 23 \cdot 10^{-17}\,\nu^2$, exceed the experimental values by one order of magnitude; this is related to the hypothesis that energy losses of the fundamental wave are only dissipative. In obtaining the function $p_2 = p_2(x)$ [6], energy losses of the fundamental wave for the production of harmonics were not taken into consideration. When the experimental absorption coefficient in water is used for the determination of the stabilization distance, the relation given for x_2' can result in values which agree with experiment in order of magnitude.

We note in conclusion that the distortion of a sound wave and the associated production of harmonics is well known for gases. It is widely believed that for liquids at moderate ultrasonic intensities these distortions must be extremely small because of the high internal pressure of liquids. However, as the above measurements show, the amplitudes of ultrasonic harmonics with moderate intensity are of very considerable magnitude; this can be explained by the small damping of ultrasonic waves in liquids compared with gases and the resultant "accumulation" of distortions from nonlinear effects in the course of propagation of the wave.

LITERATURE CITED

[1] G. D. Mikhailov, Doklady Akad. Nauk SSSR 89, 4, 663 (1953).

[2] F. E. Fox and W. A. Wallace, J. Acoust. Soc. Amer. 26, 6, 994 (1954).

[3] A. G. Gorelik and V. A. Zverev, Acoust. J. (USSR) 1, 4, 339 (1955).

[4] M. Kornfel'd, Elasticity and Strength of Liquids (1951).

[5] R. D. Fay, J. Acoust. Soc. Amer. 3, 2, 222 (1931).

[6] A. L. Thuras, R. T. Jenkins and H. T. O'Neill, Bell System Tech. J. 14, 1, 159 (1935).

Anisotropic Structures Laboratory,
Academy of Sciences, U.S.S.R.

Received February 28, 1956

• It should be noted that these are isothermal values of B/A.

GENERALIZATION OF THE METHOD OF SUPPLEMENTARY VARIABLES

D. N. Zubarev

(Presented by Academician N. N. Bogoliubov January 17, 1956)

For the purpose of describing the interacting electrons of a plasma it is convenient to introduce collective variables – the Fourier components of the particle density operator [1,2]. In these variables the collective portion of the particle motions can be described, i.e. the plasma oscillations. The existence of collective motion is characteristic not only of a plasma but of Fermi and Bose gases in general [3-6]. A considerable number of papers have recently appeared on the collective model of the nucleus [7-11] in which an attempt was made to construct a nuclear model which would be a natural generalization of the Bohr liquid drop model and the nuclear shell model. It is easily seen that the problems involved in the development of a collective nuclear model are closely related to collective-variable methods. Indeed, the nucleus possesses, on the one hand, intrinsic collective motions, which are revealed in the liquid drop model, and on the other hand, individual nucleonic motions, which are described by the nuclear shell model. Consequently, there arises the problem of distinguishing the collective motions [10,11]. In the present paper we shall show that the method of supplementary variables [4] can be generalized in such a way that it is applicable not only to nonideal Fermi and Bose gases but also the collective model of the nucleus.

Let a quantum mechanical system of N fermions be described by the N coordinates $\mathbf{r}_1, \ldots, \mathbf{r}_N$ of the particles. We shall attempt to distinguish collective motions of this system of as general a nature as possible. We note, first of all, that the particle density operator is of the form

$$\rho(\mathbf{r}) = \sum_{1<j<N} \delta(\mathbf{r} - \mathbf{r}_j). \tag{1}$$

The Fourier coefficients of $\rho(\mathbf{r})$ in a complete system of orthogonal functions $\varphi_\lambda(\mathbf{r})$ will be

$$\rho_\lambda = \sum_{1<j<N} \varphi_\lambda(\mathbf{r}_j) \quad (\lambda < \lambda_0), \tag{2}$$

where the ρ_λ are symmetrical functions of the particle coordinates. The quantities ρ_λ can be considered to be supplementary variables which describe the collective motions of the system.

Let us assume that ρ_0 = const and that $\lambda \neq 0$. We note, in addition that we shall consider ρ_λ only for $\lambda < \lambda_0$, where λ_0 is a limiting value of λ. This is associated with the fact that a collective motion cannot have a too short wavelength: for example, less than the distance between particles. The system of $\varphi_\lambda(\mathbf{r})$ is determined by the character of the system under consideration. For example, for a gas in a large volume it is convenient to choose for the φ_λ the plane waves $\varphi_\lambda(\mathbf{r}) \rightarrow \frac{1}{\sqrt{N}} e^{-i(\mathbf{kr})}$. Therefore in [2,4] the collective variables were given by

$$\rho_{\mathbf{k}} = \frac{1}{\sqrt{N}} \sum_{1<j<N} e^{-i(\mathbf{kr}_j)}, \quad k < k_0 \quad (k \neq 0). \tag{3}$$

We shall assume that the wave function of the system depends on the variables $\mathbf{r}_j$ not only explicitly but also implicitly through the ρ_λ : $\psi = \psi(\mathbf{r}_1 \ldots \mathbf{r}_N \,|\, \ldots \rho_\lambda \ldots)$. Thus the number of variables is greater than the number of particles, although this does not introduce serious complication; the relation of ρ_λ to the particle coordinates is a supplementary condition which can be taken into consideration in the calculation of mean values.

We shall write the Hamiltonian of the system as

$$H = \sum_j \frac{-\hbar^2 \nabla_j^2}{2m} + \frac{1}{2} \sum_{j_1 \neq j_2} \Phi(\,|\,\mathbf{r}_{j_1} - \mathbf{r}_{j_2}\,|\,) \tag{4}$$

in this representation, which we shall designate as the $(\mathbf{r}, \rho_\lambda)$ representation. For this purpose it is necessary to remember that the differential equation for ψ depends both explicitly and implicitly on the coordinates $\mathbf{r}_j$ and that the interaction energy must be expressed in terms of the variables ρ_λ.

We shall express the potential energy of particle interactions

$$U = \frac{1}{2} \sum_{j_1 \neq j_2} \Phi(\,|\,\mathbf{r}_{j_1} - \mathbf{r}_{j_2}\,|\,) \tag{5}$$

in terms of the variables ρ_λ. For this purpose we expand $\Phi(\,|\mathbf{r}_{j_1} - \mathbf{r}_{j_2}|\,)$ in a series of $\varphi_\lambda(\mathbf{r}_{j_1})\,\varphi_{\lambda'}(\mathbf{r}_{j_2})$:

$$U = \frac{1}{2} \sum_{\lambda, \lambda', j_1, j_2} c_{\lambda\lambda'} \varphi_\lambda(\mathbf{r}_{j_1})\, \varphi_{\lambda'}(\mathbf{r}_{j_2}) - \frac{N\Phi(0)}{2}. \tag{6}$$

By using (2) we finally obtain:

$$\begin{aligned} U = {} & \frac{1}{2} \sum_{\lambda, \lambda' < \lambda_0} c_{\lambda\lambda'} \rho_\lambda \rho_{\lambda'} + N\varphi_0 \sum_{\lambda < \lambda_0} c_{\lambda_0} \rho_\lambda + \sum_{\lambda < \lambda_0,\, \lambda' > \lambda_0,\, j} c_{\lambda'\lambda} \varphi_{\lambda'}(\mathbf{r}_j)\, \rho_\lambda + \\ & + \frac{1}{2} \sum_{\lambda, \lambda' > \lambda_0,\, j_1,\, j_2} c_{\lambda\lambda'} \varphi_\lambda(\mathbf{r}_{j_1})\, \varphi_{\lambda'}(\mathbf{r}_{j_2}) + N\varphi_0 \sum_{\lambda > \lambda_0,\, j} c_{\lambda_0} \varphi_\lambda(\mathbf{r}_j) + \frac{N^2}{2} c_{00} \varphi_0^2 - \frac{N\Phi(0)}{2}. \end{aligned} \tag{7}$$

Thus the interaction energy is a quadratic form in the variables ρ_λ. This occurs not only for the special choice (3) of the supplementary variables, as was shown in [2,4], but also in the general case for variables of the type in (2).

For the Hamiltonian of the system in the $(\mathbf{r}, \rho_\lambda)$ representation by using (7) we obtain

$$H = E_0 + H_F + H_B + H_{FB}, \tag{8}$$

where

$$E_0 = \frac{N^2}{2} c_{00} \varphi_0^2 - \frac{N\Phi(0)}{2}; \tag{8a}$$

$$H_F = \sum_j - \frac{\hbar^2 \nabla_j'^2}{2m} + N\varphi_0 \sum_{\lambda > \lambda_0,\, j} c_{\lambda 0} \varphi_\lambda(\mathbf{r}_j) + \frac{1}{2} \sum_{\lambda, \lambda' > \lambda_0,\, j_1,\, j_2} c_{\lambda\lambda'} \varphi_\lambda(\mathbf{r}_{j_1})\, \varphi_{\lambda'}(\mathbf{r}_{j_2}); \tag{8b}$$

$$H_B = \sum_{\lambda<\lambda_0} \left\{ -\frac{\hbar^2}{2m} \left[A_\lambda^0 N \varphi_0 + \sum_{\mu<\lambda_0} A_\lambda^\mu \rho_\mu \right] \frac{\partial}{\partial \rho_\lambda} + c_{\lambda 0} N \varphi_0 \rho_\lambda \right\} +$$
$$+ \sum_{\lambda,\, \lambda'<\lambda_0} \left\{ -\frac{\hbar^2}{2m} \left[B_{\lambda\lambda'}^2 N \varphi_0 + \sum_{\mu<\lambda_0} B_{\lambda\lambda'}^\mu \rho_\mu \right] \frac{\partial^2}{\partial \rho_\lambda \partial \rho_{\lambda'}} + \frac{1}{2} c_{\lambda\lambda'} \rho_\lambda \rho_{\lambda'} \right\}; \tag{8c}$$

$$H_{FB} = -\sum_{j,\, \lambda<\lambda_0} \frac{\hbar^2}{m} \left\{ \left(\nabla_j \varphi_\lambda (\mathbf{r}_j) \nabla'_j \right) + \frac{1}{2} \sum_{\mu>\lambda_0} A_\lambda^\mu \varphi_\mu (\mathbf{r}_j) \right\} \frac{\partial}{\partial \rho_\lambda} +$$
$$+ \sum_{\lambda<\lambda_0,\, \lambda'>\lambda_0,\, j} c_{\lambda'\lambda} \varphi_{\lambda'} (\mathbf{r}_j) \rho_\lambda - \sum_{\lambda,\, \lambda'<\lambda_0,\, \mu>\lambda_0,\, j} \frac{\hbar^2}{2m} B_{\lambda\lambda'}^\mu \varphi_\mu (\mathbf{r}_j) \frac{\partial^2}{\partial \rho_\lambda \partial \rho_{\lambda'}}, \tag{8d}$$

where A_λ^0 and $B_{\lambda\lambda'}^\mu$ are the coefficients of the expansion:

$$\nabla^2 \varphi_\lambda = A_\lambda^0 \varphi_0 + \sum_{\mu \neq 0} A_\lambda^\mu \varphi_\mu, \quad (\nabla \varphi_\lambda \nabla \varphi_{\lambda'}) = B_{\lambda\lambda'}^0 \varphi_0 + \sum_{\mu \neq 0} B_{\lambda\lambda'}^\mu \varphi_\mu. \tag{9}$$

The individual terms of the Hamiltonian (8) have the following meaning: E_0 is a constant in the lowest energy state; H_F is the Hamiltonian of the individual degrees of freedom, – its second term means an external field and its third term is the short-range portion of the interaction energy; H_B is the Hamiltonian of the collective degrees of freedom; H_{FB} is the operator for interactions between the collective and individual degrees of freedom. We have thus shown that in the Hamiltonian of interacting particles it is possible to separate the part that depends only on the variables ρ_λ and which is thus the Hamiltonian of the collective degrees of freedom; this was done for specially selected supplementary variables in [2,4].

The Hamiltonian in (8) is not the only possible form. We can replace ρ_λ in the individual terms of the Hamiltonian by its expression in terms of the particle coordinates (2) and thus obtain another equivalent representation of the Hamiltonian in supplementary variables.

For example, the operator

$$\sum_{\lambda,\, \mu<\lambda_0} \frac{-\hbar^2}{2m} A_\lambda^\mu \rho_\mu \frac{\partial}{\partial \rho_\lambda} = \sum_{\lambda,\, \mu<\lambda_0,\, j} -\frac{\hbar^2}{2m} A_\lambda^\mu \varphi_\mu (\mathbf{r}_j) \frac{\partial}{\partial \rho_\lambda},$$

in H_B can be applied to a term of H_{FB}. Then H_B and H_{FB} become

$$H_B = \sum_{\lambda<\lambda_0} \left\{ -\frac{\hbar^2}{2m} A_\lambda^0 N \varphi_0 \frac{\partial}{\partial \rho_\lambda} + c_{\lambda 0} N \varphi_0 \rho_\lambda \right\} +$$
$$+ \sum \left\{ -\frac{\hbar^2}{2m} \left[B_{\lambda\lambda'}^0 N \varphi_0 + \sum_{\mu<\lambda_0} B_{\lambda\lambda'}^\mu \rho_\mu \right] \frac{\partial^2}{\partial \rho_\lambda \partial \rho_{\lambda'}} + \frac{1}{2} c_{\lambda\lambda'} \rho_\lambda \rho_{\lambda'} \right\}; \tag{10}$$

$$H_{FB} = -\sum_{\lambda<\lambda_0,\, j} \frac{\hbar^2}{m} \left\{ (\nabla_j \varphi_\lambda (\mathbf{r}_j) \nabla'_j) + \frac{1}{2} \sum_{\mu \neq 0} A_\lambda^\mu \varphi_\mu (\mathbf{r}_j) \right\} \frac{\partial}{\partial \rho_\lambda} +$$
$$+ \sum_{\lambda<\lambda_0,\, \lambda'>\lambda_0,\, j} c_{\lambda'\lambda} \varphi_{\lambda'} (\mathbf{r}_j) \rho_\lambda - \sum_{\lambda,\, \lambda'<\lambda_0,\, \mu>\lambda_0,\, j} \frac{\hbar^2}{2m} B_{\lambda\lambda'}^\mu \varphi_\mu (\mathbf{r}_j) \frac{\partial^2}{\partial \rho_\lambda \partial \rho_{\lambda'}}. \tag{11}$$

The form of the Hamiltonian (14) for the variables (3) corresponds to the author's results in [4], while the form of (11) and (12) corresponds to those of Bohm and Pines [2]. The representation in (9) possesses the advantage that a large number of its terms are expressed in the supplementary variables, so that dispersion in the plasma is obtained even in the zeroth approximation, but (10) and (11) are somewhat simpler – for example, in the variables (3) the quadratic part of H_B is diagonal.

The operator H_B can be diagonalized. Thus it is possible in the Hamiltonian of the interacting particles to separate the elementary Bose type of interactions which represent the collective motions.

The above discussed method of separating the collective motions is of interest in connection with the collective nuclear model [7-10]. The surface vibrations of the nucleus in the incompressible liquid drop model can be described, as was shown by Bohr and Mottelson [8] by the collective variables:

$$\alpha_{lm} = \frac{4\pi}{3A} \sum_{1<j<N} \left(\frac{r_j}{R_0}\right)^l Y^*_{lm}(\vartheta_j \varphi_j), \tag{12}$$

where $Y_{\ell m}$ is a spherical harmonic, A is the atomic weight and R_0 is the nuclear radius. If we also allow for compressibility of the nucleus, which results in three-dimensional vibrations, it is necessary to use a more general type of collective variables:

$$\alpha_{klm} = \sum_{1<j<N} f_{kl}(\mathbf{r}_j)\, Y^*_{lm}(\vartheta_j \varphi_j), \tag{13}$$

where the quantum number $\underline{k}$ characterizes the spatial vibrations of the nucleus. The collective variables (13) can be derived by the general method which has been discussed in this article.

In conclusion I take this opportunity to thank Academician N. N. Bogoliubov for discussions and for a number of valuable comments.

LITERATURE CITED

[1] D. Bohm and D. Pines, Phys. Rev. 82, 625 (1951).

[2] D. Bohm and D. Pines, Phys. Rev. 92, 609 (1953).

[3] S. Tomonaga, Progr. Theoret. Phys. (Japan) 5, 544 (1950).

[4] D. N. Zubarev, J. Exptl.-Theoret. Phys. (USSR) 25, 548 (1953).

[5] N. N. Bogoliubov and D. N. Zubarev, J. Exptl.-Theoret. Phys. (USSR) 28, 129 (1955). [Soviet Physics – JETP, p. 83].

[6] R. P. Feynman, Phys. Rev. 94, 262 (1954).

[7] A. Bohr, Kgl. Danske Videnskab. Selskab Mat.-fys. Medd. 26, 14 (1952).

[8] A. Bohr and B. Mottelson, Kgl. Danske Videnskab. Selskab Mat.-fys. Medd. 27, 16 (1953).

[9] G. Süssmann, Z. Physik 139, 543 (1954).

[10] T. Marumory and J. Yukawa, Tanaka, Progr. Theoret. Phys. (Japan) 13, 442, 557 (1955).

[11] S. Tomonaga, Progr. Theoret. Phys. (Japan), 13, 467 (1955).

V. A. Steklov Mathematical Institute,
Academy of Sciences, U. S. S. R.

Received January 15, 1956

THE ELASTIC PROPERTIES OF β-QUARTZ AT HIGH TEMPERATURES

V. G. Zubov and M. M. Firsova

(Presented by Academician I. K. Kikoin February 22, 1956)

1. The values and the temperature dependence of the adiabatic elastic constants of quartz above the α-β transition have not been studied in detail. Osterberg and Cookson [1] determined C_{44} at 600° and Atanasoff and Kammer [2] have given values of all the constants at the same temperature as well as the change of C_{44} between 575 and 630°. The values of C_{44} obtained from these two sources are not in agreement.

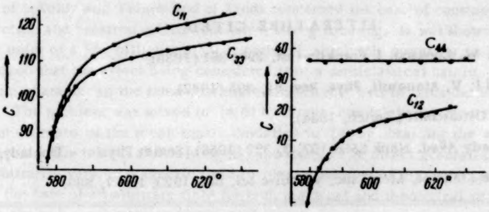

Fig. 1.

The present paper gives the temperature dependence of the adiabatic elastic constants of β-quartz which were measured by the Bergmann-Schaefer method [3] over the range 578-635°.

2. The measurements were made with the apparatus described in [4]. The good uniformity of the furnace temperature field enabled us to take 20 x 20 x 20 mm cubic quartz samples through the phase transition point. Each sample went through the phase transition several times in both directions while fully retaining its elastic properties.

The shadow method was used to observe the phase transition. All stages of the creation of new phase nuclei were photographed as well as movement of the phase interface in the samples.

The piezoelectrical activity of the quartz after the phase transition was so high that we were able to obtain complete diffraction patterns along the three principal crystal axes.

The appreciable simplification of the calculational equations which resulted from the increased symmetry of the quartz following the transition and the completeness of the diffraction patterns enabled us to make independent direct measurements of all of the elastic constants of β-quartz in the temperature range mentioned above with errors which did not exceed 1%, with the exception of C_{13}, for which the error was somewhat greater.

3. The results for C_{11}, C_{33}, C_{44} and C_{12} are given in Fig. 1, from which it can be seen that C_{11}, C_{33} and C_{12} increase monotonically with rising temperature, while C_{44} is constant within experimental error. Close to 580°, C_{11} becomes equal to C_{33}; in the same region C_{12} changes sign by passing through zero. The relation of the temperature coefficients of C_{11} and C_{12} always remains such that $C_{66} = \frac{1}{2}(C_{11}-C_{12})$ monotonically and increases slowly from $50 \cdot 10^{10}$ to $51 \cdot 10^{10}$ d/cm. C_{13} also increases from $17 \cdot 10^{10}$ d/cm near 580° to $36 \cdot 10^{10}$ d/cm at 615-620°.

The values which we obtained for C_{44} and C_{66} at 600° agree within experimental error with the data of Atanasoff and Kammer, thus supporting their conclusions concerning the error in the data of Osterberg and Cookson.

Perrier and Mandrot [5] used a statistical method to investigate the temperature dependence of the isothermal moduli. There is satisfactory agreement between our values for C_{11} and C_{33} and the calculations of Perrier and Mandrot, thus showing that the temperature dependence of the adiabatic constants and of the isothermal constants are similar.

It is noteworthy that at higher temperatures none of the elastic constants of β-quartz is diminished and that its elasticity is generally increased with temperature.

4. The Bergmann-Schaefer method made it possible to perform independent measurements of all the elastic constants of β-quartz. We have obtained the temperature dependence of these constants from 578 to 630°. Our values for C_{44} and C_{66} at 600° agree with the data of Atanasoff and Kammer. It has been established that the elasticity of β-quartz increases at higher temperatures. It has also been established that in this region β-quartz possesses quite good piezoelectric properties which enable us to obtain complete patterns of light diffraction by ultrasound.

LITERATURE CITED

[1] H. Osterberg and J. W. Cookson, J. Franklin Inst. 220, 361 (1935).

[2] E. W. Kammer and I. V. Atanasoff, Phys. Rev. 62, 395 (1942).

[3] L. Bergmann, Der Ultraschall (Zurich, 1954).

[4] V. G. Zubov, Doklady Akad. Nauk SSSR 107, 3, 392 (1956) [Soviet Physics - Doklady, p. 187].

[5] A. Perrier and B. de Mandrot, Mem. soc. vaudoise sci. nat. 1923, No. 7, 333.

M. V. Lomonosov Moscow State University

Received February 18, 1956

ELECTRON MOTION IN CYCLICAL ACCELERATORS AS A STOCHASTIC PROCESS

A. N. Matveev

(Presented by Academician N. N. Bogoliubov February 21, 1956)

In their examination of the influence of radiation emitted by an electron on its trajectory in a constant axially symmetric magnetic field, A. A. Sokolov and I. M. Ternov [1,2] found that the trajectory is broadened by the emission. A little later Sands [3] examined the influence of radiation emission on the synchrotron oscillations of the electrons. The excitation mechanism of these oscillations is identical with the mechanism studied in [1,2].

The findings of Sokolov and Ternov and of Sands concerned the case of constant weak focusing. Later we [4,5] studied synchrotron and betatron oscillations under strong focusing. It was shown, in particular, that for electron energies of the order of a few billion volts it is probably absolutely necessary to have strong focusing. In [4,5] it was emphasized that the effect being considered is of a semiclassical nature. The excitation of the oscillations is of quantum character in the sense that there are discrete acts of emission but the oscillations are of classical character. The problem was solved in [4,5] by direct, one might say dynamical, methods, and it was possible to obtain an estimate of the mean square deviation in [4] by obtaining the solution of a practically infinite set of algebraic equations with arbitrary right-hand sides. The direct generalization of the method in [4] to the case of an arbitrarily varying magnetic field involves a number of mathematical difficulties. But it is important to examine the case of an arbitrary field for both practical and theoretical reasons. In this connection it is necessary to carry through a general examination of the phenomenon.

The mathematical apparatus which must be used is dictated by the physical nature of the phenomenon. This physical nature is determined by the fact that by far the larger portion of the radiation is due not to the betatron and synchrotron oscillations but to the cyclical motion of the electrons. Consequently, the acts of emission are independent of the phase of these oscillations, and this means that the cyclical electron motion which is accompanied by betatron or synchrotron oscillations must be regarded as a stochastic process.

We have obtained the following stochastic equations which describe betatron and synchrotron oscillations induced by emission:

$$(\sqrt{E_s}x)'' - \beta(\sqrt{E_s}x)''' + F(\zeta)\sqrt{E_s}x = \frac{\mu(\zeta)}{\sqrt{E_s}}\Big\{\sum_{g}\mu(\zeta,\zeta_g)\,eV_0(\cos\varphi - \cos\varphi_s) - \Big[\sum_{\nu}\mu(\zeta,\zeta_\nu)\,\varepsilon_\nu - \int_0^{\zeta}\mu(\zeta')\,W_s\,d\zeta'\Big]\Big\}; \tag{1}$$

$$\ddot{\varphi} + \gamma\dot{\varphi} + \Omega^2\varphi = -\frac{k\omega\alpha}{\lambda}\sum_i \frac{\varepsilon_i}{E_i}\,\delta(t - t_i) + \frac{k\omega\alpha}{\lambda E_s}\,W_{st}. \tag{2}$$

The following notation has been used: R_0 is the radius of curvature of the curved parts of the synchrotron; $x = (R - R_0)/R_0$; R is the radial coordinate of the electron, i.e. $\underline{x}$ includes both the betatron and the synchrotron parts of the radial deflection; $\zeta = ct/R_0$; ζ_0 will denote the value of ζ for the straight parts and ζ_γ for the curved parts; $\mu(\zeta_0) = 0$; $\mu(\zeta_\gamma) = 1$; $\mu(\zeta,\zeta') = 0$ for $\zeta < \zeta'$; $\mu(\zeta,\zeta') = 1$ for $\zeta > \zeta'$; eV_0 is the amplitude of the high frequency field; φ is the phase of passage through the high frequency field, with the subscript $\underline{s}$ denoting its equilibrium value; e is the charge of the electron;

$$\beta \sim \frac{r_0}{R_0}\frac{E}{mc^2}; \quad r_0 = \frac{e^2}{mc^2}; \quad \psi = \varphi - \varphi_s; \quad \gamma = (4-\alpha)\frac{2}{3}\frac{c}{R_0\lambda}\frac{r_0}{R_0}\left(\frac{E}{mc^2}\right)^3;$$

$\Omega^2 = \frac{k\omega^2\alpha}{2\pi\lambda}\frac{eV_0 \sin\varphi_s}{E_s}$; $\omega = \frac{c}{R_0\lambda}$; k indicates the high frequency harmonic which produces acceleration; $\lambda = 1 + L/2\pi R_0$; L is the combined length of all straight parts of the synchrotron; $F(\zeta) = 1 + \frac{R}{H}\frac{dH}{dR}$; $W_s = \frac{2}{3}\frac{e^2}{R_0}\left(\frac{E}{mc^2}\right)^4$; ϵ is the energy of an emitted photon at an instant denoted by its subscript. The definition of α will be given below. Primes denote derivatives with respect to ζ; dots denote derivatives with respect to t.

β in (1) takes into consideration the damping of the radial oscillations due to radiation damping. Since $r_0/R_0 \sim 10^{-15}$ this quantity is negligibly small in practice and radiation damping can be neglected.

We shall denote by $y_1(\zeta)$ and $y_2(\zeta)$ the two linearly independent solutions of the equation $y'' + Fy = 0$ and the Wronskian by $W = y'_1 y_2 - y'_2 y_1$. Let $Y_i(\zeta)$ be the primitive:

$$Y_i(\zeta) = \int^{\zeta} \mu(\zeta')\, y_i(\zeta')\, d\zeta', \tag{3}$$

whose constant of integration is determined by $\langle Y_i \rangle_{\zeta_\gamma} = 0$, where the symbol $\langle\ \rangle_{\zeta_\gamma}$ denotes averaging over the values of ζ_γ.

Let

$$\alpha(\zeta, \zeta') = [y_1(\zeta)\, Y_2(\zeta') - y_2(\zeta)\, Y_1(\zeta')]\,/\,W. \tag{4}$$

Then α in Equation (2) is $\langle \alpha(\zeta, \zeta) \rangle_{\zeta_\gamma}$.

It should be noted, furthermore, that the stochastic Equations (1) and (2) must be solved simultaneously since ψ is associated with the synchrotron part of x.

Let ℓ be the width of the vacuum chamber in the radial direction and $a = \ell/2R_0$. Then a calculation with allowance for absorption of electrons in the walls gives the following equation for the distribution function $F_a(x,t)$:

$$F_a(x,t) = \\ = \frac{1}{a}\sum_{n=0}^{\infty}(-1)^n \sin\left[\frac{2n+1}{2a}\pi(a+x)\right]\exp\left\{-\frac{\pi^2(2n+1)^2}{8a^2}\langle x^2(t)\rangle\right\}, \tag{5}$$

where

$$\langle x^2(t)\rangle = \langle x_s^2(t)\rangle + \langle x_\beta^2(t)\rangle, \tag{5a}$$

$$\langle x_s^2(t)\rangle = \frac{55}{32\sqrt{3}}\frac{\langle|\alpha(\zeta,\zeta)|^2\rangle_\zeta}{4-\alpha}\frac{hc}{e^2}\frac{r_0}{R_0}\left(\frac{E}{mc^2}\right)^2, \tag{5b}$$

$$\langle x_\beta^2(t)\rangle = \frac{55}{24\sqrt{3}}\langle|\alpha(\zeta,\zeta')|^2\rangle_{\zeta'_\gamma}\frac{hc^2}{ER_0^2\lambda}\frac{r_0}{R_0}\int_0^t\left(\frac{E}{mc^2}\right)^6 dt. \tag{5c}$$

If the absorbing walls of the synchrotron are removed to infinity (i.e. assuming no absorption by the walls) (5) yields the following Gaussian distribution:

$$F(x,t) = \lim_{n\to\infty} F_n(x,t) = \frac{1}{2\pi}\int_{-\infty}^{\infty} e^{-1/2\langle x^2\rangle \xi^2}\cos(\langle x^2\rangle \xi)\,d\xi = \tag{6}$$

$$= \frac{1}{\sqrt{2\pi\langle x^2\rangle}}\,e^{-x^2/2\langle x^2\rangle}$$

with the mean square deviation $\left\langle x^2(t)\right\rangle$.

From (5) we can obtain the probability density of electron losses in the interval $(t, t+dt)$ due to collisions with the walls, and on this basis we can calculate the law for the loss of beam intensity due to loss of electrons to the walls. If $N(t)$ denotes the number of electrons at time t we obtain

$$N(t) = N(0)\,\Phi(t), \tag{7}$$

where

$$\Phi(t) = \frac{4}{\pi}\sum_{n=0}^{\infty}\frac{(-1)^n}{2n+1}\exp\left\{-\frac{\pi^2(2n+1)^2}{8a^2}\langle x^2(t)\rangle_\zeta\right\},$$

with the symbol $\left\langle x^2(t)\right\rangle_\zeta$ denoting the average of $\left\langle x^2(t)\right\rangle$, as defined in (5), over ζ. It should be emphasized that these equations are very useful for calculations because of the rapid convergence of the series. When there is appreciable absorption the first term is sufficient.

Similar equations apply to the phase oscillations. Assuming that during acceleration the equilibrium phase is shifted a little so that the allowable limits of phase deviation are also changed, the equations become a little more complicated and for lack of space will not be given here. We shall write only the equation for the mean square phase deviation neglecting electron losses due to phase losses:

$$\langle\psi^2(t)\rangle = \frac{55\sqrt{3}}{64}\,\frac{k\alpha}{\lambda(4-\alpha)}\,\mathrm{ctg}\,\varphi_s\,\frac{hc}{e^2}\,\frac{mc^2}{E}, \tag{8}$$

where the right-hand side has been transformed on the assumption that at the end of an accelerating cycle the energy acquired in the accelerating gap is approximately equal to the energy radiated per revolution.

The equations can be applied to any synchrotron. Further improvement of the theory is possible through allowance for the linearity of both the radial and phase oscillations. This means obtaining corrections for nonlinearity when the amplitudes of the oscillations are not too great. It is also possible to obtain corrections for deviation from adiabaticity.

The axial oscillations of the electrons which are induced by radiation are to be treated in analogous fashion, although their amplitude is considerably smaller than that of the radial oscillations. In this connection, for synchrotrons with strong focusing it is clearly reasonable to increase the statistical weight of the radially focusing sectors. To what extent this can be done must be decided by calculation for each specific case.

The analysis for specific cases of weak- and strong-focusing synchrotrons on the basis of the equations given above supports the conclusion in [4,5] that strong focusing is absolutely required when the electron energy is of the order of a few billion electron volts, and we are enabled to make a number of suggestions regarding the design of high energy electron synchrotrons.

The stochastic theory of electron oscillations in synchrotrons provides the solution of problems which arise in connection with these oscillations. It is obvious that this theory can be generalized to apply to other types of cyclical accelerators, different from the synchrotron.

LITERATURE CITED

[1] A. A. Sokolov and I. M. Ternov, Doklady Akad. Nauk SSSR 92,537 (1953); J. Exptl.-Theoret. Phys. (USSR) 25, 698 (1953).

[2] A. A. Sokolov and I. M. Ternov, Doklady Akad. Nauk SSSR 97, 823 (1954); J. Exptl.-Theoret. Phys. (USSR) 28, 431 (1955) [Soviet Physics – JETP, p.227].

[3] M. Sands, Phys. Rev. 97, 470 (1955).

[4] A. N. Matveev, Doklady Akad. Nauk SSSR 107, 5, 671 (1956) [Soviet Physics – Doklady, p. 211].

[5] A. N. Matveev, Doklady Akad. Nauk SSSR 108, 3, 432 (1956) [Soviet Physics – Doklady, p. 321].

M. V. Lomonosov Moscow State University

Received February 21, 1956

MAGNETIC ANALYSIS OF THE REACTIONS (I) pp $\rightarrow$ npπ^+, (II) pp $\rightarrow$ ppπ^0 AND (III) pp $\rightarrow$ dπ^+ AT 660 MEV

M. G. Meshcheriakov, Corresponding Member of the Academy of Sciences, USSR, B. S. Neganov, I. K. Vzorov, V. P. Zrelov and A. F. Shabudin

Our present knowledge regarding inelastic (p – p) collisions for synchrocyclotron energies concerns the total cross sections for the production of π^+ mesons [1-3], the meson energy distribution in reaction I [4-6] and the angular distribution of mesons in reaction III [7-9]. In order to obtain further information regarding the nature of the process which produces π^+ mesons in (p – p) collisions we have studied experimentally the momentum spectra and angular distributions of secondary protons which were ejected in reactions I and II at 660 Mev.

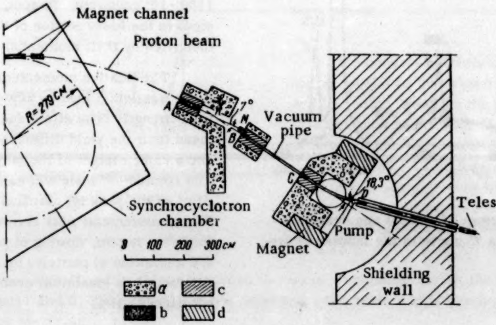

Fig. 1. Diagram of spectrometer.
a) Concrete- b) brass; c) lead; d) steel.

It was interesting, in addition, to establish the possibility of separating from the total beam of secondary particles the deuterons which are produced in reaction III in order to determine to what extent they are polarized. This experiment in conjunction with the measurements of the total cross section of reaction III as a function of energy, as well as of the angular distribution and asymmetric production of pions by protons with known polarization, enables us to carry through a complete phenomenological analysis of reaction III, including the determination of the two possible transitions which are responsible for the emission of mesons in the p-state: $^1S_0 \rightarrow {}^3S_1$ and $^1D_2 \rightarrow {}^3S_1$.

The experiments were performed on the 6-meter synchrocyclotron of the Institute of Nuclear Problems, Academy of Sciences, USSR. We used a proton beam with a density of $3 \cdot 10^9$ protons/cm^2 · sec extracted into the atmosphere through the excitation of radial oscillations during the final revolutions. The proton energy was 660 ± ± 3 Mev. The half width of the proton spectrum was $\pm$ 5 Mev.

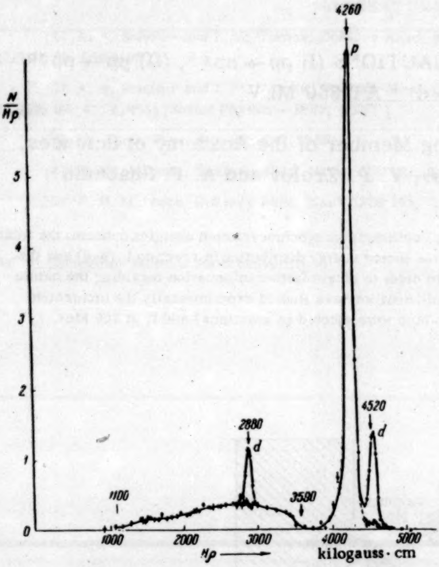

Fig. 2. Momentum spectrum of protons and deuterons from (p–p) collisions at a 7° angle in the laboratory system of coordinates.

A diagram of the spectrometer and its position with respect to the primary beam and the concrete shield during measurements at a 7° angle are shown in Fig. 1. The spectrometer was based on a magnet with circular poles of 100 cm diameter and air gap of 10 cm. The first slit of the spectrometer was a target 1 cm wide and 2.5 cm long. The secondary particles which were ejected from the target at an angle of 7° with respect to the primary beam passed through collimators B and C, whose cross sections were 2 × 3 cm and 3 × 3 cm, respectively, then through the analyzing field, the collimator D of 1 × 3 cm cross section and a channel in the 3.6 meter concrete wall and entered the experimental laboratory. The particle detector at the spectrometer outlet was a telescope consisting of four scintillation counters connected for triple and quadruple coincidences. The recording threshold was $1100 \cdot 10^3$ gauss-cm. Protons, deuterons, and also pions in the lower portion of the spectrum, were identified by their momentum and range.

The relative momentum spectrum of the particles was determined by changing the magnetic field strength. The effect due to hydrogen was found from the yield difference of a polyethylene and a carbon target of the same stopping power. The momentum scale was calibrated from the position of the peak for elastically scattered protons. The measurements were corrected for errors of the recording system, slowing of particles in the target and absorption of particles by the target and scintillators. The maximum over-all correction did not exceed 15%.

Fig. 2 is the momentum spectrum of secondary protons and deuterons for equal H_ρ ranges at 7°. The highest peak at $H_\rho = 4260 \cdot 10^3$ gauss-cm corresponds to protons scattered elastically by protons at 17° in the center-of-mass system. The spreading of this peak on the lower energy side is caused by scattering and retardation of protons in the collimators.* The peaks at $H_\rho = 4520 \cdot 10^3$ and $H_\rho = 2880 \cdot 10^3$ gauss-cm represent deuterons from reaction III scattered at 43° and 153.5°, respectively, in the c.m. system. The position of the deuteron peaks with respect to the peak for elastically scattered protons differs from the calculated value by not more than 1%.

The continuous spectrum is that of the secondary protons from reactions I and II. Its upper limit agrees with calculations which give $3560 \cdot 10^3$ and $3590 \cdot 10^3$ gauss-cm, respectively, for these reactions. From the background level close to the upper boundary of the continuous spectrum we were enabled to conclude that the protons which are scattered elastically by protons and which are partly slowed down in the collimators contribute not more than 3% to the continuous spectrum. It is noteworthy that in the continuous proton spectrum there is no appreciable distinction of two contributions, each corresponding to about half of the momenta of two groups of deuterons. This experimental fact is definite proof of the fact that the proton and neutron in reaction I and the two protons in reaction II are seldom ejected with small momentum of relative motion.

---

*In the immediate vicinity of the synchrocyclotron the background level due to incidental radiation was extremely high; this made it impossible to separate the beam of secondary particles at the spectrometer inlet by using a set of scintillation counters.

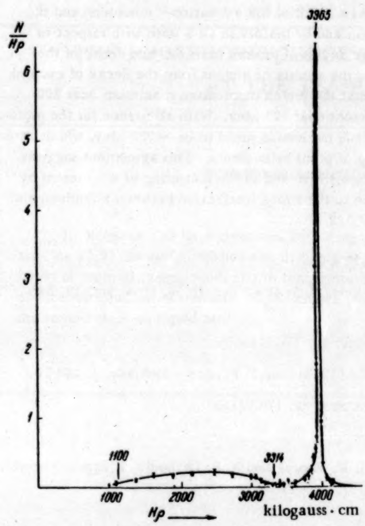

Fig. 3. Momentum spectrum of protons from (p–p) collisions at an angle of 18° in the laboratory system.

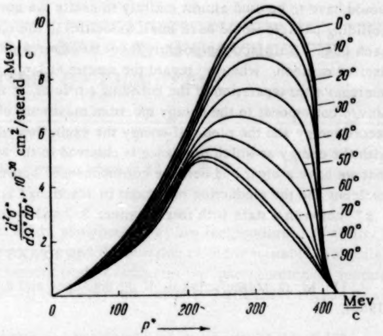

Fig. 4. Proton momentum spectra in the center-of-mass system.

A secondary particle spectrum from (p–p) collisions similar to that described above was also taken at 12.2° with respect to the primary beam. In this case deuteron peaks were observed, to the left of the peak of elastically scattered protons, at $H_\rho = 3220 \cdot 10^3$ and $3950 \cdot 10^3$ gauss-cm. Fig. 3 gives the spectrum of secondary protons from (p–p) collisions at 18°, where deuterons from reaction III are no longer observed. The spectra at 24 and 30° have the same form as at 18°.

The spectra were normalized in absolute units in two ways: 1) by determining the integral yield of secondary protons from reactions I and II; 2) by comparing the areas under the peak of elastically scattered protons and under the continuous proton spectrum.

The spectra observed in the laboratory system were used to construct the momentum spectrum of secondary protons from reactions I and II at different angles in the c.m. system. The plots are shown in Fig. 4.* This figure shows that the shape of the secondary proton momentum spectrum changes sharply with the angle of emission. Protons above 250 Mev/c are ejected predominantly forward and backward, while protons with lower momenta are distributed almost isotropically.

From a comparison of the areas under the curves in Fig. 4 it is found that the dependence of $d\sigma^*/d\omega^*$ on the proton emission angle θ^* obeys the equation

$$\frac{d\sigma^*}{d\omega^*} \approx 1.3\,(0.8 + \cos^2\theta^*) \times 10^{-27} \ \text{cm}^2/\text{sterad}$$

It is significant that at large angles the momentum spectra show a clear peak near 220 Mev/c. This characteristic of the spectra can be explained qualitatively by the assumption that at a given energy the production of pions in (p–p) collisions in some cases takes place through an intermediate excited state of the nucleon, whose lifetime is comparable with the duration of the collision. In our experiments the available energy of 305 Mev would have to be used almost entirely to excite the nucleon. As a result of the excitation the nucleon and the colliding particle would have small velocities in the c.m. system and be mainly in an S state with respect to each other. This fact can possibly favor the observation at large angles of protons from the free decay of the excited nucleon. When we regard the spectra at large angles as the spectra of protons from the decay of excited nucleons after separation of the colliding particles, it appears that the proton momentum maximum near 220 Mev/c corresponds to the energy spectrum maximum of π^+ mesons near 125 Mev. With allowance for the proton recoil energy and the pion self-energy the excitation energy of the nucleon is found to be ~ 290 Mev, which agrees with the energy at which resonance is observed in the scattering of pions by nucleons. This agreement suggests that we have a clear and definite correspondence between processes involved in the scattering of π^+ mesons by nucleons and the production of mesons in reactions I and II, due to the strong interaction between a nucleon and a π^+ meson in a state with total moment 3/2 and isotopic spin 3/2.

---

* All values which refer to the c.m. system are indicated by asterisks.

LITERATURE CITED

[1] M. G. Meshcheriakov, N. P. Bogachev and B. S. Neganov, Bull. Acad. Sci. USSR, Phys. Ser. 19, 548 (1955).

[2] L. W. Smith, A. W. McReynolds and G. Snow, Phys. Rev. 97, 1186 (1955).

[3] N. P. Bogachev, Doklady Akad. Nauk SSSR 108, 5, 806 (1956) [Soviet Physics - Doklady, p. 361].

[4] M. M. Block, S. Passman and W. W. Havens, Jr., Phys. Rev. 88, 1239 (1952).

[5] A. H. Rosenfeld, Phys. Rev. 96, 130 (1954).

[6] M. G. Meshcheriakov, V. P. Zrelov, B. S. Neganov, I. K. Vzorov and A. F. Shabudin, J. Exptl.-Theoret. Phys. (USSR) 31, 7 (1) (1956) [Soviet Physics - JETP, p.79].

[7] H. L. Stadler, Phys. Rev. 96, 496 (1954).

[8] M. G. Meshcheriakov, B. S. Neganov, N. P. Bogachev and V. M. Sidorov, Doklady Akad. Nauk SSSR 100, 673 (1955).

[9] M. G. Meshcheriakov and B. S. Neganov, Doklady Akad. Nauk SSSR 100, 677 (1955).

Institute of Nuclear Problems,
Academy of Sciences, USSR

Received June 4, 1956

THE PHOSPHORESCENCE SPECTRA OF SOME AROMATIC ACIDS AT THE TEMPERATURE OF LIQUID AIR

B. A. Piatnitskii

(Presented by Academician A. N. Terenin February 13, 1956)

1. Benzene and its derivatives, including aromatic acids, phosphoresce at low temperatures. In earlier articles [1,9] the author studied the damping of phosphorescence and the duration of the metastable molecular states of aromatic compounds at low temperatures. The present work investigates the phosphorescence spectra of alcohol solutions of benzoic [C_6H_5COOH], phthalic [$C_6H_4(COOH)_2$] and gallic [$C_6H_2COOH(OH)_3$] acids at the temperature of liquid air.

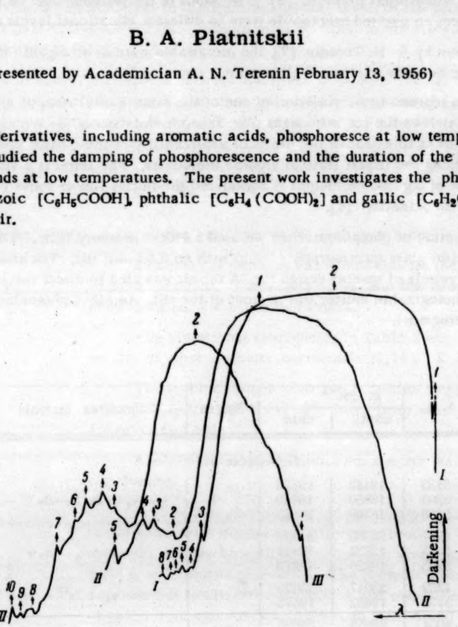

Fig. 1. Microphotograms of the visible portion of the fluorescence spectra of benzoic (I), phthalic (II) and gallic (III) acids.

TABLE 1

Phosphorescence spectrum	ν_0 cm⁻¹	Vibrational frequencies in the spectrum, cm^{-1}			
		ν'	ν''	ν'''	ν^{IV}
Benzoic acid	24685	313	608	1187	826
Phthalic acid	21739	313	608	1182	992
Gallic acid	23283	313	608	1187	—

In earlier investigations of the phosphorence spectra of aromatic compounds at low temperatures [2-6] the phosphorescence spectra of phthalic and gallic acid were not included. The phosphorescence spectrum of benzoic acid at the temperature of liquid air was first studied by Kowalski [2]. He used a quartz spectrograph and investigated the extreme violet and ultraviolet portions of the spectrum. Kowalski gave the maxima of 5 bands in these regions

from 366 to 416 mμ. We used a glass spectrograph to obtain the phosphorescence spectrum in the violet and yellow regions. We have found 8 bands with maxima from 4055 to 5388 A. In the violet region our measurements agree with those of Kowalski. We did not investigate the ultraviolet region because of our use of a glass spectrograph.

The phosphorescence spectra of aromatic compounds at liquid air temperature consist of bands of different intensities and have a vibrational structure [5]. The bands in the phosphorescence spectra result from the transition of molecules from an excited metastable state to different vibrational levels of the ground state.

As has been shown by A. N. Terenin [7], the metastable state of an organic molecule is a triplet state which is characteristic of the benzene nucleus of all aromatic compounds.

Phosphorescence represents the violation of one of the fundamental rules of spectroscopy – the forbidding of intercombinations, as well as the not infrequent simultaneous violation of the symmetry rule [5]. The study of phosphorescence enables us to establish the limits of applicability of these basic laws of spectroscopy and to obtain information regarding the triplet state of organic molecules. The latter is a vital subject, since the triplet (bivalent radical) state of organic molecules is considered the initial link in some very important chemical reactions and especially in oxidation [8].

2. For the excitation of phosphorescence we used a PRK-2 mercury lamp. The spectra were photographed by an ISP-51 triple-prism glass spectrograph (1:2.3) with an 0.04 mm slit. The aromatic-acid alcohol solutions were placed in metal vessels of special design [9]. A mirror was used to direct the luminescence radiation to the spectrograph slit. A photographic shutter was in front of the slit. An MF-2 photoelectric microphotometer was used to study the spectrograms.

TABLE 2

No. of maximum	λ, Å	ν, cm^{-1} exptl	ν, cm^{-1} calc	Series	Series formula	n
I. Benzoic acid						
4	5133	19482	19472	I	$\nu = \nu_0 - 2\nu^{IV} - 3\nu''' - n_4\nu'$	$n_1 = 0$
7	5305	18850	18846			$n_1 = 2$
8	5388	18560	18533			$n_1 = 3$
1	4051	24685	24685	II	$\nu = \nu_0 - n_2\nu''$	$n_2 = 0$
3	5045	19822	19821			$n_2 = 8$
5	5203	19220	19213			$n_2 = 9$
4	4339	23047	23033	III	$\nu = \nu_0 - 2\nu^{IV} - n_3\nu'''$	$n_3 = 0$
2	5133	19482	19472			$n_3 = 3$
1	4051	24685	24685	IV	$\nu = \nu_0 - n_1\nu'$	$n_1 = 0$
6	5254	19033	19051			$n_1 = 18$
II. Phthalic acid						
1	4600	21739	21739			
4	5433	18406	18383	I	$\nu = \nu_0 - 2\nu''' - \nu^{IV} - n_1\nu'$	$n_1 = 0$
5	5735	17437	17444			$n_1 = 3$
2	5161	19376	19375	II	$\nu = \nu_0 - 2\nu''' - n_2\nu''$	$n_2 = 0$
3	5328	18769	18767			$n_2 = 1$
III. Gallic acid						
1	4295	23283	23283	I	$\nu = \nu_0 - n_1\nu'$	$n_1 = 0$
2	4739	21101	21092			$n_1 = 7$
5	5473	18271	18275			$n_1 = 16$
6	5569	17956	17962			$n_1 = 17$
1	4295	23283	23283	II	$\nu = \nu_0 - n_2\nu''$	$n_2 = 0$
3	5252	19040	19027			$n_2 = 7$
8	6021	16608	16595			$n_2 = 11$
10	6257	15982	15987			$n_2 = 12$
4	5337	18737	18714	III	$\nu = \nu_0 - \nu' - 7\nu'' - n_3\nu'''$	$n_3 = 0$
9	6152	16355	16340			$n_3 = 2$
3	5252	19040	19027	IV	$\nu = \nu_0 - 7\nu'' - n_1\nu'$	$n_1 = 0$
7	5753	17482	17462			$n_1 = 5$

Fig. 1 gives the microphotograms of the phosphorescence spectra of alcohol solutions of benzoic (I), phthalic (II) and gallic (III) acids. The wavelengths were obtained by interpolation in Hartmann's formula between the lines of the mercury spectrum.

3. Since, as is generally believed, the bands of the phosphorescence spectrum result from a molecular transition from a (metastable) excited electron level to different vibrational levels of the ground state, the frequency differences of the band peaks in the phosphorescence spectrum must be equal to the vibrational frequencies in the unexcited state or to combinations of these.

From an analysis of the frequency differences between the maxima in each band and in all succeeding bands of each spectrum we arrive at the conclusion that in the aromatic acid phosphorescence spectra which we investigated there are definite vibrational frequencies ν', ν'', ν''', ν^{IV} (cm^{-1}) which we can use to calculate the frequencies of the band maximum by the formula

$$\nu = \nu_0 - n_1\nu' - n_2\nu'' - n_3\nu''' - n_4\nu^{IV}; \tag{1}$$

where ν_0 is the highest peak frequency, n_1, n_2, n_3, n_4 are constant for each maximum.

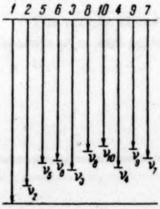

Fig. 2. Scheme for the production of band maxima in the phosphorescence spectrum of gallic acid.

Equation (1) provides series formulas for the band frequency maxima in each spectrum. The values of ν_0 and the vibrational frequencies for each spectrum are given in Table 1.

The vibrational frequencies in Table 1 were also observed in the spectra of other aromatic compounds [5,10].

The band maximum frequencies which were obtained from the microphotograms and those calculated from series of formulas such as (1) are given in Table 2.

Analysis of the phosphorescence spectra leads to the following conclusions.

1. The phosphorescence spectra of aromatic acids consists of a number of bands with maxima of different intensity. The phosphorescence spectrum of benzoic acid in the visible region extends from 4047 A to 5431 A and consists of 8 bands. The phosphorescence spectrum of phthalic acid extends from 4034 A to 5837 A and consists of 5 bands. The spectrum of gallic acid extends from 4276 A to 6293 A and consists of 10 bands.

2. The phosphorescence spectra of aromatic acids have a vibrational structure at the temperature of liquid air.

3. In all spectra there are two vibrational frequencies which are common to the spectra – $\nu' = 313\ cm^{-1}$ and $\nu'' = 608\ cm^{-1}$, corresponding to the C – H and C – C bonds of the benzene ring [5,8].

4. The frequencies of the band maxima in all of the phosphorescence spectra satisfy Formula (1).

5. The band maxima form a series in accordance with (1). The phosphorescence spectra of benzoic and gallic acid contain identical series of the form

$$\nu = \nu_1 - n_1\nu', \quad \nu = \nu_1 - n_2\nu''.$$

LITERATURE CITED

[1] B. A. Piatnitskii, Bull. Acad. Sci. USSR, Phys. Ser. 15, 5, 597 (1951).

[2] J. Kowalski, Physik Z. 12, 956 (1911).

[3] A. Kronenberger, Z. Physik, 63, 494 (1930).

[4] I. V. Obreimov and A. F. Prikhot'ko, Recollections of Sergei Ivanovich Vavilov (Acad. Sci. USSR Press, 1952), p. 197.

[5] P. P. Dikun and V. Ia. Sveshnikov, J. Exptl.-Theoret. Phys. (USSR) 19, 11, 1000 (1949).

[6] A. A. Il'ina and E. V. Shpol'skii, Bull. Acad. Sci. USSR, Phys. Ser. 15, 5, 585 (1951); J. Exptl.-Theoret. Phys. (USSR) 21, 2, 142 (1951).

[7] A. N. Terenin, Acta Physicochim. URSS, 18, 210 (1943); J. Phys. Chem. (USSR) 18, 1-2 (1944).

[8] A. N. Terenin, Photochemistry of Dyes (Acad. Sci. USSR Press, 1947).

[9] B. A. Piatnitskii, Doklady Akad. Nauk SSSR 57, 8, 771 (1947).

[10] M. V. Vol'kenshtein, M. A. El'iashevich and B. I. Stepanov, Molecular Vibrations 2 (1949).

Received December 6, 1955

A DISPERSION RELATION FOR FERMIONS

V. Fainberg and E. Fradkin

(Presented by Academician I. E. Tamm February 29, 1956)

Modern quantum field theory is based on the general requirements of relativistic invariance, causality and certain boundary conditions.[*] But attempts to solve the equations of the theory with specific types of interaction lead to the conclusion that the theory does not possess inherent mathematical completeness [1,2] (the renormalized charge is zero). In this connection it is very essential to determine those consequences of the indicated general requirements which, on the one hand, are independent of the specific form of interaction and, on the other hand, can be verified experimentally. This will enable us to determine how consistent these general requirements are with reality. One such consequence is a dispersion relation which relates the real and imaginary parts of the forward scattering amplitude. Such a formula for the scattering of bosons was established in [3-5]. The purpose of the present note is the deduction of a dispersion relation for the scattering of fermions.

The matrix element $\langle p_\lambda, q_\mu | S | p'_{\lambda'}, q'_{\mu'} \rangle$ for the scattering of two fermions from a state with the 4-momenta p',q' and polarizations λ' and μ', respectively, to a state with momenta p', q' and polarizations λ, μ is

$$\langle p_\lambda, q_\mu | S | p'_{\lambda'}, q'_{\mu'} \rangle = i \int dx\, dy\, \overline{U}^\lambda (p, x) L_x \langle q_\mu, \alpha' | T \{\Psi^*_\alpha (x) \overline{\Psi}_\beta (y)\} | q'_{\mu'}, \beta' \rangle \overline{L}_y U^{\lambda'} (p', y), \tag{1}$$

where $| q_\mu, \alpha \rangle$ is the Heisenberg state vector of one fermion with 4-momentum q ($\mathbf{q}$, $q_0 = \sqrt{\mathbf{q}^2 + M^2}$; Ψ_α is a Heisenberg fermion operator, $U^\lambda (p,x)$ is the solution of the Dirac equation for a free particle with 4-momentum p ($\mathbf{p}$, $p_0 = E = \sqrt{\mathbf{p}^2 + M^2}$ and polarization λ; $L_x = (\gamma_\mu\, \partial/\partial x_\mu + M)$; $\overline{L}_y = (-\gamma_\mu \partial/\partial y_\mu + M)$; $\overline{U} = U^* \gamma_4$; the indices α, β, α' and β' have the values 1 and 2 and characterize the charge state of the fermion; for simplicity the spinor indices are omitted $\{A, B\} = AB + BA$. Differentiating with respect to $\underline{x}$ in (1) and then integrating over $\underline{y}$, we obtain[**]

$$\begin{aligned} \langle p_\lambda q_\mu | S | p'_{\lambda'}, q'_{\mu'} \rangle &= (2\pi)^4 \delta (p + q - p' - q') \times \\ &\times i \int dx \exp[-ipx]\, \overline{U} (p) \langle q_\mu, \alpha' | T \{f_\alpha (x), \overline{f_\beta (0)}\} - \\ &- i\delta (x_0) \{f_\alpha (x), \Psi^* (0)\} | q'_{\mu'}, \beta \rangle U^{\lambda'} (p'), \end{aligned} \tag{2}$$

where $f_\alpha (x) = L_x \Psi_\alpha (x)$; $\overline{f_\beta (0)} = \Psi_\beta (0) \overline{L}_0$. In the following we shall omit the factor $(2\pi)^4 \delta (p + q - p' - q')$. The term $\sim\delta (x_0)$ in (2) is zero[***] in pseudoscalar meson theory for forward scattering ($p = p'$, $q = q'$).

---

[*] For $t \to \pm\infty$ the particles are free and possess observable masses.

[**] In deriving this relation we assume, first, invariance with respect to space-time translations $x'_\mu = x_\mu + a_\mu$ and, secondly, the existence of a complete system of vectors of positive energy states.

[***] In the general case this term can also be neglected since the dispersion formulas contain the difference between the real parts of the forward scattering amplitude for two different energies [see (9)].

For forward scattering we have (omitting $\sim \delta(x_0)$ and transforming to a system in which a fermion with 4-momentum $\underline{q}$ is at rest)

$$F^{\mu\mu'}_{\lambda\lambda'}(\mathbf{p}, E) = i\int dx\, e^{-ipx}\, \overline{U}^{\lambda}(p) \langle \mu, \alpha' \,|\, T\{f_{\alpha}(x), \overline{f_{\beta}(0)}\} \,|\, \mu', \beta' \rangle\, U^{\lambda'}(p). \tag{3}$$

In this system because of invariance with respect to spatial reflections

$$F^{\mu\mu'}_{\lambda\lambda'}(-\mathbf{p}, E) = F^{\mu\mu'}_{\lambda\lambda'}(\mathbf{p}, E), \tag{4}$$

i.e. the matrix element depends only on the energy of the incoming fermion. For simplicity we shall temporarily omit charge indices. Instead of $F^{\mu\mu'}_{\lambda\lambda'}(E)$ it is convenient to consider the quantity [3]

$$M^{\mu\mu'}_{\lambda\lambda'}(E) = i\int \cos \mathbf{p}x\, e^{iEx_0}\, \eta(x)\, f^{\mu\mu'}_{\lambda\lambda'}(E, x)\, dx, \tag{5}$$

where $f^{\mu\mu'}_{\lambda\lambda'}(E, x) = \langle \mu \,|\, \{\overline{U}^{\lambda} f(x), \overline{f(0)}\, U^{\lambda'}\} \,|\, \mu' \rangle \left(\eta(x) = \begin{pmatrix} 1 \\ 0 \end{pmatrix} \text{ for } x_0 \gtrless 0\right)$, which coincides with $M^{\mu\mu'}_{\lambda\lambda'}(E)$ for $E > M$. We separate $M^{\mu\mu'}_{\lambda\lambda'}(E)$ into its real and imaginary parts:

$$M^{\mu\mu'}_{\lambda\lambda'}(E) = D^{\mu\mu'}_{\lambda\lambda'}(E) + iA^{\mu\mu'}_{\lambda\lambda'}(E); \tag{6}$$

$$D^{\mu\mu'}_{\lambda\lambda'}(E) = i\int \cos \mathbf{p}x\, e^{iEx_0}\, \varepsilon(x)\, f^{\mu\mu'}_{\lambda\lambda'}(E, x)\, dx,$$

$$A^{\mu\mu'}_{\lambda\lambda'}(E) = \int \cos \mathbf{p}x\, e^{iEx_0} f^{\mu\mu'}_{\lambda\lambda'}(E, x)\, dx. \tag{7}$$

D(E) and A(E) will be represented in the form

$$D(E) = D^{(1)}(E) + D^{(2)}(E); \quad A(E) = A^{(1)}(E) + A^{(2)}(E), \tag{8}$$

where $D^{(1)}(E)$, $A^{(2)}(E)$ and $D^{(2)}(E)$, $A^{(1)}(E)$ are, respectively, even and odd functions of E. The quantity $f^{\mu\mu'}_{\lambda\lambda'}(E,x)$ has no poles as a function of E.* From the causality requirement ($f^{\mu\mu'}_{\lambda\lambda'}(E,x) \equiv 0$ for $x^2 > 0$) we obtain (by analogy with [3])

$$D^{(1)}(E) - D^{(1)}(E_0) = \frac{2(E - l^{2}_{0})}{\pi}\, P\int_0^{\infty} \frac{E' A^{(1)}(E')\, dE'}{(E'^2 - E^2)(E'^2 - E_0^2)};$$

$$\frac{D^{(2)}(E)}{E} - \frac{D^{(2)}(E_0)}{E_0} = \frac{2(E^2 - E_0^2)}{\pi}\, P\int_0^{\infty} \frac{A^{2)}(E')\, dE'}{(E'^2 - E^2)(E'^2 - E_0^2)} \tag{9}$$

Thus the relations obtained by Goldberger [3] are general in character.** There are differences in the physical interpretations of $A^{(1)}(E)$ and $D^{(1)}(E)$ in (9). In nucleon-nucleon scattering $D^{(1)}(E)$ and $A^{(1)}(E)$ represent the sum and $D^{(2)}(E)$ and $A^{(2)}(E)$ the difference, respectively, of the real and imaginary parts of the forward scattering amplitude for the nucleon-nucleon and antinucleon-antinucleon cases. Indeed, by definition

---

* $f^{\mu\mu'}_{\lambda\lambda'}(E,x)$ contains terms $\sim E$ or entirely independent of E.

** They are valid when the integrals in the right-hand sides of (9) converge.

$$D^{(1),(2)}(E) = {}^1/_2\,(D_+(E) \pm D_+(-E)),$$
$$A^{(1),(2)}(E) = {}^1/_2\,(A_+(E) \mp A_+(-E)), \tag{10}$$

where the plus sign indicates nucleon-nucleon scattering. It is easily shown (the momentum **p** is taken along the z axis) that[•]

$$U^{\lambda}(-E) = iV^{\nu}(E)\,S_{\nu\lambda}, \tag{11}$$

where $V^{\nu}(E)$ is a spinor which is the charge conjugate of $\bar{U}(E)$ and S is the matrix $\begin{pmatrix} \cdot & 1 \\ 1 & \cdot \end{pmatrix}$. Using (11) we finally obtain[••]

$$D^{\mu\mu'}_{\lambda\lambda',+}(-E) = S_{\lambda\nu}\,D^{\mu\mu'}_{\nu\nu',-}(E)\,S_{\nu'\lambda'}, \quad A^{\mu\mu'}_{\lambda\lambda',+}(-E) = -\,S_{\lambda\nu}\,A^{\mu\mu'}_{\nu\nu',-}(E)\,S_{\nu'\lambda'}, \tag{12}$$

where the minus sign indicates that the matrix elements refer to antinucleon-nucleon scattering.

Thus the nucleon-nucleon scattering matrix element for negative energies can be expressed according to (12) in terms of the antinucleon-nucleon matrix element for positive energies, thus giving a definite physical meaning to the relations (10).

In isotopic space the relation between $D_+(-E)$, $A_+(-E)$ and $D_-(E)$, $A_-(E)$ is[•••] (the indices are explained in [1])

$$D^{\alpha\alpha'}_{\beta\beta',+}(-E) = D^{\alpha\alpha'}_{\beta\beta',-}(E); \quad A^{\alpha\alpha'}_{\beta\beta',+}(-E) = -\,A^{\alpha\alpha'}_{\beta\beta',-}(E). \tag{13}$$

Consequently, for example, the sum of the proton-proton and antiproton-proton forward scattering amplitudes will be an even function of the energy (and the difference will be an odd function). Analogous parity properties are possessed by the sum (difference) of the proton-neutron and antiproton-neutron amplitudes (with the neutron at rest at the beginning and end of the process), etc.

In the region $M \leq E < \infty$ the quantities $A_{\pm}(E)$ can be associated with the total cross section of the corresponding process:

$$A^{\mu\varkappa}_{\lambda\lambda,\pm}(E) = \frac{p}{4\pi}\,\sigma^{\mu\lambda}_{\pm}(E). \tag{14}$$

In the region $0 \leq E < M$, unlike the case of meson-nucleon scattering (where in the region $0 \leq \omega < \mu$ only one state with energy $\omega = \mu^2/2M$ contributes) we have an entire spectrum of states including a real bound state – the deuteron . In fact, from the conservation laws and the form of $A_{\pm}(E)$ it is easily seen that the imaginary part of $A_+(E)$ in this energy region includes contributions from: 1) a single-meson state with energy $E_n = \mu^2/2M$; 2) in the region $0 \leq E \leq M - 2\mu^2/M$, states with $\underline{n}$ mesons within the limits $2 \leq n \leq \sqrt{2M/\mu}$; and,

---

[•] $U^{\lambda}(-E)$ is a spinor which is obtained from $U^{\lambda}(E)$ by formally replacing with $-E$ everywhere (including the normalization).

[••] Since the matrix element for antinucleon-nucleon scattering is defined similarly to (1) except for the minus sign [that is, instead of $\eta(x)$ in (5) we must write $\eta(-x)$].

[•••] The polarization direction must be chosen in accordance with (12).

finally, 3) for neutron-proton scattering, the deuteron state ($E_n = M - \epsilon$, where ϵ is the deuteron binding energy). $A_-(E)$ in the region $0 \le E \le M - 2\mu^2/M$ contains a contribution from the state with $\underline{n}$ mesons within the limits $2 \le n \le 2M/\mu$

Without going into detail we note that the contributions of all of the states indicated in the region $0 \le$ $\le E < M$ can be associated with physical quantities or be expressed in terms of certain physical constants. Thus: 1) the contribution of the single-meson state can be expressed in terms of the pseudoscalar interaction constant f; 2) for the deuteron state, in terms of the deuteron binding energy ϵ; 3) for all other states contributing in the region $0 \le E \le M - 2\mu^2/M$ by analytic continuation of the annihilation part of the total cross section for the nucleon-antinucleon interaction.

By taking all of the above into consideration we can obtain from (9) the following dispersion relation:

$$
\begin{aligned}
D_+(E) - \frac{1}{2}\left(1+\frac{E}{M}\right)D_+(M) - \frac{1}{2}\left(1-\frac{E}{M}\right)D_-(M) = \frac{p^2}{4\pi^2}\int\limits_M^\infty \frac{dE'}{p'}\left\{\frac{\sigma_+(E')}{E'-E} + \right.\\
\left. + \frac{\sigma_-(E')}{E'+E}\right\} + \widetilde{\left(\frac{2f^2}{\mu^2}\right)}\frac{p^2\delta_{\lambda\mu}(2-\delta_{\alpha\alpha'})}{M-\mu^2/2M-E} + C_{\lambda\mu}\frac{p^2(1-\delta_{\alpha\alpha'})}{E+\epsilon-M} + \\
+ \frac{p^2}{4\pi^2}\int\limits_0^{M-2\mu^2|M} \frac{i\,dE'}{p'}\left\{\frac{\sigma_1(E')}{E'+E} + \frac{\sigma_2(-E')}{E'-E}\right\};
\end{aligned}
\tag{15}
$$

$$
\begin{aligned}
D_-(E) - \frac{1}{2}\left(1+\frac{E}{M}\right)D_-(M) - \frac{1}{2}\left(1-\frac{E}{M}\right)D_+(M) = \frac{p^2}{4\pi^2}\int\limits_M^\infty \frac{dE'}{p'}\left\{\frac{\sigma_-(E')}{E'-E} + \right.\\
\left. + \frac{\sigma_+(E')}{E'+E}\right\} + \left(\frac{2f^2}{\mu^2}\right)\frac{p^2\delta_{\lambda u}(2-\delta_{\alpha\alpha'})}{M-\mu^2/2M+E} - C_{\lambda\mu}\frac{p^2(1-\delta_{\alpha\alpha'})}{E-\epsilon+M} + \\
+ \frac{p^2}{4\pi^2}\int\limits_0^{M-2\mu^2|M} \frac{i\,dE'}{E'-E}\left\{\frac{\sigma_1(E')}{E'-E} + \frac{\sigma_2(-E')}{E'+E}\right\},
\end{aligned}
\tag{16}
$$

where the polarization and charge indices in $D_\pm(E)$, $\sigma_\pm(E)$ and $\sigma_{1,2}(E)$ are selected to correspond with (12) and (13). The constant $C_{\lambda\mu}$ in (15) and (16) can be expressed to a good approximation in terms of the deuteron binding energy ϵ: $C_{\lambda\mu} \cong \delta_{\lambda\mu}\ \epsilon^{-1/2} M^{-3/2}$; $\sigma_1(E)$ is the total annihilation cross section in a nucleon-antinucleon collision yielding mesons numbering from 2 to $2M/\mu$ analytically continued in the region $E < M$; $\sigma_2(-E)$ is the total annihilation cross section to mesons numbering from 2 to $\sqrt{2M/\mu}$, analytically continued in the region $M < E < 0$.

LITERATURE CITED

[1] E. S. Fradkin, J. Exptl.-Theoret. Phys. (USSR) 28, 750 (1955) [Soviet Physics – JETP, p. 604].

[2] L. D. Landau and I. Ia. Pomeranchuk, Doklady Akad. Nauk SSSR 102, 489 (1955).

[3] M. L. Goldberger, Phys. Rev. 99, 979 (1955).

[4] M. Goldberger, H. Miyakawa and R. Oehme, Phys. Rev. 99, 986 (1955).

[5] R. Karplus and M. Ruderman, Phys. Rev. 98, 771 (1955).

P. N. Lebedev Physics Institute,
Academy of Sciences, USSR

Received February 22, 1956

ON THE THEORY OF ALTERNATING-GRADIENT FOCUSING

E. L. Burshtein and L. S. Solov'ev

(Presented by Academician L. A. Artsimovich February 10, 1956)

The calculations for alternating-gradient focusing in accelerators [1], as well as certain other problems, leads to a differential equation of the form

$$\ddot{x} + \varepsilon p(\varepsilon t, \theta)\,\dot{x} + q(\varepsilon t, \theta)\,x = 0, \tag{1}$$

where ϵ is a small parameter; $\underline{p}$ and $\underline{q}$ are periodical functions with argument Θ; and $d\Theta/dt = \nu(\epsilon t)$. As functions of $\underline{t}$ the coefficients of Equation (1) are "periodic" with slowly changing "amplitude" and "period".

We shall assume that we know two linearly independent solutions $f_n(t)$ and $\varphi_n(t)$ of Equation (1) in any nth "period" of the change in t of the coefficients $\underline{p}$ and $\underline{q}$. We shall count t from the beginning of each period and shall use τ_n to denote the duration of the nth "period" of the coefficients. Because of the linearity of (1) any solution in the nth "period" and its derivative can be represented by

$$x = af_n(t) + b\varphi_n(t), \quad \dot{x} = af'_n(t) + b\varphi'_n(t). \tag{2}$$

We choose f_n and φ_n to satisfy the initial conditions $f_n(0) = \varphi'_n(0) = 1$, $f'_n(0) = \varphi_n(0) = 0$; then the continuity requirement for x and $\dot{x}$ at the boundary between the nth and (n+1)th "periods" leads to the equations

$$x_{n+1} = \alpha_{11}x_n + \alpha_{12}\dot{x}_n, \quad \dot{x}_{n+1} = \alpha_{21}x_n + \alpha_{22}\dot{x}_n, \tag{3}$$

where x_n and $\dot{x}_n$ denote the values of the desired solution and of its derivative at the beginning of the nth "period" and the matrix of the coefficients $\alpha_{ik} = \alpha_{ik}(n)$ is

$$(\alpha_{ik}) = \begin{pmatrix} f_n(\tau_n) & \varphi_n(\tau_n) \\ f'_n(\tau_n) & \varphi'_n(\tau_n) \end{pmatrix}. \tag{4}$$

We must now determine x_n and $\dot{x}_n$. Given $x_n = a$ and $x_n = b$ the solution within any "period" τ_n is obtained by using (2).

By virtue of the small difference of the coefficients in Equation (1) in two adjacent "periods" the coefficients α_{ik} are slowly varying functions of the number $\underline{n}$. Thus (3) can be regarded as a set of two linear equations in finite differences with respect to the unknown functions x_n and $\dot{x}_n$ with slowly varying coefficients α_{ik}.

Let us first consider the case of constant α_{ik} (corresponding to (1) with coefficients which are purely periodic in $\underline{t}$). The solution of the difference Equations (3) with constant coefficients is, as usual, sought in the form [2]:

$$x_n = c_1\lambda^n, \quad \dot{x}_n = c_2\lambda^n. \tag{5}$$

Substituting (5) in (3) we obtain a set of homogeneous equations from which to determine the constants c_1 and c_2:

$$(\alpha_{11}-\lambda)\,c_1+\alpha_{12}c_2=0, \quad \alpha_{21}c_1+(\alpha_{22}-\lambda)\,c_2=0.$$

The requirement that nontrivial solutions exist leads to an equation for λ:

$$\lambda^2-2g\lambda+D=0, \tag{6}$$

where $g = (\alpha_{11}+\alpha_{22})/2$, $D=\alpha_{11}\alpha_{22}-\alpha_{12}\alpha_{21}$. Using the notation $\cos\mu = g/\sqrt{D}$ we obtain

$$\lambda=\sqrt{D}e^{\pm i\mu}. \tag{7}$$

The general solution of (3) can be written as

$$x_n=D^{n/2}(c_1e^{i\mu n}+\overset{*}{c}_1e^{-i\mu n}), \quad \dot{x}_n=D^{n/2}(c_2e^{i\mu n}+\overset{*}{c}_2e^{-i\mu n}). \tag{8}$$

a) Subject to the condition $|g/\sqrt{D}|<1$, μ is real. Transforming to trigonometric functions and satisfying the initial conditions, we obtain

$$\begin{aligned}x_n&=D^{n/2}\left[x_0\cos\mu n+\left(\frac{\alpha_{11}-\alpha_{22}}{2\sqrt{D}\sin\mu}\,x_0+\frac{\alpha_{12}}{\sqrt{D}\sin\mu}\,\dot{x}_0\right)\sin\mu n\right],\\ \dot{x}_n&=D^{n/2}\left[\dot{x}_0\cos\mu n+\left(\frac{\alpha_{22}-\alpha_{11}}{2\sqrt{D}\sin\mu}\,\dot{x}_0+\frac{\alpha_{21}}{\sqrt{D}\sin\mu}\,x_0\right)\sin\mu n\right].\end{aligned} \tag{9}$$

b) When $|g/\sqrt{D}|>1$, μ is purely imaginary and the solution is obtained from (9) through replacement of the trigonometric functions by hyperbolic functions and μ by $|\mu|$, where $|\mu|$ is defined by $\cosh|\mu| = g/\sqrt{D}$.

c) When the characteristic Equation (6) has multiple roots, with $|g/\sqrt{D}|=1$, the Solution (9) loses its meaning, although suitable solutions can be obtained from it in the limit:

1) $$g\to\sqrt{D},\ \mu\to 2m\pi,\ m=1,2,3,\ldots:$$

$$x_n=D^{n/2}\left[x_0+\left(\frac{\alpha_{11}-\alpha_{22}}{2\sqrt{D}}\,x_0+\frac{\alpha_{12}}{\sqrt{D}}\,\dot{x}_0\right)n\right],$$

$$\dot{x}_n=D^{n/2}\left[\dot{x}_0+\left(\frac{\alpha_{22}-\alpha_{11}}{2\sqrt{D}}\,\dot{x}_0+\frac{\alpha_{21}}{\sqrt{D}}\,x_0\right)n\right];$$

2) $$g\to-\sqrt{D},\ \mu\to(2m+1)\pi:$$

$$x_n=D^{n/2}\cos\pi n\left[x_0-\left(\frac{\alpha_{11}-\alpha_{22}}{2\sqrt{D}}\,x_0+\frac{\alpha_{12}}{\sqrt{D}}\,\dot{x}_0\right)n\right],$$

$$\dot{x}_n=D^{n/2}\cos\pi n\left[\dot{x}_0-\left(\frac{\alpha_{22}-\alpha_{11}}{2\sqrt{D}}\,\dot{x}_0+\frac{\alpha_{21}}{\sqrt{D}}\,x_0\right)n\right].$$

We note that the determinant of the matrix (α_{ik}) is the Wronskian determinant of Equation (1) and is given by $D=\exp\left(-\epsilon\int_0^{\tau_n}p_n(t)\,dt\right)$, where $p_n(t)$ is the coefficient of the first derivative in Equation (1) in the nth "period". In this case, when $p_n(t)$ or its mean value in the "period" τ_n is zero, $D = 1$.

We now proceed to construct solutions of the difference Equations (3) for slowly varying $\alpha_{ik}(n)$. By analogy with the B.W.K. method for ordinary differential equations we obtain the solution of (3) in the form

$$x_n = c_1(n)\,\lambda_0\lambda_1\ldots\lambda_{n-1}, \qquad \dot{x}_n = c_2(n)\,\lambda_0\lambda_1, \ldots, \lambda_{n-1}, \tag{10}$$

where λ_n are roots of the characteristic Equation (6) for $g = g(n)$, $D = D(n)$. $c(n)$ and λ_n are assumed to be slowly varying functions of $\underline{n}$. Substituting (10) in (3) and replacing the increments by derivatives, we obtain

$$c_1'\lambda = (\alpha_{11} - \lambda)\,c_1 + \alpha_{12}c_2, \qquad c_2'\lambda = \alpha_{21}c_1 + (\alpha_{22} - \lambda)\,c_2,$$

where primes denote derivatives with respect to $\underline{n}$ and $\underline{n}$ is omitted as an index. Separating the variables c_1 and c_2, substituting for λ its value in (7) and neglecting the products of derivatives and the second derivatives of the slowly varying functions c and λ, we obtain as a result of integration

$$c_1 = \text{const}\cdot\left(\frac{\alpha_{12}}{\sqrt{D}\sin\mu}\right)^{1/2}\exp\left[\mp i\int_0^n \frac{\alpha_{12}}{4\sqrt{D}\sin\mu}\left(\frac{\alpha_{11}-\alpha_{22}}{\alpha_{12}}\right)' dn\right],$$

$$c_2 = \text{const}\cdot\left(\frac{\alpha_{21}}{\sqrt{D}\sin\mu}\right)^{1/2}\exp\left[\mp i\int_0^n \frac{\alpha_{21}}{4\sqrt{D}\sin\mu}\left(\frac{\alpha_{22}-\alpha_{11}}{\alpha_{21}}\right)' dn\right].$$

The product of the roots of the characteristic equation, which appear in (10), is given approximately by

$$\lambda_0\lambda_1\ldots\lambda_{n-1} = \sqrt{D_0D_1\ldots D_{n-1}}\exp\left[\pm i\sum_{k=0}^{n-1}\mu_k\right] \simeq$$

$$\simeq \exp\left(\frac{1}{2}\int_0^n [\ln D - (\ln D)'/2]\,dn\right)\cdot\exp\left[\pm i\int_0^n\left(\mu - \frac{\mu'}{2}\right)dn\right].$$

For simplicity we shall consider μ to be real. Constructing linear combinations of the Solutions (10) and transforming from exponential to trigonometric functions we obtain the general solution of (3):

$$x_n = \left(\frac{\alpha_{12}}{\sqrt{D}\sin\mu}\right)^{1/2}\exp\left(\frac{1}{2}\int_0^n [\ln D - (\ln D)'/2]\,dn\right)\cdot(A_1\cos\Phi_1 + B_1\sin\Phi_1),$$

$$\dot{x}_n = \left(\frac{\alpha_{21}}{\sqrt{D}\sin\mu}\right)^{1/2}\exp\left(\frac{1}{2}\int_0^n [\ln D - (\ln D)'/2]\,dn\right)\cdot(A_2\cos\Phi_2 + B_2\sin\Phi_2),$$

where

$$\Phi_1 = \int_0^n\left[\mu - \mu'/2 - \frac{\alpha_{12}}{4\sqrt{D}\sin\mu}\left(\frac{\alpha_{11}-\alpha_{22}}{\alpha_{12}}\right)'\right]dn,$$

$$\Phi_2 = \int_0^\infty\left[\mu - \mu'/2 - \frac{\alpha_{21}}{2\sqrt{D}\sin\mu}\left(\frac{\alpha_{22}-\alpha_{11}}{\alpha_{21}}\right)'\right]dn.$$

The constants A and B are determined from the initial conditions. Omitting terms of the first order of smallness we finally obtain

$$x_n = P_1(n)\left[x_0\cos\Phi_1 + \left(\frac{\alpha^0_{11}-\alpha^0_{22}}{2\sqrt{D_0}\sin\mu_0}\,x_0 + \frac{\alpha^0_{12}}{\sqrt{D_0}\sin\mu_0}\,\dot{x}_0\right)\sin\Phi_1\right],$$

$$\dot{x}_n = P_2(n)\left[\dot{x}_0\cos\Phi_2 + \left(\frac{\alpha^0_{22}-\alpha^0_{11}}{2\sqrt{D_0}\sin\mu_0}\,\dot{x}_0 + \frac{\alpha^0_{21}}{\sqrt{D_0}\sin\mu_0}\,x_0\right)\sin\Phi_2\right], \qquad (11)$$

where

$$P_1 = \frac{(\alpha_{12}/\alpha^0_{12})^{1/2}\exp\left(\frac{1}{2}\int\limits_0^n [\ln D - (\ln D)'/2]\,dn\right)}{(D/D_0)^{1/4}(\sin\mu/\sin\mu_0)^{1/2}},$$

$$P_2 = \frac{(\alpha_{21}/\alpha^0_{21})^{1/2}\exp\left(\frac{1}{2}\int\limits_0^n [\ln D - (\ln D)'/2]\,dn\right)}{(D/D_0)^{1/4}(\sin\mu/\sin\mu_0)^{1/2}}.$$

Here quantities with the index 0 refer to the initial (zero) "period" and quantities without this index refer to the nth "period" of the coefficients p and q. Equations (11) give an error of the order ϵ/μ in the interval $n \sim 2\pi/\epsilon\mu$.

With the aid of (11) we can write an approximate formula for the product of the four-element matrices with slowly varying elements:

$$(\alpha)_{n-1}(\alpha)_{n-2}\ldots(\alpha)_0 =$$

$$= \begin{pmatrix} P_1\left(\cos\Phi_1 + \dfrac{\alpha^0_{11}-\alpha^0_{22}}{2\sqrt{D_0}\sin\mu_0}\sin\Phi_1\right), & P_1\dfrac{\alpha^0_{12}}{\sqrt{D_0}\sin\mu_0}\sin\Phi_1 \\ P_2\dfrac{\alpha_{21}}{\sqrt{D_0}\sin\mu_0}\sin\Phi_2, & P_2\left(\cos\Phi_2 + \dfrac{\alpha^0_{22}-\alpha^0_{11}}{2\sqrt{D_0}\sin\mu_0}\sin\Phi_2\right) \end{pmatrix} \qquad (12)$$

These relations enable us to calculate for alternating-gradient focusing in accelerators with slowly varying parameters. It is sometimes more convenient to utilize (12) directly for the multiplication of matrices without reference to the initial differential Equation (1).

LITERATURE CITED

[1] E. D. Courant, M. S. Livingston and H. S. Snyder, Phys. Rev. 88, 1190 (1952).

[2] A. O. Gel'fond, Calculation of Finite Differences (1952).

Received November 24, 1955

HYPERFINE STRUCTURE OF PARAMAGNETIC RESONANT LINES IN SUPERCOOLED SOLUTIONS OF $^{51}V^{++}$, $^{53}Cr^{+++}$ AND $^{55}Mn^{++}$

N. S. Garif'ianov

(Presented by Academician G. S. Landsberg March 6, 1956)

The effect of nuclear spin on paramagnetic resonant absorption was discovered in 1948 by S. A. Al'tshuler, B. M. Kozyrev and S. G. Salikhov [1-3]. The experiments were conducted with magnetic field oscillations of the order of 100 Mc and with very dilute aqueous solutions of Mn^{++} and Cu^{++} salts, that is, under conditions which give the Zeeman effect in weak and intermediate fields. Later a hyperfine structure was observed in solutions of salts of VO^{++}, Mn^{++} and Cu^{++} at frequencies of the order of 1000 Mc, that is, under the conditions of the strong field case [4-8].

We give below the results of investigations of the hyperfine structure of paramagnetic resonant lines in supercooled solutions of $^{51}V^{++}$, $^{53}Cr^{+++}$ and $^{53}Mn^{++}$ with frequencies of 520, 150, 91 and 58 Mc at 90° K. Ethyl alcohol and glycerine were used as solvents. The experimental method has been described in [9]. An anthracene line was used to calibrate the magnetic field.

TABLE 1

Solution	Concentration in M/l	Frequency in Mc			
		520	150	91	58
		g-factor			
$^{55}MnCl_2$	0.5	1.2	1.0	1.0	-
$^{53}Cr(NO_3)_3$	0.05	3.0	1.7	1.5	1.2
$^{51}VCl_2$	0.5-0.1	1.0	0.6	0.5	0.5

All three solutions show the dependence of the g-factor for the single resonant absorption peak on the field frequency, $g = h\nu/\beta H^*$; here h is Planck's constant; β is the Bohr magneton, H^* is the static field strength at the absorption maximum. This dependence is given in Table 1.

As was shown in [1-3] for aqueous solutions of ^{55}Mn, the experimental data are in full agreement with the theory of the Zeeman effect in weak fields, that is, the following condition is satisfied:

$$g_F = g_e \frac{F(F+1) + J(J+1) - I(I+1)}{2F(F+1)}, \tag{1}$$

where g_e is the Lande factor for the orbital electrons; F is the resultant moment of the nucleus and orbital electrons; J is the resultant electronic moment and I is the nuclear spin.

For $^{55}Mn^{++}$ in the ground state $^6S_{5/2}$, $J = 5/2$, $I = 5/2$ and $g \simeq 2$. Therefore for all values of F, Equation (1) gives $g_F \simeq 1$. This value of g_F is confirmed by experiment.

In supercooled solutions of $^{55}Mn^{++}$ at 150-91 Mc and lower, (1) is also in good agreement with experiment (see Fig. 1,a). The discrepancy at 520 Mc (see Table 1) can be explained as a case of the Zeeman effect in intermediate fields.

The ground state of free $^{51}V^{++}$ and $^{53}Cr^{+++}$ ions is $^4F_{3/2}$. But the local nonspherical electric field "freezes the orbit", so that in (1) we must replace J by S, and g_e by the effective g-factor for spectroscopic splitting.

For $^{53}Cr^{+++}$, $S = 3/2$, $I = 3/2$ and $g \simeq 2$. Therefore (1) gives $g_F \simeq 1$. As can be seen from Table 1, at lower frequencies g for $^{53}Cr^{+++}$ actually approaches unity (see Fig. 1,b). It may be concluded that the conditions for the Zeeman effect in weak fields are realized for $^{53}Cr^{+++}$ at frequencies ≤ 58 Mc.

For $^{52}Cr^{+++}$ the g-factor of the absorption peak is independent of the field frequency (I = 0).

For $^{51}V^{++}$, if we take $S = {}^3/_2$, $I = {}^7/_2$ and $g \simeq 2$, (1) gives $g_{F_1} = 0.6$, $g_{F_2} = 0.4$, $g_{F_3} = 0$ and $g_{F_4} = -1$. Experiment reveals a single broad resonance curve with a g-factor which approaches the value 0.5 as the frequency is reduced; we consider this to be a superposition of three broad peaks with $g_{F_1} = 0.6$, $g_{F_2} = 0.4$ and $g_{F_4} = 1$. Thus for $^{51}V^{++}$ the conditions for the Zeeman effect in weak fields are realized at frequencies ≤ 100 Mc.

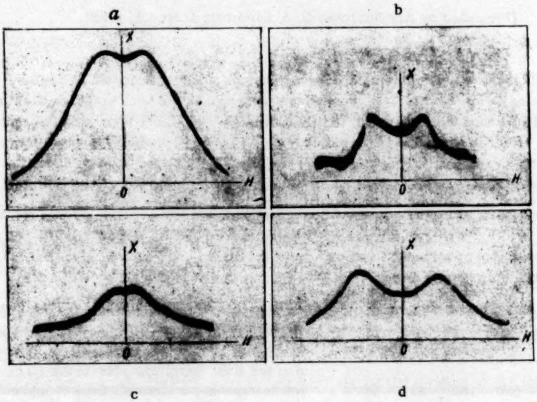

Fig. 1. a) $^{55}MnCl_2$ in alcohol 0.5 M/ℓ, ν = 150 Mc, T = 90°K; b) $^{53}Cr(NO_3)_3$ in alcohol 0.05 M/ℓ, ν = 91 Mc, T = 90°K; c) $^{52}Cr(NO_3)_3$ in alcohol 0.05 M/ℓ, ν = 91 Mc, T = 90°K; d) $^{51}VCl_2$ in alcohol 0.5 M/ℓ, ν = 150 Mc, T = 90°K. The photographs show double curves.

At 9580 Mc and 90°K in supercooled solutions of 0.05 M/ℓ $^{53}Cr(NO_3)_3$ and $^{51}VCl_2$ there were observed paramagnetic resonant absorption curves whose widths are ΔH = 260 oerst and 600 oerst, respectively, without resolution of the hyperfine structure. Ethyl alcohol was used as solvent.

The absence of an observed hyperfine structure may be due to smallness of the hyperfine splitting constant as well as to the fact that the absorption curve is broadened at higher frequencies.

In conclusion the author wishes to thank B. M. Kozyrev and S. A. Al'tshuler for discussions, and E. I. Semenova for preparing the samples.

LITERATURE CITED

[1] S. A. Al'tshuler, B. M. Kozyrev and S. G. Salikhov, Doklady Akad. Nauk SSSR 71, 855 (1950).

[2] B. M. Kozyrev, Bull. Acad. Sci. U.S.S.R., Phys. Ser. 16, 5, 533 (1952).

[3] B. M. Kozyrev, Report at All-Union Conference on Radiospectroscopy, Kazan, 1955.

[4] E. E. Schneider and T. S. England, Physica 17, 221 (1951).

[5] M. Tinkham, R. Weinstein and R. F. Kip, Phys. Rev. 84, 848 (1951).

[6] N. S. Garif'ianov and B. M. Kozyrev, Doklady Akad. Nauk SSSR 98, 929 (1954).

[7] N. S. Garif'ianov and B. M. Kozyrev, Scientific Records of the V. I. Ul'ianov-Lenin Kazan Univ. 114, 8 (1954).

[8] N. S. Garif'ianov, Doklady Akad. Nauk SSSR 103, 41 (1955).

[9] N. S. Garif'ianov, Doklady Akad. Nauk SSSR 101, 503 (1955).

[10] N. S. Garif'ianov and B. M Kozyrev, Report at all-Union Conference on Radiospectroscopy, Kazan, 1955.

Physicotechnical Institute,
Kazan Affiliate,
Academy of Sciences, U.S.S.R.

Received January 2, 1956

ELECTRICAL PHENOMENA IN THE DISRUPTION MECHANISM OF SOME SOLIDS

Corresponding Member of the Academy of Sciences of the U.S.S.R.
B. V. Deriagin, N. A. Krotova and V. V. Karasev

In earlier articles [1] we described electrical phenomena (luminescence, electron emission) which we observed during the stripping off of polymer films and the splitting of various crystals – quartz, Rochelle salt, mica, gypsum, tourmaline and a number of others. In one of our articles [2] it was shown that the effect which we observed must be associated with the mechanical properties of the crystals.

Luminescence during splitting in air, which is usually called triboluminescence, has been familiar for a very long time. It was observed by Boyle during the splitting of rock salt and quartz, by B. Severgin, N. Gezukhus, L. A. Chugaev and others. Systematic investigations of this phenomenon as a function of the structure of various minerals were carried out by V. I. Vernadskii and B. Lindener [3].

I. V. Obreimov [4] split mica (muscovite) in a high vacuum (10^{-4} - 10^{-5} mm Hg) and observed a phenomenon which, in our opinion, must be regarded as a special type of autoelectric emission. However, Obreimov gave no explanation and did not compare the phenomenon with the change in the work of cleavage for mica as a function of the pressure of the ambient, which the same author also observed.

The increased work of cleavage of mica in a vacuum is explained by Obreimov as being due to the removal of adsorbed layers from the internal surfaces of the mica – these are layers which exercise a loosening effect and weaken the adhesion of mica leaves. The work of cleavage was identified with surface energy on the assumption that cleavage occurs when the molecular forces at the point of contact O balance the moment M which is bending the leaf of mica.

Cleavage was performed by driving a wedge into a space between leaves of mica. Obreimov observed the following: when the wedge is introduced the crack either grows gradually and slowly or suddenly with a snap. The latter effect is usually observed in a vacuum. Equilibrium is not established immediately after introducing the wedge; under atmospheric conditions a few seconds are required for this purpose and in a high vacuum as much as a few days. It follows from his account that Obreimov was not concerned with the effect of speed on the work of cleavage of mica; the advance of the wedge and the growth of the crack took place with different speeds in different experiments. This is a possible explanation of the large scatter of points in the graphs.

In our experiments on the cleavage of mica we used a fundamentally different method in which special attention was paid to determining the work of cleavage as a function of time. We assumed that during the fracture of crystalline bodies (especially mica) the space between the cleavage surfaces can contain strong fields (which Obreimov also observed) because of the separation of opposite charges which form a mosaic of alternate signs.

In the experiments described in one of our articles [2] we observed electron emission during the cleavage of mica, gypsum and other crystals in a high vacuum (10^{-4} mm Hg). These experiments were repeated by N. A. Krotova and V. V. Karasev, who obtained photographs which show clearly that maximum emission is observed in the space between the cleaved leaves and that the surfaces of the fracture also emit electrons (Fig. 1,a). Our method also enabled us during the cleavage of gypsum to observe the fine structure of the cleavage surfaces. In Fig. 1,b the strong light-struck region corresponds to the place where the blade cut through, the fine lines are regions where the gypsum split along cleavage planes (a pre-existing disruption zone with the direction of splitting parallel to the cleavage planes). Fig. 1,c shows the ends of broken gypsum fibers (the direction of the break

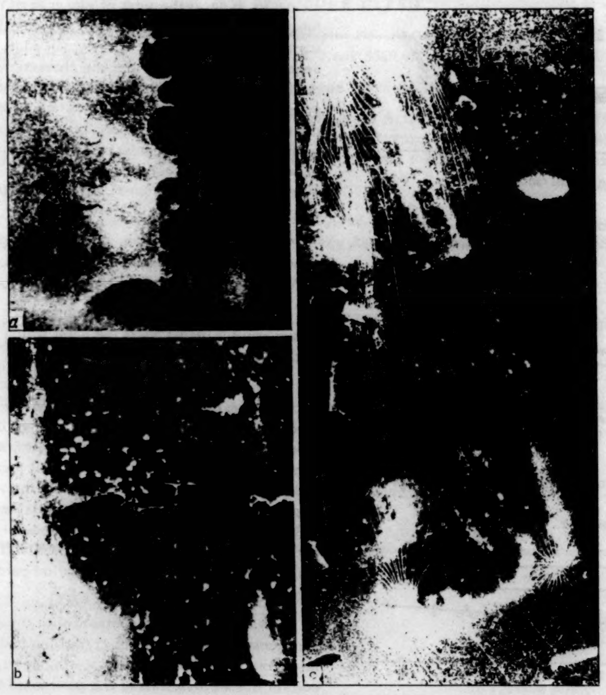

Fig. 1.

is perpendicular to the cleavage planes). Thus when splitting occurs parallel to the cleavage planes, we observe the separation of fibers. When the break is perpendicular to the cleavage planes the fibers are broken with their ends appearing as bright spots in the photograph.

On the basis of our work on adhesion [5] we were able to postulate (assuming an analogous mechanism for stripping off) that, first, the work of cleavage of mica must depend on the speed of the process and, secondly, it must be affected by such factors as the pressure and nature of the gas in which the splitting takes place.

For our experiments on the cleavage of mica we used an adhesiometer with a rotating plate [5]; the split-off leaf was a few microns thick. A weight was attached to the end of the leaf and the work of cleavage was determined from the equation

$$A = \frac{Pl}{S}(1 - \cos\alpha)$$

also the corresponding speed $v = \ell / t$, where ℓ is the length of the split-off strip, P is the load, t is the time, S is the area of the strip and α is the angle of splitting.

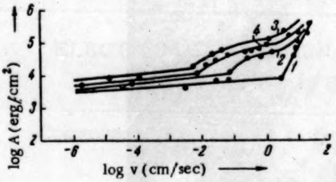

Fig. 2. Cleavage of mica at various pressures.
1) P = 760 mm; 2) 160 mm; 3) 100 mm; 4) 10 mm.

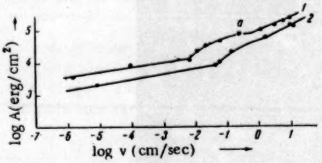

Fig. 3. Cleavage of mica in air (1) and in argon (2) at P = 10 mm.
a) Start of luminescence.

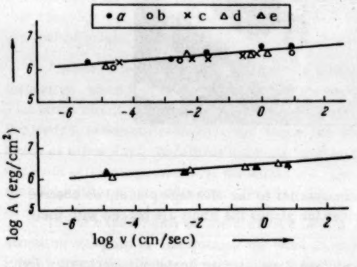

Fig. 4. Removal of a layer of nitrile-based rubber.
a) P = 760 mm; b) 160 mm; c) 100 mm; d) 10 mm;
e) argon, P = 10 mm.

Fig. 2 shows the work of cleavage of mica as a function of speed at various pressures, on a logarithmic scale. These curves show clearly (in addition to the dependence on the rate) that the character of the adhesiograms differs with the pressure and that at lower pressure the work of cleavage is increased similarly to the effects observed when polymer films are stripped from a backing, in accordance with the electrical theory of adhesion. In the curves of A for given $\underline{v}$ and P (Fig. 2) a peak value of the work of cleavage is observed at a given pressure.*

When mica is split in argon the work of cleavage is reduced in comparison with air. This takes place at different pressures of the ambient (see Fig. 3).

It is characteristic that luminescence is observed during rapid splitting ($\underline{a}$ is the point which corresponds to the start of luminescence).

When polymer films are removed from various backings luminescence is also observed during a fast process in argon. Discharges are observed during fast processes, to which Paschen's law applies, and A is reduced in argon. It should be noted that argon is inert and poorly adsorbed. Thus changes in the work of splitting under these conditions can be explained only as an influence of the argon on the magnitude of the discharge potential during the separation of double electrical layers corresponding to the low ionization potential of argon.

It is interesting to compare with the described experiments on the fracture of crystalline bodies, especially mica, our experiments on the tearing apart of rubbers and certain fibrous materials of the pasteboard type. When these materials are torn apart in a vacuum no trace of electronic emission is observed. Rubber and pasteboard are heterogeneous systems in which the particles of the filler (fibers, carbon black, kaolin, etc.) are encased in a high polymer. When the filler content is not too high the separation takes place in the high polymer coating. Consequently there is no reason to expect electrical phenomena in this case, since the separation does not take place in a phase interface.

The curves log A = f (log v) for rubber also show no strong dependence on speed, and the curves at different pressures coincide. The argon atmosphere in which the experiment was conducted did not affect the work of separation nor the character of the curves.

A comparison of the behavior of mica and rubber materials (Fig. 4) when disrupted in air and in a vacuum demonstrates graphically the relation between the electrical phenomena observed in the cleavage of mica and its mechanical properties – a relation which should also be expected to hold in the fracture of other crystalline bodies and, possibly, in the disruption of some heterogeneous systems when internal phase interfaces are separated.

N. E. Golynskii performed a portion of the experimental work.

---

* It should be noted that the curves A = f (P) for the removal of polymer films from a backing show no peaks.

LITERATURE CITED

[1] V. V. Karasev, N. A. Krotova and B. V. Deriagin, Doklady Akad. Nauk SSSR 88, 776 (1953); 89, 108 (1953); V. V. Karasev, and N. A. Krotova, Doklady Akad. Nauk SSSR 99, 715 (1954).

[2] N. A. Krotova and V. V. Karasev, Doklady Akad. Nauk SSSR 92, 606 (1953).

[3] Boyle, Opera Varia 1680, 164-168; B. Severgin, Nova Acta Acad. Petrop. 12, 11 (1793); N. Gezekhus, J. Russ. Phys. Chem. Soc., Phys. Sect. 13 (1902); L. A. Chugaev, J. Russ. Phys. Chem. Soc. 32, 837 (1900); V. I. Vernadskii, Bull. Imp. Acad. Sci. (Russia) 24, 69 (1906); B. Lindener, Bull. Imp. Acad. Sci. (Russia) 4, 999 (1910).

[4] I. V. Obreimov, Proc. Roy. Soc. 127, 290 (1930).

[5] B. V. Deriagin and N. A. Krotova, Adhesion (Acad. Sci. U.S.S.R. Press, Moscow and Leningrad, 1949); B. V. Deriagin, N. A. Krotova and Iu. M. Kirillova, Doklady Akad. Nauk SSSR 97, 475 (1954); B. V. Deriagin, Vestnik Akad. Nauk SSSR 7, 10 (1954).

Institute of Physical Chemistry,
Academy of Sciences, U.S.S.R.

Received March 3, 1956

THE ABSORPTION OF ULTRASONIC WAVES OF FINITE AMPLITUDE IN LIQUIDS

L. K. Zarembo, V. A. Krasil'nikov and V. V. Shklovskaia-Kordi

(Presented by Academician M. A. Leontovich March 2, 1956)

1. It has been shown that at frequencies from 4 to 10 Mc the absorption coefficient of ultrasound in liquids depends on intensity [1-3]. Increased absorption with intensity does not result from the development of cavitation processes since the increase of absorption is gradual; the medium in which the wave of finite amplitude is propagated is optically empty [1] and cavitation is impeded at high ultrasonic frequencies [4]. A wave of finite amplitude propagated in a liquid undergoes a distortion of its shape with consequent formation of harmonics [5]. The formation of harmonics must be accompanied by increased absorption, and the relative increase of the absorption coefficient which is associated with the production of harmonics must be greater at lower frequencies [2]. In addition, the effect of sound streaming is diminished at low frequencies. It was therefore of interest to investigate the absorption of waves of finite amplitude with fundamental frequencies below 4 Mc.*

2. The absorption measurements were performed in a 68 × 10 × 11 cm tank damped with a layer of sponge rubber at the end. The radiator was a circular quartz plate with an air cushion on its inoperative side of 3.0 cm diameter and a silver coating of 2.8 cm diameter; this was excited by a fundamental frequency of 1.5 Mc. The quartz circuit was inductively coupled to the oscillator output, which had a high-frequency output of 350 w. With 3 kv applied to the quartz the intensity in the immediate neighborhood of the plate was ~ 18 w/cm^2. Various types of copper-constantan thermocouples were used as ultrasonic receivers. The operating junction of the thermocouple was placed in a soft rubber absorber; the inoperative end was in the ultrasonic field at a distance from the other junction (in order to eliminate errors due to temperature changes in the medium). For the purpose of increasing the sensitivity and of obtaining more uniform reception throughout the beam cross section, we used receivers of 4.5 cm diameter and 25 thermocouples connected in series.

Thermal methods of making measurements in a medium-intensity ultrasonic field at these frequencies possess a number of advantages over piezoelectric and radiometric methods, the principal advantage being the simultaneous combination, in thermal methods, of nonresonant thermal receivers, easier shielding from the effects of sound streaming and large inertia of the thermal receivers. The latter fact results in time averaging of intensity fluctuations which are possibly associated with turbulent sound streaming at radiated intensities above $\sim$1.5-2.0 w/cm^2. In order to reduce the scattering of heat due to thermal conductivity as well as the effect of sound streaming, the thermocouple junctions and the absorber were placed in an ebonite capsule. We also used the following procedure: voltage was applied to the quartz for a period of $\tau = 2$-10 sec (the majority of measurements were made with $\tau = 2$ sec). This also led to diminished heating of the medium during the measurements (during a measuring cycle with $\tau = 2$ sec this did not exceed 1.5-2.0°). Absolute intensity measurements were performed by calorimetry with a Dewar at the points where the absorption coefficient was to be determined. The relative experimental error did not exceed 15-20%.

3. Results obtained for the absorption coefficient are given in Table 1. Figs. 1 and 2 show the dependence of the absorption coefficient in methyl alcohol, glycerine and transformer oil. The fluids, with the natural exception of the transformer oil, were chemically pure.

An increase of the absorption coefficient by two orders of magnitude at ~ 4w/cm^2 intensity compared with its values at small amplitudes was observed in ethyl amd methyl alcohol and toluene, somewhat less in distilled

---

* This work was begun jointly with S. A. Akhmanov in 1953.

TABLE 1

I*, w/cm^2	$2\alpha_l$, 1/cm	$\frac{2\alpha_l}{\nu^2}\cdot 10^{17}$, sec^2/cm	t, °C
96% ethyl alcohol			
Small amplitudes**	0.0025	110	20
0.9	0.075	3340	20
0.93	0.065	2890	21.5
1.1	0.084	3740	21.5
1.35	0.075	3340	21.5
1.8	0.121	5380	21.5
1.86	0.107	4760	21.5
1.9	0.118	5250	20
2.25	0.095	4220	21.5
3.5	0.159	7070	21.5
3.7	0.168	7470	21.5
Toluene			
Small amplitudes**	0.0036	160	20
0.4	0.043	1910	17
0.65	0.079	3510	17
0.8	0.05	2220	20
1.0	0.068	3020	20
1.2	0.06	2670	20
1.33	0.10	4450	17
1.8	0.11	4890	20
2.1	0.13	5780	20
5.3	0.28	12440	20
Distilled water			
Small amplitudes**	0.00103	46	20
2.0	0.012	530	20
4.0	0.015	670	
4.7	0.029	1290	20
7.0	0.024	1070	
9.0	0.038	1690	19
85% formic acid			
1.0	$\alpha =$ 0.074***	$\frac{\alpha}{\nu^2} = 3290$	23
80% acetic acid			
1.4	$\alpha =$ 0.256***	$\frac{\alpha}{\nu^2} = 11370$	31.5

---

* Intensities are given for the middle of the region in which the absorption coefficient is determined.

** The values of $2\alpha_0/\nu^2$ for small amplitudes were taken from [8]; $2\alpha_0$ was calculated for 1.5 Mc.

*** Measured with a piezoelectric receiver.

water and an insignificant amount in viscous liquids: transformer oil and glycerine. The absorption coefficients at intensities of the order of 1 w/cm^2 in acetic and formic acid fit well on extrapolated curves for the dependence of α on ν which were obtained by P. A. Bazhulin [6].

4. In order to determine the influence of cavitation at this frequency in some liquids, we measured absorption at a higher static pressure. The liquids were poured into a brass tube with an inside diameter of 4.6 cm and 41 cm length, with a 1.5 Mc quartz radiator at the bottom. A piston, which was moved by a screw, bore a holder for the ebonite capsule in which the operating junctions of the copper-constantan thermocouples were placed in the rubber absorber. The surface of the piston facing the radiator was damped with sheets of vacuum rubber. The pressure gauge was connected to the tube very close to the radiator. Absorption measurements in methyl alcohol and tap water at excess pressures of 15, 10, 5 and 0 kg/cm^2, like the measurements in the tank at atmospheric pressure, were made with τ = 2 sec and

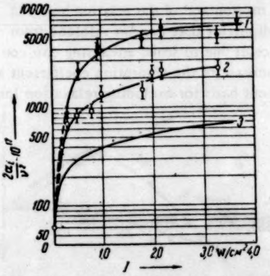

Fig. 1. Intensity dependence of $2\alpha_1/\nu^2$ in methyl alcohol:
1) Measured by a thermoelectric receiver (t = 21°); 2) measured by an unshielded radiometer (t - 16°); 3) calculated by Fox and Wallace [2].

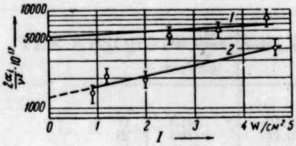

Fig. 2. Intensity dependence of $2\alpha_i/\nu^2$. 1) In glycerine (t = 20°) in transformer oil (t = 19°).

V = 2 kv(intensity at the radiator ~7.8 w/cm²; acoustic pressure $P_0 \simeq (2\rho_0 c_0 I)^{1/2}$ = 4.85 atmos for water). No difference was detected between absorption in methyl alcohol at 15 kg/cm² excess pressure and without excess pressure. In tap water this difference is within experimental error. We can thus assume that at 1.5 Mc, at least for τ = 2 sec, cavitation cannot develop with intensities of the order of a few watts per cm². Since the majority of the absorption measurements were made with τ = 2 sec, it can be assumed that cavitation does not cause the marked increase of absorption.

5. The absorption of ultrasonic waves of finite amplitude in liquids is influenced by the distortion of the wave during its propagation and resulting harmonics [2,5]. According to [2] the coefficient $2\alpha_i$ of a "relatively stable" wave of finite amplitude with θ curvature of the wave front is given by $2\alpha_i = 2R_\theta\alpha_0$, where α_0 is the absorption coefficient for small amplitudes; the relative increase of the absorption coefficient is given by

$$R_\theta = \left(\frac{B}{A}\pi P_0\delta_k^{(1)} + 0.1\alpha_0\rho_0 c_0^2\lambda\right)(0.1\,\alpha_0\rho_0 c_0^2\lambda)^{-1}$$

(assuming that the pressure is dependent on the compression s through the equation $p = p_0 + As + \frac{B}{2}s^2$); P_0 is the acoustic pressure amplitude; $\delta_k^{(1)}$ is a factor which determines the transfer of energy from the fundamental wave to the harmonics; ρ_0 is the density; c_0 is the velocity; λ is the wavelength. Fig. 1 gives the experimental dependence of the absorption coefficient in methyl alcohol (Curve 1) and the curve calculated from the formula with $\delta_k^{(1)} = 0.01$ [2] and B/A = 6.6 [7] (Curve 3). The discrepancy between the theoretical and experimental values lies far outside the limits of experimental error. We note, however, that some of the qualitative laws of the approximate theory of Fox and Wallace [2] are obeyed: 1) within experimental error the relative increase of the absorption coefficient is proportional to the acoustic pressure; 2) for liquids with small α_0 (ethyl and methyl alcohol, toluene, water) the relative increase of the absorption coefficient is greater than in liquids with larger α_0 (transformer oil, glycerine). It should also be noted that the relative increase of absorption at 1.5 Mc is greater than is given in the literature at higher frequencies; this also follows from the relation for R_θ. When absorption coefficients are compared it should be kept in mind that the experimental methods used in [1-3], considering the "nonmonochromaticity" of the wave of finite amplitude and the effect of sound streaming, are not free of certain shortcomings.

Thus the marked increase of the absorption coefficient at 1.5 Mc cannot be attributed entirely to distortion of the wave shape which is associated with nonlinearity of the equation of motion and of the relation between compression and pressure. A comparison of measurements made with a radiometer that was not shielded from sound streaming (Fig. 1,2) with thermoelectric measurements shows that losses due to sound streaming can contribute significantly to the absorption. The absence of any considerable increase of the absorption coefficient at these frequencies in formic and acetic acid is not, in our opinion, a sufficient basis for excluding relaxation losses from consideration in a wave of finite amplitude.

LITERATURE CITED

[1] F. E. Fox, Nuovo Cimento 7, Ser. IX, Suppl. No. 2, 198 (1951).

[2] F. E. Fox and W.A. Wallace, J. Acoust. Soc. Am. 26, 994 (1954).

[3] D. M. Towle and R. B. Lindsay, J. Acoust. Soc. Am. 27, 530 (1955).

[4] W. Gaertner, J. Acoust. Soc. Am. 26, 977 (1954).

[5] L. K. Zarembo, V.A. Krasil'nikov and V.V. Shklovskaia-Kordi, Doklady Akad.Nauk SSSR 109,3 (1956).

[6] P. A. Bazhulin, J. Exptl.-Theoret. Phys. (U.S.S.R.) 8, 4,457 (1938).

[7] M. Kornfel'd, Elasticity and Strength of Liquids (1951).

[8] I. G. Mikhailov, Propagation of Ultrasonic Waves in Liquids (1949).

Laboratory of Anisotropic Structures,
Academy of Sciences of the U.S.S.R.

Received February 28, 1956

THE TRANSVERSE PHOTOMAGNETIC EFFECT IN n- AND p-TYPE GERMANIUM

Academician I. K. Kikoin and Iu. A. Bykovskii

One of the authors [1] has shown that when a semiconductor (copper oxide) is irradiated in a magnetic field, in addition to the ordinary photomagnetic effect there is observed the so-called "transverse" photomagnetic effect.

As we know, the ordinary photomagnetic effect is the following: When a sample is irradiated along the $\underline{y}$ axis while the magnetic field is directed along the $\underline{x}$ axis, an emf is produced in the $\underline{z}$ direction which is proportional to the field strength H. When in addition to the field component H_x we have a component H_y, there is another emf generated in the $\underline{x}$ direction, which is proportional to the product H_xH_y. This is the transverse photomagnetic effect.

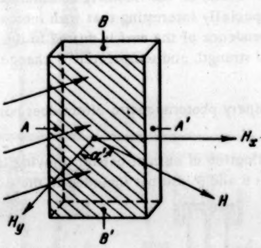

Fig. 1

It is evident that for observation of this effect the sample in the form of a rectangular plate must form an angle α with the direction of the field H (see Fig. 1). Then when the plate is irradiated in the direction L between the electrodes B and B' a photomagnetic emf is generated which is proportional to H_x; but between the electrodes A and A' the transverse photomagnetic emf is produced, which is proportional to $H_xH_y = H^2 \sin 2\alpha$. This is the experimental method which gave the results that will be presented below.

The samples used were flat plates (12 × 6 × 0.8) cut from a single crystal of germanium (the resistivity of the samples was 45 ohm·cm for p-type germanium and 40 ohm·cm for n-type germanium.

The samples were mounted on a slide in a glass tube. The tube and samples were then placed between the poles of a large electromagnet. By rotating the slide around its axis it was possible to change the angle between the plane of the sample and the direction of the magnetic field.

As might be expected, the transverse emf (between electrodes A and A') was zero for $\alpha = 0$ and reached its maximum at $\alpha = 45°$.

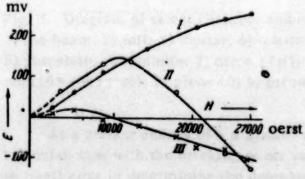

Fig. 2. p-Type germanium.
I) t = + 20°; II) t = − 20°; III) t = − 100°.

The dependence of the transverse photomagnetic emf on the field strength was very distinct, as is shown in Fig. 2. For weak fields this emf E was proportional to H^2 as expected. In strong fields the character of the dependence of the emf on the field strength is strongly affected by the temperature of the sample. At room temperature the emf increases monotonically with the field (Curve I),

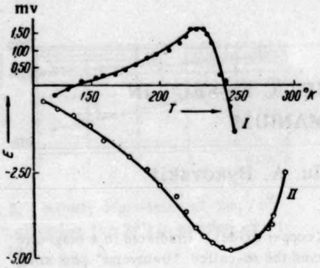

Fig. 3. I) p-Type germanium; II) n-type germanium; H = 20,000 oerst.

but at lower temperatures (Curves II and III) it reaches a maximum, passes through zero and finally changes sign. When the direction of the magnetic field is changed the magnitude and sign of the transverse emf are preserved under all conditions.

The magnetic field strength corresponding to the maximum emf is reduced at lower temperatures (it is possible that for the observation of the maximum emf at room temperature the fields available to us were not of sufficient magnitude).

We also investigated the temperature dependence of the transverse photomagnetic effect for p-type and n-type germanium, as shown in Fig. 3.

It is essential to note that for p-type germanium the transverse photomagnetic emf changes sign twice as it passes through its maximum. For n-type germanium in the investigated temperature range no change of sign of the effect is observed.

The magnitude of the transverse photomagnetic emf depends, of course, on the intensity of irradiation (at low intensities the emf is proportional to the illumination). It is especially interesting that with increased intensity of irradiation the peak of the curve representing the field dependence of the emf is shifted in the direction of stronger fields. This indicates that at a given value of the field strength and temperature a change in the illuminating intensity produces a change in the sign of the effect.

The above refers only to samples of p-type germanium. The ordinary photomagnetic effect does not show these anomalies in the same samples.

The transverse photomagnetic effect is evidently the result of deflection of current carriers moving in the direction of the photomagnetic emf (in spite of the fact that electrodes B and B' are not included in the external circuit).

LITERATURE CITED

[1] I. K. Kikoin, Doklady Akad. Nauk SSSR 3, 418 (1934).

Received March 23, 1956

A STUDY OF THE REACTION OF He^3 WITH DEUTERONS

A. P. Kliucharev, B. N. Esel'son and Academician A. K. Val'ter
of the Academy of Sciences of the Ukrainian S.S.R.

A considerable number of papers [1, 4] have been devoted to the nuclear reaction resulting from the bombardment of the light helium isotope with deuterons. But the results thus far obtained by different investigators show marked divergence. We studied the excitation function of the $He^3(dp)He^4$ reaction and measured the absolute cross section of the reaction during 1953 [5].

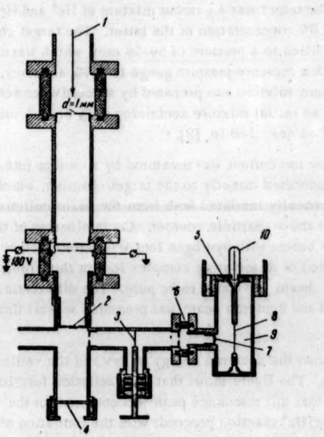

Fig. 1. Diagram of target chamber and counter. 1) Ion beam; 2) foil; 3) shutter; 4) quartz glass; 5) porcelain; 6) insulator; 7) mica (4 μ); 8) platinum (d = ~ 0.1 mm); 9) glass; 10) to preamplifier.

The deuterons with which the target were bombarded were accelerated in the high-voltage discharge tube of an electrostatic generator whose high voltage was stabilized by a corona triode and measured by an oscillating voltmeter in a compensating circuit. The oscillating voltmeter was calibrated by the resonance maxima of the excitation function for the $F^{19}(p, \alpha\gamma)O^{16}$ reaction. We used a shielded gas target so that the voltage on the conductor of the electrostatic accelerator did not completely determine the deuteron energy for which interactions with target nuclei took place. It is necessary to take into account the deuteron energy losses due to passage through the shielding foil. We used an aluminum foil whose thickness was of the order of 5 μ. This thickness (and not less) was chosen because our accelerator was able to provide a stable potential of not less than 900 kev and sufficient current for the experiment (focused on the target). Therefore the lowest value of the deuteron energy is 450 kev if we use the molecular component D_2^+ of the ion beam. For lower energies thicker foils had to be used.

The coil thickness is determined in two ways – by direct measurement using an optical gauge and by weighing. Both methods gave 5.1 μ for the thickness of our foils within 2-3%. Energy losses were obtained from the data of Parkinson, et al. [6] and of Warshaw [7] for low energies, and from Bethe [8] for energies above 400 kev.

At a current density of 1 μ a/mm² we did not detect the carbon film which appears on a foil under a beam in conjunction with the cracking of oil vapor; this was the current density which we used for low energies. The over-all error in determining the deuteron energy was ± 30 kev for energies in the range of resonant excitation.

A diagram of the target and counter for recording α-particles from the reaction is given in Fig. 1. The total beam of accelerated deuterons passed through a magnetic analyzer and the required component was sent into the shielded gas target through a collimator which was bounded by two diaphragms of 1 mm diameter.

TABLE 1

$\sigma_{90°}$, mbarn/ /steradian	E_{res}, kev	Years and authors
55.0±2.7	400±10	1952(1)
71.5±8	430±30	1953(2)
63.4±3.2	435±30	Our experiment
75.0±7.5	430	1954(3)
55.6±1.1	427	1955(4)

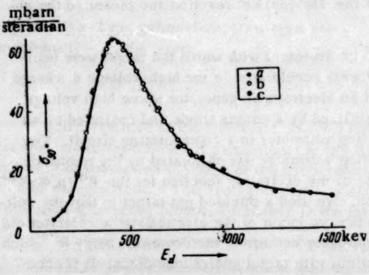

Fig. 2. Cross section of $He^3(dp)He^4$ ($\theta = 90°$) as a function of deuteron energy.
a) Measured with D_2^+; b) with DH^+; c) with D^+.

After passing through an auxiliary diaphragm of 4 mm diameter bearing a −180 v potential, the deuteron beam entered the target through a 3 mm opening sealed with aluminum foil. The bottom of the target chamber was a quartz glass which permitted adjustment of the target along the beam axis; α-particles from the reaction were recorded by a counter whose entrance window was sealed with 4 μ mica. Before entering the counter the α-particles traversed a "long" diaphragm measuring 3.1 × 7.2 mm. The "long" diaphragm was used so that at low energies the ion beam, because of multiple scattering in the foil, will limit the effective target volume to a cone whose entire base can be "seen" from the center of the detector. A screen could be put in the path of the α-particles so that the counter background could be measured.

The target was a gaseous mixture of He^4 and He^3 with 57.6% concentration of the latter. The target chamber was filled to a pressure of 50-56 mm, which was measured with a mercury pressure gauge to ± 1% accuracy. Our helium mixture was prepared by successive enrichment of an initial mixture containing 2.4% of He^3, using the method described in [9]. •

The ion current was measured by a current integrator connected directly to the target chamber, which was electrically insulated both from the beam collimator and from the α-particle counter. Contamination of the deuteron beams with hydrogen ions was determined by the method of dissociating complex ions in thin films. The D_2^+ beam was found to be pure. The differential cross section of the $He^3(dp)He^4$ reaction at 90° to the direction of the deuteron beam was measured several times using different components of the deuteron beam.

The results are given in Fig. 2, where the horizontal axis shows the deuteron energy in kev and the vertical axis gives the differential cross section in millibarns per steradian. The figure shows that the excitation function has a resonance peak at deuteron energy 435 ± 30 kev. We note that this resonance peak was obtained for the first time by us in 1949. The resonance indicates that the $He^3(dp)He^4$ reaction proceeds with the formation of a compound Li^5 nucleus with an excitation level at 16.8 Mev. The absolute value of the cross section at resonance is 63.4 ± 3.2 millibarns per steradian according to our measurements.

In conclusion we give in Table 1 the differential cross sections for resonance at 90° taken from various authors.

LITERATURE CITED

[1] T. W. Bonner, J. P. Conner and A. B. Lillie, Phys. Rev. 88, 473 (1952).

[2] J. L. Yarnell, R. H. Lovberg and W. R. Stratton, Phys. Rev. 90, 292 (1953).

[3] G. Freier and H. Holmgren, Phys. Rev. 93, 825 (1954).

• The He^3 concentration was determined by N. E. Alekseevskii in the Institute of Physical Problems of the Academy of Sciences of the U.S.S.R., with ± 1.5% accuracy.

[4] W. E. Kunz, Phys. Rev. 97, 456 (1955).

[5] A. K. Val'ter, A. P. Klincharev and B. N. Esel'son, Tech. Report of the Physicotechnical Institute, Academy of Sciences of the U.S.S.R., 1954.

[6] D. B. Parkinson, et al., Phys. Rev. 52, 75 (1937).

[7] S. D. Warshaw, Phys. Rev. 76, 1759 (1949).

[8] H. A. Bethe, Rev. Mod. Phys. 22, 213 (1950).

[9] B. N. Esel'son and B. G. Lazarev, J. Exptl.-Theoret. Phys. (U.S.S.R.) 20, 742 (1950).

Physicotechnical Institute,
Academy of Sciences of the U.S.S.R.

Received November 17, 1955

THE SPECTRAL REPRESENTATION AND THE RENORMALIZATION GROUP

A. A. Logunov

(Presented by Academician N. N. Bogoliubov March 12, 1956)

In several articles a spectral (interaction) representation has been given for the Green's function in quantum field theory [1-3]. In this representation the Green's function of interacting fields can be represented as a superposition of Green's functions for free-particle fields with different masses. The spectral functions are real and characterize the field in detail.

In quantum electrodynamics the spectral representation of the Green's function for photons can be written as [3]:

$$d_c(k^2) = -1 + \int_0^\infty \frac{dM^2}{M^2} \frac{k^2}{M^2 - k^2 - i\varepsilon} f\left(\frac{M^2}{m^2}, e_0^2\right), \tag{1}$$

where f is a real function.

From considerations of homogeneity in momentum space and introducing the λ-normalization [4] we can transform from the correct function $d_c\left(\frac{k^2}{m^2}, e_0^2\right)$ to $d(x, y, e^2)$ [4]. The spectral representation of $d(x, y, e^2)$ can be written as:

$$d(x, y, e^2) = A(y, e^2) - \int_0^\infty I(\nu, y, e^2) \frac{x}{\nu - x - i\varepsilon} d\ln\nu, \tag{2}$$

where

$$A(y, e^2) = 1 - \int_0^\infty \frac{I(\nu, y, e^2)}{\nu + 1} d\ln\nu. \tag{3}$$

Substituting the above expression for d in the functional equation [4,5]

$$t > 0, \quad d(x, y, e^2) = d(-t, y, e^2)\, d\left(\frac{x}{t}, \frac{y}{t}, e^2 d(-t, y, e^2)\right), \tag{4}$$

we obtain

$$\begin{gathered} A(y, e^2) = d(-t, y, e^2)\, A\left(\frac{y}{t}, e^2 d(-t, y, e^2)\right), \\ I(\nu, y, e^2) = d(-t, y, e^2)\, I\left(\frac{\nu}{t}, \frac{y}{t}, e^2 d(-t, y, e^2)\right), \end{gathered} \tag{5}$$

whence, setting $t = \nu$, we have

$$I(\nu, y, e^2) = d(-\nu, y, e^2)\, I\left(1, \frac{y}{\nu}, e^2 d(-\nu, y, e^2)\right). \tag{6}$$

From the functional Equation (5) we can obtain the following Lie differential equation for the spectral function I:

$$\frac{\partial}{\partial\nu} \ln I(\nu, y, e^2) = \frac{1}{\nu}\left[\frac{\partial}{\partial\xi} \ln I\left(\xi, \frac{y}{\nu}, e^2 d(-\nu, y, e^2)\right)\right]_{\xi=1}. \tag{7}$$

Since the spectral function $\underline{I}$ is real the Green's function for a photon is real for $k^2 < 0$ and complex for $k^2 > 0$.

On the basis of the spectral representation (2) it is easy to establish the relation between the imaginary part of $\underline{d}$ and the spectral function I:

$$I(x, y, e^2) = -\frac{1}{\pi} \operatorname{Im} d(x, y, e^2). \tag{8}$$

On the basis of the properties of the spectral function the group equation for the Green's function when $x > 0$ can be written separately for the imaginary and real parts:

$$\begin{aligned} \frac{\partial}{\partial x} \ln d_R(x, y, e^2) &= \frac{1}{x}\left[\frac{\partial}{\partial\xi} \ln d_R\left(\xi, \frac{y}{x}, e^2 d(-x, y, e^2)\right)\right]_{\xi=1}; \\ \frac{\partial}{\partial x} \ln d_I(x, y, e^2) &= \frac{1}{x}\left[\frac{\partial}{\partial\xi} \ln d_I\left(\xi, \frac{y}{x}, e^2 d(-x, y, e^2)\right)\right]_{\xi=1}. \end{aligned} \tag{9}$$

By repeating the above discussion for the spectral functions R_1 and R_2 for an electron we obtain equations for R_1 and R_2 which are analogous to Equations (5-9).

The equations for the spectral functions enable us, through the use of perturbation theory, to obtain spectral functions both for small ν (infrared region) and for large ν ($e^2 d < 1$). Approximate calculations of the Green's functions from these or other equations distort their analytical structure. The spectral representation and the group equations obtained for the spectral functions enable us to calculate the Green's functions without affecting their analytical structure.

Let us now consider the asymptotic region of large momenta $\nu \gg y$.

Substituting the asymptotic expressions for the spectral functions in the range $\nu \gg y$ which were obtained from perturbation theory, as well as the expressions for the functions $\underline{d}$ and $\underline{s}$ obtained by group renormalization [5], in the functional equations for I, R_1 and R_2 in the form of (6), we obtain

$$\begin{aligned} I(\nu, y, e^2) &\sim \frac{e^2}{3\pi}\left(1 - \frac{e^2}{3\pi} \ln\nu\right)^{-2}; \\ R_1(\nu, y, \omega^2, e^2) &\sim -\frac{e^2\omega^2}{4\pi} \exp\left[\frac{e^2\omega^2}{4\pi} \int\limits_{\ln(1/y)}^{\ln(\nu/y)} d_e(z)\, dz\right]; \\ R_2(\nu, y, \omega^2, e^2) &\sim -\frac{e^2}{4\pi}(\omega^2 - 3d)\left(1 - \frac{e^2}{3\pi} \ln\nu\right)^{9/4} \exp\left[\frac{e^2\omega^2}{4\pi} \int\limits_{\ln(1/y)}^{\ln(\nu/y)} d_e(z)\, dz\right]. \end{aligned} \tag{10}$$

These expressions are valid only for momenta $\frac{e^2}{3\pi}$ ln $\nu < 1$. Therefore it is not legitimate to draw conclusions regarding the existence of a singularity of the Green's function for a photon and of the spectral function I, on the basis of the formulas given above.

In conclusion, let us examine the region $\nu \sim y$. Since the Green's function for an electron is known to have a singularity [4,5] the spectral functions R_i do not have a δ-type singularity for $\nu \sim y$, as was assumed in [1-3], but a much stronger singularity.

In this case, by virtue of the diverging spectral integral for a and b in the region of small ν it is necessary to work with the spectral representations of the functions $\partial a/\partial \bar{p}^2$, $\partial b/\partial \bar{p}^2$, where $(p^2-m^2)G = a\hat{p} + bm$.

Elementary calculations give the following expression for the spectral functions in the region of $\nu \sim y$:

$$R_l(\nu, y, \omega^2, e^2) \sim \left(\frac{\nu}{y} - 1\right)^{-1-\frac{e^2}{3\pi}(3-\omega^2 d_e^0)}$$

In conclusion I wish to express my deep gratitude to Academician N. N. Bogoliubov, who directed the present work.

LITERATURE CITED

[1] G. Källen, Helv. Phys. Acta 25, 417 (1952).

[2] H. Lehmann, Nuovo Cimento 11, 342 (1954).

[3] M. Gell-Mann and F. Low, Phys. Rev. 95, 1300 (1954).

[4] N. N. Bogoliubov and D. V. Shirkov, Doklady Akad. Nauk SSSR 103, 203 (1955); 103, 391 (1955).

[5] A. A. Logunov, J. Exptl.-Theoret. Phys. (U.S.S.R.) 30, 793 (1956).

M. V. Lomonosov Moscow State University

Received February 24, 1956

ON MEASURING THE RESOLVING POWER OF AN OPTICAL INSTRUMENT

S. G. Rautian

(Presented by Academician G. S. Landsberg March 10, 1956)

1. The amplitude distribution $\varphi(x)$ in the image of a one-dimensional object is given [1] by the integral expression

$$\varphi(x) = \int_{-\infty}^{\infty} a(x-y)\,\psi(y)\,dy, \tag{1}$$

where $\psi(x)$ is the amplitude distribution in the object. A Fourier transformation of (1) leads [2] to the algebraic relation

$$\Phi_f = \sqrt{2\pi}\,A_f \Psi_f \tag{2}$$

between the Fourier transforms Φ_f, A_f and Ψ_f of the functions $\varphi(x)$, $a(x)$ and $\psi(x)$, respectively. If the optical instrument with a slit aperture is ideal from the standpoint of geometric optics it is usually assumed that*

$$a(x) = \frac{1}{\pi}\frac{\sin x}{x}; \quad A_f = \begin{cases} 1, & |f| < \frac{1}{2\pi}, \\ 0, & |f| > \frac{1}{2\pi}. \end{cases} \tag{3}$$

Consequently, in the spectrum Φ_f of the function $\varphi_f(x)$ which describes the image, no frequencies will be present which exceed the limit $1/2\pi$.

According to Kotel'nikov's theorem [3] a function with a bounded spectrum is determined uniquely by its values at points separated by the distance $1/2\ \Omega$, where Ω is the frequency limit, which in our case is equal to $1/2\pi$. Hence it follows that in the length X an optical image can contain not more than

$$N = \frac{X}{\pi} \tag{4}$$

independent data.

2. An analysis of the above situation led Toraldo di Francia [4,5] to the following conclusion. It is usually assumed, either explicitly or implicitly, that the image can reveal all changes of the object if the accuracy of measurement is sufficiently great (see, for example, [6]). It was shown in [4], however, that when condition (3) is satisfied different objects can give identical images. According to Kotel'nikov's theorem this fact is directly

---

* Coordinates in the image plane are measured in the so-called optical units $\lambda F/\pi D$.

associated with the finiteness of N (the number of degrees of freedom of the image). If it is assumed, following Toraldo di Francia, that N remains finite even in the ideal case of complete absence of errors of measurement, one easily deduces that the finite width of a light beam passing through the instrument determines, strictly speaking, not the finiteness of the resolving power but the finiteness of the "number of degrees of freedom of the image." Therefore N will be a characteristic of an optical instrument which is sufficient to describe its power as an instrument of research independently of the light receiver.

Toraldo di Francia's concept was criticized by Linfoot [7], who showed that the number of degrees of freedom of the response of any system is finite only in the presence of noise, when there are errors of measurement. Thus N is a doubly statistical characteristic which is determined by the noise level. Toraldo di Francia assumes [5], however, that optical instruments are an exception in this regard, that is, that they can be described rigorously by the functions A_f in (3).

In the present note it will be shown that this is erroneous since the spectrum of the image is, strictly speaking, unbounded.

3. In an optical image the absence of frequencies which exceed a certain frequency limit is associated with the approximate nature of the expressions obtained for diffraction. Such is not the case when diffraction at the aperture is calculated accurately. This can be shown by a direct calculation of the Fourier transform of the rigorous solution obtained by Morse and Rubinstein [8], although the same result can be arrived at from more general considerations.

Let us consider the two-dimensional problem of the diffraction of a light wave at a plane screen. The field behind the screen can be expressed in terms of the wave function and its normal derivative at the screen in accordance with the well-known Kirchhoff equation (see, for example, [9]):

$$2\pi\varphi_p = \int\left[\varphi\frac{\partial Z(kr)}{\partial n} - Z(kr)\frac{\partial\varphi}{\partial n}\right]df. \qquad (5)$$

Here $k = 2\pi/\lambda$; r is the distance from a point of the screen to the point of observation P; Z is proportional to the zeroth-order Hankel function of the second kind. For the transition to Fraunhofer diffraction it is possible to use the asymptotic expression:

$$Z(kr) \cong \sqrt{\frac{\pi}{2kr}}\, e^{-i(kr-\pi/4)}.$$

Expressing r in the exponent in terms of the distance R from the center of the diaphragm to the point P:

$$kr \cong kR - 2\pi f x$$

and differentiating, we arrive at the following expression for the field distribution in the image:

$$\varphi(x) \cong A\int\limits_{-\infty}^{\infty}\left[ik\varphi(f) + \frac{\partial\varphi}{\partial n}\right]e^{i2\pi f x}\,df. \qquad (6)$$

Thus the spectrum of Φ_f is proportional to the linear combination $ik\varphi + \partial\varphi/\partial n$ at the screen.

Therefore A_f in the form given in (3) denotes that at the screen both φ and $\partial\varphi/\partial n$ are simultaneously equal to zero. Yet it can be shown that this boundary condition corresponds to a physically absurd solution [10]: if φ and $\partial\varphi/\partial n$ are zero on any finite portion of a surface they vanish at all points of the space enclosed by that surface, or φ does not satisfy the wave equation.

Since, therefore, φ and $\partial\varphi/\partial n$ cannot vanish simultaneously in any finite region the spectrum of the optical image is, strictly speaking, unbounded. Therefore, the conditions of Kotel'nikov's theorem are not satisfied and $\varphi(x)$ cannot be determined uniquely by its values at a set of discrete points. Such a representation can only serve as a more or less exact interpolation. The degree of the approximation is then necessarily determined by the accuracy of the measurements.

It follows from the foregoing that optical instruments are no exception among linear transmitting systems. A difference can only lie in the fact that the number N of the degrees of freedom depends on the noise level; in other words, it is impossible to have a quantitative measure of the resolution which is independent of errors of measurement.

All of the above conclusions also apply to the three-dimensional case as well as for self-luminous objects.

4. The foregoing affects only the problem of the number of degrees of freedom, whereas the basic problem of a unique solution for the integral Equation (1) remains unsolved. Of course, one of the possible sources of nonuniqueness has been removed, but this is certainly not a solution.

LITERATURE CITED

[1] L. I. Mandel'shtam, Complete Works, Vol. 1 (1948), p. 211.

[2] E. C. Titchmarsh, Introduction to the Theory of Fourier Integrals (1948), p. 80 (Russian translation).

[3] A. A. Kharkevich, Outline of General Communication Theory (1955), p. 23.

[4] G. Toraldo di Francia, J. Opt. Soc. Am. 45, 7, 497 (1955).

[5] G. Toraldo di Francia, J. Opt. Soc. Am. 46, 1, 72 (1956).

[6] G. S. Gorelik, Doklady Akad. Nauk SSSR 83, 549 (1952).

[7] E. H. Linfoot, J. Opt. Soc. Am. 46, 1, 72 (1956).

[8] P. M. Morse and P. J. Rubinstein, Phys. Rev. 54, 11, 895 (1938).

[9] L. I. Mandel'shtam, Complete Works, Vol. 5 (1950), p. 20.

[10] J. A. Stratton, Electromagnetic Theory (1948), p. 408 (Russian translation).

P. N. Lebedev Physics Institute,
Academy of Sciences of the U.S.S.R.

Received March 5, 1956

ON THE POSSIBILITY OF A TRANSITION BETWEEN TWO TYPES OF CONCENTRATION QUENCHING OF FLUORESCENCE

B. Ia. Sveshnikov, L. A. Kuznetsova and V. A. Molchanov

(Presented by Academician A. N. Terenin January 18, 1956)

The concentration quenching of luminescent solutions, which was discovered by Stokes [1] more than 100 years ago, has frequently attracted attention. At present three hypotheses exist for the explanation of the phenomenon: energy migration, association and diffusion. The first two of these are the principal hypotheses; the last hypothesis [2] is used for only a few cases of concentration quenching.

The theory established by S. A. Vavilov [3] on the basis of energy migration* has been applied successfully by him to explain concentration quenching and concentration depolarization in solutions. On the one hand, this theory has received thorough experimental verification in the work of Vavilov's pupils [6], and on the other hand, it has been confirmed by experiments on sensitized fluorescence [7] and investigations of sensitized phosphorescence, which was discovered by A. N. Terenin and V. L. Ermolaev [8].

At the same time, after almost 15 years of development of the migration theory, it has been shown that its application to luminescence quenching is limited to not very high concentrations and that the theory, at least in its present form, cannot explain a number of effects observed in very high concentrations of a dissolved substance such as: the change of absorption and fluorescence spectra, the dependence of quenching on the wavelength of the exciting light, the marked discrepancy between the change of duration of the excited state in quenching and the change of the yield**, etc.

There has recently been renewed interest in attempts to explain concentration phenomena in fluorescent solutions on the basis of the association theory. The most detailed attempt to apply this theory to concentration quenching was that of V. L. Levshin as long ago as 1927 [10]. At that time he was able to explain many concentration effects but the association hypothesis was not able to explain the experimentally observed change of duration of the excited molecular state with increased concentration.

At the present time both hypotheses possess a range of application: concentration quenching in nonaqueous solutions and for not very high concentrations of the dissolved substance is usually explained by the energy migration theory; concentration quenching in aqueous solutions and sometimes in nonaqueous solutions with large concentrations of the activator are explained by the association hypothesis. This is a very artifical division. Frequently for the same activator either the first or second mechanism is assumed depending on the solvent. In a single series of related compounds one quenching mechanism is assumed for some compounds and the other mechanism for the remaining compounds [11]. And, finally, when the concentration quenching of any substance in a given solvent is not in accord with one hypothesis, both types of concentration quenching are assumed to exist simultaneously.

---

* The suggestion that concentration quenching is caused by energy migration was advanced earlier by J. Perrin [4] and F. Perrin [5].

** M. D. Galanin [9] attempts to explain this discrepancy by nonexponential fluorescence damping in quenched solutions. The nonexponential character is attributed by him to the fact that as a result of fluctuations of molecular distribution the probability of a transition from excited to unexcited molecules during the first moments of time after excitation is greater than at a later time.

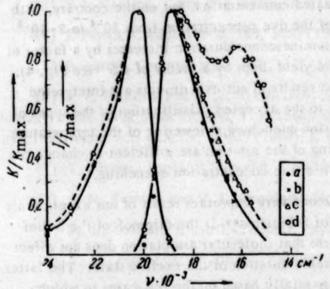

Fig. 1. Absorption and fluorescence spectra of alcohol solutions of acridine orange at 20° for different concentrations of the dye: a) $1 \cdot 10^{-4}$ M/ℓ ; b) $1 \cdot 10^{-3}$ M/ℓ; c) $1 \cdot 10^{-2}$ M/ℓ; d) $2.5 \cdot 10^{-2}$ M/ℓ.

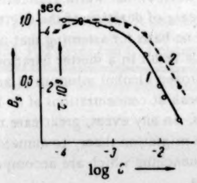

Fig. 2. Change of relative yield $B_s = B/B_0$ (1) and fluorescence duration (2) of an alcohol solution of acridine orange as a function of dye concentration at – 20° (excitation by 436 mμ mercury line).

These facts should have long ago stimulated both the formulation of a single theory of concentration quenching which would include as special cases both of the hypotheses mentioned and the expansion of experimental work which would establish a relationship between the two types of quenching. Unfortunately, after the unsuccessful attempts of F. Perrin [5] and F. Dushinskii [12] to combine the two hypotheses purely mechanically, no new attempts were made.

The present article aims to give new proofs of the existence of a close relation between the indicated types of concentration quenching. We have investigated the effect of dye concentration on the luminescence of alcohol solutions of acridine orange at room temperature and at the temperature of liquid air. According to Förster [13] quenching in nonaqueous solutions of dyes are typical of quenching through energy migration. In particular, the concentration quenching of acridine orange in nonaqueous solutions (in glycerine*) was one of the cases for which the energy migration theory was verified [3,9].

The fluorescence spectrum of an alcohol solution of acridine orange at 20° in the concentration range from $1 \cdot 10^{-4}$ to $1 \cdot 10^{-2}$ M/ℓ** is practically unchanged*** (see Fig. 1); considerable change occurs only in concentrations of $2.5 \cdot 10^{-2}$ M/ℓ. The absorption spectrum according to Zanker's data [14], which are reproduced by us in the same figure, also changes very little from $1 \cdot 10^{-4}$ to $1 \cdot 10^{-2}$ M/ℓ. The fluorescence yield and duration**** are markedly reduced with increased concentration (see Fig. 2) with the yield dropping more rapidly than the duration. Thus the concentration quenching of alcohol solutions of a given dye at room temperature, at least up to concentrations of 10^{-2} M/ℓ, possesses all the indications of quenching by means of energy migration: unchanged absorption and fluorescence spectra and concordant changes of yield and duration of the excited molecular state.

On the other hand, as we noted in [16], concentration quenching of alcohol solutions of the same dye at the temperature of liquid air possesses all the typical indications of quenching by molecular association: the fluorescence and absorption spectra are strongly deformed even for relatively low dye concentrations (see Fig. 3) and the concentration quenching depends on the exciting wavelength; and not only is there no accord between the changes of

---

* There is only a small quantitative difference between the quenching of acridine orange in alcohol and glycerine.

** We used a vessel of 5 mm width for which the exciting light was completely absorbed even at a concentration of $1 \cdot 10^{-2}$ M/ℓ.

*** Zanker obtained greater changes in the fluorescence spectrum and a marked shift to the long-wave region with increase of the dye concentration from $1 \cdot 10^{-4}$ to $1 \cdot 10^{-2}$ M/ℓ. We have shown by special experiments that this shift and spectral distortion were caused by strong reabsorption since Zanker used for excitation the 366 mμ mercury line, which is absorbed by an alcohol solution of acridine orange much more weakly than the 436 mμ line.

**** Measurements of the fluorescence duration were performed with the phase fluorometer of A. M. Bonch-Bruevich, V. I. Shirokov and V. A. Molchanov [15].

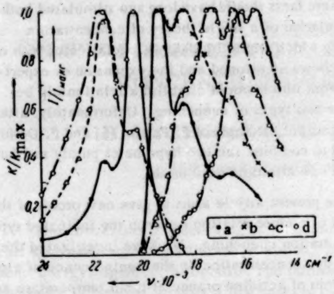

Fig. 3. Absorption and fluorescence spectra of alcohol solutions of acridine orange for various dye concentrations at the temperature of liquid air. a) $1 \cdot 10^{-5}$ M/ℓ; b) $1 \cdot 10^{-4}$ M/ℓ; c) $1 \cdot 10^{-3}$ M/ℓ; d) $1 \cdot 10^{-2}$ M/ℓ.

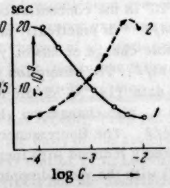

Fig. 4. Change of relative yield $B_s = B/B_0$ (1) and duration of fluorescence (2) of an alcohol solution of acridine orange as a function of dye concentration at the temperature of liquid air.

yield and the duration of the excited molecular state with increased concentration, but on the contrary, with increase of the dye concentration from 10^{-4} to $2 \cdot 10^{-2}$ M/ℓ the luminescence duration increases by a factor of 4 while the yield drops by a factor of 4.5 (see Fig. 4). Thus if the results of our experiments are interpreted according to the accepted classification of the types of concentration quenching,* lowering of the temperature and freezing of the solution are sufficient to change the mechanism of the concentration quenching.

A second very important result of our experiments and those of Schmillen** is the disproof of the belief held hitherto that molecular association does not affect the measurable duration of the excited state. The latter belief is essentially based on the few cases in which, within a certain range of concentrations of a few compounds, stability of the emission spectra was demonstrated while the absorption spectra were strongly deformed.*** Subsequently, however, a decreased duration of molecular excitation began to be considered a sufficient indication of migration quenching without giving sufficient attention to the deformation of the absorption and especially the fluorescence spectra. Förster's book [18] is an example. It is entirely obvious that while association can lead to a great increase of duration of the excited molecular state there is no basis for assuming that under other conditions it cannot result in a shorter duration. Fig. 4 shows that τ in frozen alcohol solutions of acridine orange attains its peak at concentrations of $5 \cdot 10^{-3}$ M/ℓ and then decreases. In any event, great care must be taken in applying the migration theory to numerous cases of concentration quenching which are accompanied by changes of the spectra.

At the same time the ease with which migration quenching changes to association quenching with change of the solvent and of temperature and at fairly high concentrations of the dissolved substance proves the close relation between the two quenching mechanisms. It is clear that the function which describes the interaction of two molecules must be more complicated and more flexible than that which is used in the energy migration theory. An expression for the wave function is needed which would give the transition from dispersion energy to association energy primarily as a function of distance. It is interesting that a detailed study of the dispersion interaction between two asymmetrical molecules by Davies and Coulson [18] shows that for small separations of such molecules strong forces act to orient and hold them in a definite relative position.

LITERATURE CITED

[1] G. Stokes, Phil. Trans. Roy. Soc. (London) 142, 463 (1852).

[2] E. Bowen and A. Norton, Trans. Farad. Soc. 35, 44 (1939).

---

* See, for example, [13], p. 244.

** Schmillen [17] observed greatly increased fluorescence duration for acridine orange when the concentration in aqueous solutions was increased at room temperature.

*** In this case it is evident that associated molecules do not participate in the emission.

[3] S. I. Vavilov, Complete Works, 7, 2 (Moscow, 1952).

[4] J. Perrin, Comptes rend. 184, 1097 (1927).

[5] F. Perrin, Comptes rend. 192, 1727 (1931); Ann. Phys. 17, 283 (1932).

[6] P. P. Feofilov and B. Ia. Sveshnikov, J. Exptl.-Theoret. Phys. (U.S.S.R) 10, 1372 (1940); F. M. Pekerman, Doklady Akad. Nauk SSSR 52, 405, 773 (1946); Dissertation (State Optical Institute, 1947); M. D. Galanin, Trans. Phys. Inst., Acad. Sci. U.S.S.R. 5, 339 (1950); J. Exptl.-Theoret. Phys. (U.S.S.R.) 21, 126 (1951).

[7] T. Förster, Angew. Chem. 59, 181 (1947); 60, 163 (1948).

[8] A. N. Terenin and V. L. Ermolaev, Doklady Akad. Nauk. SSSR 85, 547 (1952).

[9] M. D. Galinin, J. Exptl.-Theoret. Phys. (U.S.S.R.) 28, 455 (1955).

[10] V. L. Levshin, Z. Physik 43, 230 (1927); Photoluminescence of Liquids and Solids (Moscow, 1951).

[11] L. V. Levshin, J. Exptl.-Theoret. Phys. (U.S.S.R.) 28, 201, 213 (1955).

[12] F. Dushinskii, Doklady Akad. Nauk SSSR 14, 73 (1937).

[13] T. Förster, Fluoreszenz organischer Verbindungen (Göttingen, 1951).

[14] W. Zanker, Z. physik. Chem. 200, 250 (1952).

[15] A. M. Bonch-Bruevich, V. A. Molchanov and V. I. Shirokov, Bull. Acad. Sci. U.S.S.R., Phys. Ser. 20, 5 (1956).

[16] L. A. Kuznetsova and B. Ia. Sveshnikov, Bull. Acad. Sci. U.S.S.R., Phys. Ser. 20, 4 (1956).

[17] A. Schmillen, Z. Naturforsch. 9a, 1036 (1954).

[18] P. Davies and C. Coulson, Trans. Faraday Soc. 48, 777 (1952).

Received January 11, 1956

MAGNETORESISTANCE AND HOLE CONDUCTION IN TELLURIUM

S. S. Shalyt

(Presented by Academician A. F. Ioffe March 15, 1956)

An investigation of magnetoresistance in tellurium at the temperature of liquid helium ($T \leq 4.2°$ K) shows that the valence band of tellurium is split into two energy bands of different widths; in terms of the theory of electrical conductivity of solids this indicates that tellurium contains two groups of hole carriers of different mobility.

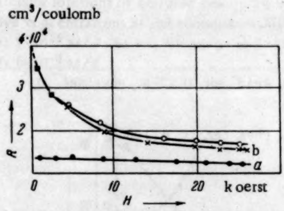

Fig. 1. The Hall coefficient as a function of magnetic field strength for tellurium.
a) 77.4° K; b) 4.2° K; c) 1.3° K.

Such a conclusion can be reached on the basis of the following experimental facts and comparisons.

1. It is known that in the impurity region, where $T < 200°$ K, tellurium always possesses only hole conduction independently of the chemical nature of the impurities.

Figures 1 and 2 give the experimental measurements of the Hall coefficient and the change of electrical resistance in a magnetic field at different temperatures. We obtained these results with a single-crystal tellurium rod of semicircular cross section ($d = 5$ mm) and 40 mm length. The sample was purified by zone melting repeated 10 times. The crystal axis [0001] formed an angle of 5° with the axis of the sample.

If it is assumed that tellurium contains one type of hole, and we use the Hall coefficient R for $H \rightarrow 0$ and the resistivity ρ_0 at liquid helium temperatures to determine the carrier mobility u from the formula

$$u = 0.52 \frac{R\,(\mathrm{cm}^3/\mathrm{coulomb})\ \mathrm{cm}^2}{\rho_0\,(\mathrm{ohm \cdot cm})\ \mathrm{v \cdot sec}}$$

we obtain $u = 1200$ cm²/volt·sec. This relatively low mobility makes it hard to understand the relatively large change of the Hall coefficient which is observed experimentally when the magnetic field is raised from 600 to 26,000 oerst (see Fig. 1). According to the theoretical calculation of Johnson and Lark-Horovitz [1], for these values of u and H the Hall coefficient should be reduced by only 13%. To account for the large reduction of the Hall coefficient which is observed (to less than half) it must be assumed the mobility of some fraction of the carriers is much greater than the value which follows from the single-group model.

2. The valence band of tellurium is formed by the triply degenerate 5 p^4 state of free tellurium atoms. According to Callen [2] this valence band splits into two bands in the crystal: one of these bands rises high in the energy level scheme and thus remains empty in the solid; the other band remains doubly degenerate, contains 4 electrons per atom and is thus completely filled at absolute zero. The latter fact explains why tellurium is a semiconductor. However, Callen's conclusions are not based on a consideration of the actual complicated crystal structure of tellurium but on a simplified tetragonal lattice model without the screw axes of real tellurium.

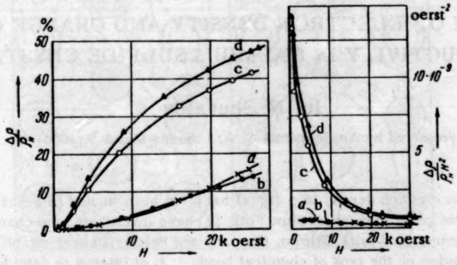

Fig. 2. Electrical resistance of tellurium as a function of the magnetic field.

a) 290° K; b) 77.4° K; c) 4.2° K; d) 1.3° K.

Because our experimental findings are not in accord with the single-group model of electrical conductivity we can assume that in the real complex tellurium crystal the valence band, which is doubly degenerate according to Callen, splits into two bands of different widths represented by two kinds of holes of unlike mobility.

3. The experimental fact that the curves representing resistivity as a function of the magnetic field (see Fig. 2) contain no quadratic region even in the weak operating fields indicates that $uH/c \gg 1$ and confirms the conclusion that we are dealing here with carriers of a high mobility which is considerably above the value obtained in a calculation that allows for only one kind of hole.

A theoretical analysis of magnetoresistance in an isotropic semiconductor containing two groups of undegenerate carriers of the same sign scattered by ionized impurities has been carried through by Iu. N. Obraztsov. Using his formulas for the Hall effect and change of resistivity in a magnetic field, together with the above experimental data, we calculated the concnetrations and mobilities of the two groups of holes which we have assumed to exist in tellurium. The concentrations are $n_1 = 7 \cdot 10^{-14}$ cm^{-3} and $n_2 = 4 \cdot 10^{12}$ cm^{-3}; the mobilities are $u_1 = 550$ cm^2/volt·sec and $u_2 = 9500$ cm^2/volt·sec.

The concentrations and mobilities calculated in this way are only approximate values since, first, the theoretical formulas which we used apply to an isotropic semiconductor, whereas tellurium shows marked anisotropy of its electrical properties and, secondly, the unavoidable extrapolation (to H = 0) in a steep section of the experimental curves (Figs. 1 and 2) is not sufficiently reliable. However, our qualitative conclusion that tellurium contains two groups of holes of unlike mobility, based on the experimental data, can be considered confirmed. In this connection it would be very interesting to investigate diamagnetic (cyclotron) resonance in tellurium.

I am grateful to the directors and to the head of the laboratories of the Leningrad Physicotechnical Institute, N. M. Reinov, for making it possible to carry out this investigation.

LITERATURE CITED

[1] V. A. Johnson and K. Lark-Horovitz, Phys. Rev. 79, 1, 176 (1950).

[2] H. Callen, J. Chem. Phys. 22, 518 (1954).

Semiconductor Institute,
Academy of Sciences of the U.S.S.R.

Received March 13, 1956

REDISTRIBUTION OF ELECTRON DENSITY AND CHANGE OF ELECTRICAL CONDUCTIVITY IN CADMIUM SULFIDE CRYSTALS

Iu. N. Shuvalov

(Presented by Academician A. A. Lebedev March 9, 1956)

The distribution of the electron density in a crystal has often been studied in connection with different properties and under different conditions. James and Firth [1] have investigated the change in the electron distribution with rising temperatures and Brill, Grimm, Hermann and Peters [2] have established the dependence of the character of this distribution on the type of chemical bond. It is of interest to determine the relation between the electron density distribution in a semiconductor crystal and its electrical conductivity.

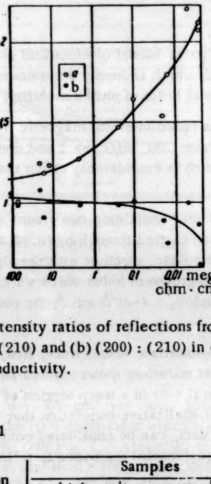

Fig. 1. Intensity ratios of reflections from planes: (a) (110) : (210) and (b) (200) : (210) in crystals of unlike conductivity.

We investigated hexagonal crystals of cadmium sulfide with well-developed faces over a range of conductivity and photosensitivity. With radiation from molybdenum we took rotating-crystal x-ray photographs by the Weissenberg method [3] and measured the reflection intensities. The reflection intensity ratios from adjacent planes in crystals of unlike conductivity were compared.

This comparison showed the law followed by the change of reflection intensities in going from samples of high resistivity to those of low resistivity. When the conductivity is increased some of the reflection intensity ratios increase regularly, others decline and others show no definite tendency. Fig. 1 gives the conductivity dependence of one of the increasing and one of the decreasing ratios on a logarithmic scale. Table 1 gives these ratios averaged for several samples of the high-resistance group (from 110 to 2 megohm · cm), intermediate group (from 0.25 to 0.02 megohm · cm) and low-resistance group (from 0.02 to 0.0025 megohm · cm) of crystals with the ratios of the high-resistance group taken as unity.

TABLE 1

Reflection ratios	Samples		
	high resistance	intermediate resistance	low resistance
(110) : (100)	1.00	1.19	1.23
(110) : (200)	1.00	1.29	1.62
(220) ; (310)	1.00	1.12	1.40
(200) : (210)	1.00	0.97	0.81
(300) : (210)	1.00	0.92	0.82
(300) : (220)	1.00	0.90	0.76

From the measurements of reflection intensities and the summation of Fourier series [4] by the stencil method, we constructed projections of the electron density in CdS crystals along the hexagonal axis for one of the high-resistance crystals (78 megohm · cm) and for one of the low-resistance crystals (0.016 megohm · cm). The values of the relative electron density were averaged over symmetrical points of each projection. In order to reveal the details of the electron density distribution in the interatomic space,

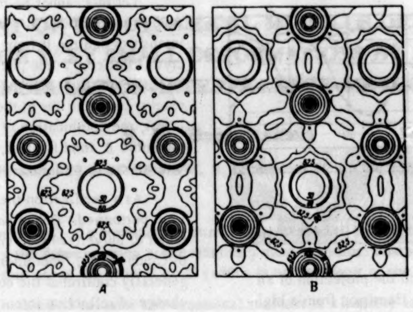

Fig. 2. Projections of the electron density distribution in the (001) plane of a high-resistance crystal (A) and of a low-resistance crystal (B).

besides the principal isolines through 50 units, additional isolines were drawn for 60, 62.5 and 70 units (see Fig. 2). In addition, curves were constructed on an enlarged scale for the electron density distribution at a distance of 1/6 a $\sqrt{3}$ around an atom, that is, half the separation between closest projections of atoms (see Fig. 3). The lower portion of the figures shows schematically the redistribution of the electron density in going from a high-resistance crystal (H) to a low-resistance crystal (L), by the difference in the line density.

TABLE 2

Reflections	Samples											Average over-all illumination
	35	56	56'	42	42	42'	42'	49	53	43	31	
	Effect											
	light	light	light	light	heat 100°	heat 130°	light & heat 150°	light	light	light	light	
	Photosensitivity											
	3	32	32	38		38		58	84	130	400	
(110) : (100)	1.09	1.16	1.07	1.04	1.01	1.09	1.18	1.11	1.06	1.22	1.25	1.13
(110) : (200)	0.97	1.07	1.18	1.03	1.13	1.27	1.34	1.06	1.28	1.18	1.05	1.13
(220) : (310)		1.16	1.22	1.74	1.05				1.10		0.96	1.24
(200) : (210)	1.00	0.91	0.78	0.85	0.84	0.89	0.79	0.92	0.80	0.98	0.66	0.85
(300) : (210)	1.02	0.92	0.63	0.88	0.78	0.92	0.87	0.94	0.89	0.98	0.55	0.85
(300) : (220)	0.87	0.86	0.91	0.85	0.89	1.00	0.83	0.98	0.81	0.87	0.72	0.85

From this figure it can be seen that when we go from a high-resistance crystal to a low-resistance sample the electron density distribution changes regularly. The electron density increases along lines which connect the projections of the closest atoms (0 to 120°) and also in the direction of the most distant atom (60°), and decreases in other directions (30 and 90°). Thus, along definite directions in the crystal the electron density increases, producing "electronic bridges."

When we consider the wurtzite structure of the CdS crystal and the characteristics of the selected projection it is easy to see that the nearest atoms at small and large separations between their projections are atoms which lie in different neighboring layers, that is, cadmium and sulfur atoms, respectively. But for the intermediate separation between atom projections the nearest atoms are of the same kind, either both of cadmium or both of sulfur.

Hence it follows that increased conductivity can be attributed to the creation of electronic bridges between unlike atoms.

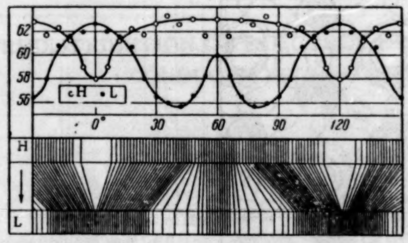

Fig. 3. Electron density around the projection of an atom and redistribution in the transition from a high-resistance (H) to a low-resistance (L) crystal.

Yet this cannot be regarded as the only possible interpretation. Indeed, a change of reflection intensities can result from various phenomena in the crystal lattice. These phenomena can result from microscopic disruptions of the lattice such as microcracks, irregularities in the positions of the atomic layers, the combination of hexagonal α-CdS with the cubic β modification, different degrees of mosaic structure, etc.

As a verification the following experiments were performed. Debye powder photographs were taken of pulverized CdS crystals with various values of conductivity. Photometric study of these patterns generally confirmed the observed regularity of the change of reflection intensities.

We also took Weissenberg photographs of CdS while subjected to illumination and heating. The samples were illuminated by a powerful incandescent lamp combined with a system of lenses for focusing. The light heated the crystals 15 to 20° above the surrounding temperature. In other experiments the samples were heated during the photographing by special heaters, to 100 or 130°. Sometimes illumination and heating were simultaneous. In order to eliminate random effects rotating-crystal photographs were taken on the same film before, during and after illumination and heating. The results are given in Table 2, which contains the quotients resulting from the division of reflection intensity ratios from illuminated and heated crystals by the ratio of the same intensities from the same crystals when unexcited. The samples are placed in order of increasing photosensitivity, which is indicated by the ratio of the light current to the dark current under small but identical illumination.

Despite the large scattering of the observed values which resulted from the impossibility of illuminating all samples identically, it is apparent that some reflection intensity ratios increase when the crystal is excited by light or heat (ratios above unity) and others decrease (ratios below unity). It can also be noticed that these characteristic changes of reflection intensities are very small in slightly photosensitive sample No. 35, unusually large in very photosensitive sample No. 31 and for sample No. 42 increase under high excitation – increased temperature or simultaneous illumination and heating.

A comparison of these results makes it possible to state that increased conductivity of a CdS crystal resulting from any cause is associated with a change of reflection intensities, that is, with a redistribution of electron density in the CdS lattice; when the conductivity increases there is a formation or strengthening of electronic bridges in the directions of the chemical bonds of the crystal.

The idea of this investigation came from Academician A. A. Lebedev, who participated directly in the work.

LITERATURE CITED

[1] R. W. James and E. M. Firth, Proc. Roy. Soc. (London) A 117, 62 (1927).

[2] R. Brill, H. G. Grimm, C. Hermann and Cl. Peters, Ann. Phys. 34, 393 (1939).

[3] M. D. Burger, X-Ray Crystallography (1948).

[4] A. I. Kitaigorodskii, X-Ray Structural Analysis (1950).

A. A. Zhdanov Leningrade State University

Received February 14, 1956

MEASUREMENT OF THE DYNAMICAL MODULUS OF ELASTICITY OF RUBBER FOR VERY SMALL DEFORMATIONS BY AN OPTICAL MODULATION-INTERFERENCE METHOD

N. M. Borovitskaia

(Presented by Academician M. A. Leontovich March 29, 1956)

Articles [1-3] have described a modulation-interference method of measuring very small optical path differences which permits the determination (with relatively modest optical equipment) of the amplitudes of mechanical oscillations that are of the order 0.01 A (which is not the limit of the method).

We have used this method to measure the dynamical modulus of elasticity of rubber for very small displacements. This method is practicable for the measurement of the dynamical modulus of rubber and other highly elastic substances for two reasons. First, this method may have certain advantages in accuracy and relative simplicity over the existing acoustical methods. Secondly, this method broadens the experimental possibilities by enabling us to work with very small amplitudes and in conjunction with other methods over a very broad range of deformation amplitudes; this is of interest in connection with the general theory of the dynamical properties of rubber and especially for checking the linearity of these properties – the deformation-amplitude independence of the modulus and losses, especially for filled rubber [4,5].

We shall give a brief description of the apparatus used for the measurements. A Michelson interferometer and a source of monochromatic light are used. The interference pattern (lines of equal thickness) is projected on the cathode of a photomultiplier. The voltage from the photomultiplier is applied to the input of a narrow-band filter; the measuring instrument is connected to the output of this filter. The interferometer mirrors were adjusted in such a way that the entire interference pattern or most of it was illuminated uniformly. If one of the mirrors oscillates with the frequency ω and amplitude $\underline{z}$ the path difference between the interfering beams will change with the frequency ω, and the intensity of the light reaching the photomultiplier will also change. The current through the load of the photomultiplier will be modulated by the frequency ω. The first harmonic of the photocurrent will be

$$I_1' = AJ_1\left(\frac{4\pi}{\lambda}z\right),$$

where λ is the wavelength of the light; A is a coefficient which depends on the intensity of the interfering beams and on their path difference when the mirror is at rest; I_1 is the first-order Bessel function.

When the narrow-band filter is tuned to frequency ω the readings of the output instrument are proportional to I_1. For $4\pi z/\lambda \leq 0.5$ the relation between these readings and the amplitude of the vibrations will be (within 1% accuracy)

$$\alpha = B\frac{z}{\lambda},$$

where B is an instrumental constant which includes the factor A. Under our conditions ($\lambda = 5460$ A) this relation is correct for $z \leq 200$ A.

Our apparatus permitted the detection of displacements of the order of 0.01 A; measurements were possible with frequencies from 100 to 10,000 cps.

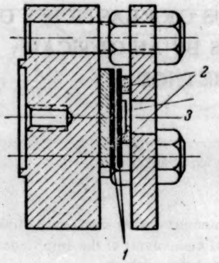

Fig. 1. Block for fastening of samples.
1) Electrodes; 2) rubber samples;
3) mirror.

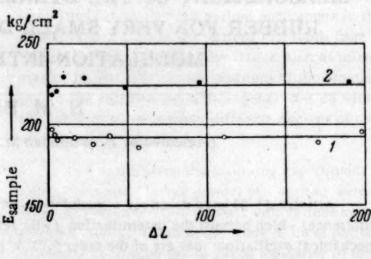

Fig. 2. Modulus of elasticity as a function of deformation amplitude.
1) No. 3 rubber; 2) No. 4 rubber.

The rubber samples were fastened (cemented) to a massive block (see Fig. 1) which was placed in one of the arms of the interferometer. Three identical samples were tested simultaneously.

The alternating voltage of frequency ω was applied to the electrodes 1; this caused attraction of the electrodes so that the rubber 2 was subjected to stretching deformation with the frequency 2ω. The right-hand electrode and disk to which the rubber was cemented were grounded so that the rubber would not be in an electrical field that would induce electrostrictive oscillations. The left-hand electrode and insulating disk were firmly fastened to the block. The mirror 3, which was cemented to the right-hand electrode and vibrated with it, was one of the interferometer mirrors. Light reached it through an opening in the disk.

The measurements gave the amplitude of deformation of the rubber; the magnitude of the force was obtained by calculation (the voltage on the electrodes, area of the electrodes and gap between them were known). The dynamical modulus of elasticity was determined as the ratio of the amplitude of mechanical stress to the amplitude of deformation.

We measured the moduli of four different rubbers. Their composition was as follows: No. 1 - vulcanized natural rubber; chalk filler; No. 2 - vulcanized natural rubber without fillers; No. 3 - vulcanized natural rubber with carbon black filler; No. 4 - vulcanized SKS-30 rubber with carbon black filler.

Samples of each rubber were prepared in the form of cylinders of diameters 2, 4, 6 and 8 mm. All measurements were made at a constant temperature of 20°.

For each type of sample we obtained the dependence of the deformation on frequency. For simplicity and greater reliability of the calculations we chose the frequencies 300 to 500 cps, which are below the resonance frequency of the rubber-electrode system. All measurements were made at these frequencies. An attempt was made to measure the modulus of a sample of rubber No. 3 as a function of frequency. Up to 8000 cps the modulus was constant within 10%; with further increase of frequency it rose very rapidly

The moduli were measured for deformation amplitudes from 1 to 200 A, which with an average sample thickness of 2 mm corresponds to a relative deformation of $5 \cdot 10^{-6}$ to 10^{-3} %. Fig. 2 gives the dependence of the modulus for

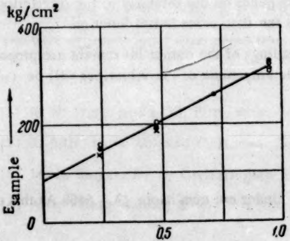

Fig. 3. Dependence of the modulus of elasticity of a sample on the shape factor.

samples of rubber No. 3 and No. 4 on the magnitude of the deformation. The figure shows that the modulus is constant (within 5%) in the entire range. Similar results were obtained for all samples of all the types of rubber.

From these results it is possible to obtain Young's modulus by the method proposed by G. M. Bartenev and V. I. Novikov [6]. For this purpose we plot the dependence of the modulus of a sample on a form factor Φ (the ratio of the cross-sectional area to the lateral surface area of a sample). This relation as obtained from our experiments is given for rubber No. 3 in Fig. 3. Each point in the graph refers to a different set of samples. By extrapolating this linear relation to the vertical axis for $\Phi = 0$, we obtain the following values of Young's modulus: rubber No. 1 - 9 kg/cm^2; rubber No. 2 - 3 kg/cm^2; rubber No. 3 - 85 kg/cm^2; rubber No. 4 - 90 kg/cm^2.

I am grateful to Doctor of Physicomathematical Science, Iu. S. Lazurkin, for his interest in this work.

LITERATURE CITED

[1] G. S. Gorelik, Doklady Akad. Nauk SSSR 83, 4, 549 (1952).

[2] I. Ia. Brusin, G. S. Gorelik and S. A. Pikovskii, Doklady Akad. Nauk SSSR 83, 4, 553 (1952).

[3] I. L. Bershtein, Doklady Akad. Nauk SSSR 94, 4, 655 (1954).

[4] R. S. Rivlin, Trans. Inst. Rubber Ind. 26, 1, 78 (1950).

[5] W. P. Fletcher and A. N. Gent, Trans. Inst. Rubber Ind. 26, 1, 45 (1950).

[6] G. M. Bartenev and V. I. Novikov, Doklady Akad. Nauk SSSR 91, 1027 (1953).

Physicotechnical Research Institute,
Gorki State University

Received March 28, 1956

DETERMINATION OF THE ORIENTATION RELAXATION TIME OF SOME LIQUIDS BY THE WIDTHS OF SCATTERED LINES

M. F. Vuks and A. K. Atakhodzhaev

(Presented by Academician A. A. Lebedev March 24, 1956)

According to the relaxation theory of modulated scattered light, which was proposed by E. F. Gross [1] and developed by M. A. Leontovich [2], the intensity distribution in the profile of a line scattered by a liquid is given by the formula

$$I = \frac{1}{1+\tau^2\Delta\omega^2}, \tag{1}$$

where I is the intensity $\Delta\omega$ from the middle of the line and τ is the anisotropy relaxation time.

In [3] a resonance filter was used to investigate the intensity distribution for anisotropic scattering in the immediate vicinity of the middle of the line. It was shown that Equation (1) is a comparatively good representation of the region within 3-4 cm^{-1} from the line middle. On the basis of this agreement of theory and experiment Equation (1) was used to determine the orientation relaxation time of a number of liquids.

In the present work we have investigated a more distant portion of the line profile. The resonance filter method is unsuitable here and we have resorted to the usual method of photographic photometry. In order to reduce the errors of this method we chose as intensity standards the lines of the exciting light, which were the three mercury lines $\lambda\lambda$ 4358, 4347 and 4339 A.

It was first necessary to determine the relative intensities of these three lines from a PRK-4 quartz mercury lamp which served as the source of exciting light. Photographs were taken with an ISP-51 spectrograph and a long focal length camera. We found that under our normal operating conditions for the lamp the intensities of the three lines were in the ratios $1:{}^{1}/_{18}:{}^{1}/_{58}$.

An MF-4 microphotometer was used to make a photometric examination of the incident and scattered spectra and a comparator was then used to measure the line widths of the direct and scattered light at three points: 1) where the intensity is reduced by the factor 3.2 – this is the width of the second line where its intensity equals the maximum of the third line (see Fig. 1 crossline a); 2) where the intensity is reduced by the factor 18 – this is the width of the first line where its intensity equals the maximum of the second line (crossline b); and 3) where the intensity is reduced by the factor 58 – this is the width of the first line when its intensity equals the maximum of the third line (crossline c).

If we assume that an exciting line has the shape of a dispersion curve and that a scattered line has the shape of a relaxation curve and consider that these curves are of similar form, we can write

$$\Delta\nu' = \Delta\nu + \Delta\nu_0, \tag{2}$$

where $\Delta\nu'$ is the experimentally measured scattered line width, $\Delta\nu$ is the true width of the scattered line and $\Delta\nu_0$ is the width of the exciting line.

We shall use $\Delta\nu_n$ to denote the true half width of a scattered line where its intensity is less by the factor n than the middle of the line. Then from Equation (1) we have

$$\frac{1}{n} = \frac{1}{1 + \tau^2 (2\pi\Delta\nu_n)^2},$$

or

$$\tau = \frac{\sqrt{n-1}}{2\pi\Delta\nu_n}. \qquad (3)$$

The last formula is the basis for our proposed method of determining τ.

In our experiments n had the values 3.2, 18 and 58. If the relaxation processes in a given liquid possess identical relaxation times the half widths $\Delta\nu_{3.2}$, $\Delta\nu_{18}$ and $\Delta\nu_{58}$ should lead to the same value of τ. Let us examine the three values of τ by $\tau_{3.2}$, τ_{18} and τ_{58}, respectively. The spectrograph slit was varied from 0.025 to 0.15 mm, giving in all cases practically the same values for τ_{18} and τ_{58}. It was also shown experimentally that the lengths of crosslines b and c are practically independent of the levels of intensity at which they are obtained. All of these observations indicate that the measurements of τ_{18} and τ_{58} were not affected by the experimental procedure. The values of $\tau_{3.2}$ were more sensitive to the experimental conditions.

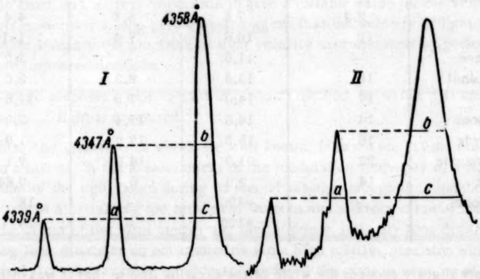

Fig. 1. Microphotograms of incident light (I) and light scattered in fluorobenzene (II).

Table 1 gives the values of $\tau_{3.2}$, τ_{18} and τ_{58} for the 20 liquids which we investigated at 28° (mainly singly substituted benzene derivatives). The table shows that $\tau_{3.2}$ is somewhat larger than τ_{18} in the majority of cases. Small excesses of $\tau_{3.2}$ over τ_{18} cannot be regarded as actual and must be attributed to the fact that close to the center of an exciting line the intensity distribution differs notably from a dispersion curve.

The table also shows that in all cases τ_{58} is appreciably smaller than τ_{18}. This difference must be due to the fact that, as earlier investigations showed [4], the more distant portion of a line contour is not associated with relaxation processes but is due to molecular vibrations and rotations, and in the region where the intensity is reduced by the factor 58 there is clearly an appreciable superposition of a vibration-rotational band on the relaxation profile.

It must thus be recognized that the most precise values of the orientation relaxation time are given by τ_{18}. This is also confirmed by a comparison of our results for carbon bisulfide, benzene, chlorobenzene and bromobenzene with the values obtained in [3] by the resonance filter method. For nitrobenzene there is a great discrepancy between our value for the relaxation time and the value obtained previously by the resonance filter method. This must clearly be attributed to the fact that nitrobenzene has two relaxation times. In benzophenone

TABLE 1

Measurements of Orientation Relaxation Times Obtained from the Widths of the Scattered Lines λλ 4358 and 4347 at 28° (Styrene at 22°)

Substance	$\tau_{3.2} \cdot 10^{12}$ sec	$\tau_{18} \cdot 10^{12}$ sec	$\tau_{58} \cdot 10^{12}$ sec	η at 20° in centipoises
Carbon bisulfide	1.9	1.75	1.45	0.37
Benzene	1.9	1.90	1.35	0.65
Pyridine	3.6	3.0	2.1	0.95
Toluene	4.3	4.0	3.0	0.58
Ethylbenzene	4.9	4.7	3.4	0.66
Fluorobenzene	4.3	3.8	2.9	0.58
Chlorobenzene	7.0	6.1	4.0	0.80
Bromobenzene	11	8.3	6.0	1.13
Iodoxybenzene	–	10.0	–	1.49
Aniline	9.3	7.8	5.3	4.4
Styrene	12	10.6	7.4	1-10
Nitrobenzene	–	11.0	–	2.0
Benzyl alcohol	14	13.6	8.3	5.6
Phenol	17	14.0	7.0	11.6
Acetophenone	14	14.5	11.4	2.0
Benzaldehyde	16	15.3	12.0	1.9
Methyl benzoate	22	21.0	14.0	2.1
Paraxylene	14	9.0	6.3	0.64
Benzophenone	–	~100	–	18
Salol	–	>100	–	26

the scattered line width very slightly exceeds the width of the exciting line so that it was difficult to obtain a precise value of τ. In salol the scattered lines cannot be distinguished at all from the exciting lines; therefore it can only be stated that $\tau > 10^{-10}$ sec.

The first conclusion derived from our work is the following: the profile of a line scattered by a liquid is undoubtedly mainly of relaxational character: in the liquids which we investigated, with the exception of nitrobenzene, the intensity distribution in the relaxation profile is in good agreement with a single relaxation time.

It can also be noted that for similar substances such as toluene and ethyl benzene, for example, or halogen substitutional derivatives of benzene, a definite relationship is observed between the relaxation time and viscosity: with an increase in viscosity and molecular size the relaxation time increases. When substances of different types are compared this is not observed. Thus five liquids – from benzyl alcohol to methyl benzoate – whose molecules differ little in size and shape, have very close relaxation times, whereas the viscosities of the first two exceed those of the three others severalfold. This indicates that the relation between the orientation relaxation time and viscosity is more complicated than the well-known Debye formula.

LITERATURE CITED

[1] E. F. Gross, Doklady Akad. Nauk SSSR 28, 788 (1940).

[2] M. A. Leontovich, J. Phys. (USSR) 4, 515 (1941).

[3] M. F. Vuks and V. L. Litvinov, Doklady Akad. Nauk SSSR 105, 696 (1955).

[4] E. F. Gross and M. F. Vuks, J. Phys. (USSR) 4, 437 (1936).

A. A. Zhdanov Leningrad State University

Received March 13, 1956

A NEW METHOD OF MEASURING THE VELOCITY OF LIGHT

K. S. Vul'fson

(Presented by Academician G. S. Landsberg January 14, 1956)

The development of electronics has brought about a considerable improvement of Fizeau's method of measuring the velocity of light. Using an ingenious null method Bergstrand [1] increased the precision of the measurement to 0.25 km/sec, i.e. to $1 \cdot 10^{-6}$. Electromagnetic methods of measuring the velocity of light have also reached a high degree of accuracy [2-5]. Nevertheless, the spread of the mean values in various articles exceeds the probable error, so that it is impossible to give a reliable value for the velocity of light. A comparison of measurements made over a long period even suggests that the velocity of light changes in time [6]. It is thus desirable to further increase the precision of light velocity measurements by perfecting existing methods and finding new and more improved methods.

The present article proposes a new variant of Fizeau's method, by which it is hoped to increase the accuracy with which the velocity of light is measured.

Fizeau's method, the essentials of which are well known, is based on: 1) the measurement of the distance from a modulator to a mirror; 2) the measurement of the modulation frequency of a light beam; 3) the fixing of the intensity minimum of the light beam during its second passage through the modulator after reflection from the mirror. Inaccuracy in ascertaining the minimum leads to an incorrect value of the modulation frequency. In order to reduce the effect of the error concerning the minimum intensity long distances must be used, but the methods of measuring long distances do not insure the same high relative precision which can be attained for short distances. Bergstrand's null method considerably reduced the error in locating of the minimum and enabled him to obtain amazing results.

In the method proposed below item 3), which is the principal source of error, is eliminated by the use of an automatic arrangement. In addition, the new method does not require long distances, so that the measurements can be made with very great relative accuracy.

The method is essentially as follows: The light source or the modulating device sends out a short light pulse whose duration is of the order 10^{-7} to 10^{-8} sec. After reflection from the mirror the beam enters a photoelectric receiver. The electrical pulse which is generated in the latter triggers the sending of a second light pulse, through the use of a special circuit. Thus, after emission of the first pulse the system begins to generate light pulses whose frequency of repetition is determined by the distance from the modulator or light source to the mirror and from the mirror to the light receiver as well as by the signal delay in the apparatus. By determining the period, or what amounts to the same, the repetition rate of the light and electrical pulses which are generated for a few easily distinguishable positions of the mirror, it is possible to establish both the velocity of the light and the signal delay in the apparatus.

Since the repetition rate of the light pulses can be determined very precisely the shift of the mirror does not have to be very large, but of the order of a few meters; therefore it can be measured with extreme accuracy by an interferometer. The mirror can be placed in a vacuum chamber in order to eliminate a correction for the refractive index of air. It is expedient to use mirror displacements of such magnitude that the repetition rate of the light pulses will coincide with the harmonics of the standard quartz oscillator which is used in the frequency measurements. The accuracy of the frequency determination will then be especially high.

The repetition rates of the light flashes can be compared with a standard generator by the use of Lissajous figures. The accuracy of such a method of comparison is limited by the average stability of both the standard generator and the measuring instrument. In principle it is possible to observe stationary Lissajous figures on the screen of a cathode ray oscilloscope as long as desired; thus the precision of the frequency comparison becomes higher than the precision of phase coincidence in other methods of measuring the velocity of light in which the duration of a single measurement is limited by the period of the measuring instrument.

A frequency comparison can be accomplished at the present time with an accuracy of as much as 10^{-7} to 10^{-8} . Distances of the order of a few meters can be measured with the same accuracy; consequently, the velocity of light will be determined with this same accuracy. For the purpose of attaining such high accuracy it is, of course, required that the component parts of the apparatus be designed and constructed in such a way as to insure great stability of its parameters.

LITERATURE CITED

[1] E. Bergstrand, Arkiv Fysik 3, 4-5, 479 (1952).

[2] W. C. Andersen, J. Opt. Soc. Am. 31, 187 (1941).

[3] K. D. Froom, Nature 169, 4290, 107 (1952).

[4] D. H. Ronk, Phys. Rev. 86, 5, 798 (1952).

[5] A. I. Kartashev, Trans. All-Union Sci. Research Inst. Meteorol. 13, 26, 17 (1955).

[6] J. H. Rush, Sci. American 193, 2, 62 (1955).

Received January 3, 1956

ON THE THEORY OF THE SPONTANEOUS MAGNETIZATION OF FERROMAGNETIC SEMICONDUCTORS AT LOW TEMPERATURES

E. I. Kondorskii, A. S. Pakhomov and T. Shiklosh

(Presented by Academician M. A. Leontovich March 22, 1956)

The theory of the magnetic and electrical properties of ferromagnetic semiconductors including ferrites began to be developed comparatively recently – during the past decade. The quasiclassical theory of ferrites was initiated by Neel [1]. His hypothesis that ferrites contain two magnetic sublattices was confirmed experimentally by work on neutron diffraction in these substances [2]. The case of several magnetic sublattices was examined from the standpoint of quantum theory by Vlasov and Ishmukhametov [3], Kaplan [4] and Vonsovskii and Seidov [5]. In articles [4] and [5] differing formulas were derived for the low temperature dependence of spontaneous magnetization.

In the present work this temperature dependence was calculated using the method of second quantization developed by N. N. Bogoliubov and S. V. Tiablikov [6]. This method has already been used by Tiablikov [7] in the theory of antiferromagnetism and by the present authors [8] in the theory of ferromagnetism of metals and alloys.

In exchange which is of indirect character (superexchange), as in ferrites, the Hamiltonian can be represented in the same form as in the case of a direct exchange interaction by introducing the so-called indirect exchange integrals [9]. If we denote an integral of indirect exchange between electrons located at nodes f_1 and f_2 of the ferrite lattice by $I(f_1, f_2)$, the Hamiltonian for this lattice can be written by analogy with the theory of ferromagnetism as follows:

$$\hat{H} = G_0 - \frac{1}{2} \sum_{f_1, f_2, \alpha} I(f_1, f_2)\, \hat{S}^{\alpha}_{f_1} \hat{S}^{\alpha}_{f_2}, \tag{1}$$

where G_0 is a constant and $\hat{S}^{\alpha}_{f}$ are spin operators with $\alpha = x, y, z$.

Let us consider a ferrite whose crystal lattice can be represented as a combination of two oppositely magnetized nonequivalent sublattices A and B. At the sites of sublattice A, denoted by the indices r, let there be located N/3 magnetic ions with spins pointing to the right, and at the sites of sublattice B, denoted by the indices ℓ, let there be 2N/3 ions with spins pointing to the left. In this special case the indices f in the general expression (1) assume the values r and ℓ independently of each other. It can be shown that if $I(r_1, r_2) > 0$, $I(\ell_1, \ell_2) > 0$, $I(r, \ell) < 0$ the energy of the ground (lowest) level is

$$E_0 = G_0 - \frac{1}{2} \sum_{r_1 \neq r_2} I(r_1, r_2) - \frac{1}{2} \sum_{l_1 \neq l_2} I(l_1, l_2) - \sum_{r, l} I(r, l). \tag{2}$$

The energy spectrum of the system, which we require in order to determine the temperature dependence of spontaneous magnetization, will be sought in the region close to the ground level E_0, i.e. for weakly excited states.

After making a transformation from the spin operator $\hat{S}^{\alpha}_{f}$ to the Fermi operators $\hat{a}^{+}_{f_\nu}$ and $\hat{a}_{f_\nu}$, $\nu = \pm 1/2$, which are associated with the former by well-known relations (see [6], for example), the Hamiltonian (1) becomes

$$\begin{aligned}\hat{H} = G_0 &+ \frac{1}{2} \sum_{\substack{r_1, r_2, \nu_1, \nu_2, \nu_1', \nu_2' \\ r_1 \neq r_2}} B(r_1, r_2, \nu_1, \nu_2, \nu_1', \nu_2')\, \hat{a}^+_{r_1\nu_1} \hat{a}^+_{r_2\nu_2} \hat{a}_{r_2\nu_2'} \hat{a}_{r_1\nu_1'} + \\ &+ \frac{1}{2} \sum_{\substack{l_1, l_2, \nu_1, \nu_2, \nu_1', \nu_2' \\ l_1 \neq l_2}} B(l_1, l_2, \nu_1, \nu_2, \nu_1', \nu_2')\, \hat{a}^+_{l_1\nu_1} \hat{a}^+_{l_2\nu_2} \hat{a}_{l_2\nu_2'} \hat{a}_{l_1\nu_1'} + \\ &+ \sum_{r, l, \nu_1, \nu_2, \nu_1', \nu_2'} B(r, l, \nu_1, \nu_2, \nu_1', \nu_2')\, \hat{a}^+_{r\nu_1} \hat{a}^+_{l\nu_2} \hat{a}_{l\nu_2'} \hat{a}_{r\nu_1'},\end{aligned} \tag{3}$$

where $B(f_1, f_2, \nu_1, \nu_2, \nu_1', \nu_2')$ are coefficients expressed in terms of the indirect exchange integrals. This equation differs from the corresponding Hamiltonian in [7] for the case of two equivalent sublattices in that the first and second summations contain a different number of terms. This difference leads to essentially different final results (in the case of two equivalent sublattices we have antiferromagnetism, and for nonequivalent sublattices we have ferromagnetism); however, the transformation of the Hamiltonian (3) and its subsequent reduction to diagonal form do not differ at all from what is described in [7]. The intermediate expressions and Equations (4) which are obtained for the determination of eigenvalues (see below) differ from the corresponding equations in [7] only in the number of terms in the summations.

The eigenvalues of the Hamiltonian E_k are determined, as in [7] by the condition for the solubility of the equations:

$$\begin{aligned}E_k U_k(r) &= 2\Big\{\sum_{(r')} I(r, r') - \sum_{(l)} I(r, l)\Big\} U_k(r) - 2\sum_{(l)} I(r, l) V_k(l) - \\ &\quad - 2\sum_{(r')} I(r, r') U_k(r'), \\ -E_k V_k(l) &= 2\Big\{\sum_{(l')} I(l, l') - \sum_{(r)} I(r, l)\Big\} V_k(l) - 2\sum_{(r)} I(r, l) U_k(r) - \\ &\quad - 2\sum_{(l')} I(l, l') V_k(l'), \\ E_k U_k(l) &= 2\Big\{\sum_{(l')} I(l, l') - \sum_{(r)} I(r, l)\Big\} U_k(l) - 2\sum_{(r)} I(r, l) V_k(r) - \\ &\quad - 2\sum_{(l')} I(l, l') U_k(l'), \\ -E_k V_k(r) &= 2\Big\{\sum_{(r')} I(r, r') - \sum_{(l)} I(r, l)\Big\} V_k(r) - 2\sum_{(l)} I(r, l) U_k(l) - \\ &\quad - 2\sum_{(r')} I(r, r') V_k(r')\end{aligned} \tag{4}$$

and the normalization conditions

$$\sum_{(r)} U_k^*(r) U_{k'}(r) - \sum_{(l)} V_k^*(l) V_{k'}(l) = \delta(k - k'),$$

$$\sum_{(l)} U_k^*(l) U_{k'}(l) - \sum_{(r)} V_k^*(r) V_{k'}(r) = \delta(k - k').$$

The solution of (4) can be written as

$$U_k(r) = \sqrt{\frac{3}{N}}\, a_k e^{-i(kr)}, \quad U_k(l) = \sqrt{\frac{3}{2N}}\, \alpha_k e^{-i(kl)}.$$
$$V_k(l) = \sqrt{\frac{3}{2N}}\, b_k e^{-i(kl)}, \quad V_k(r) = \sqrt{\frac{3}{N}}\, \beta_k e^{-i(kr)}. \tag{5}$$

The substitution of (5) in (4) gives two sets of equations for the determination of a_k, b_k, $E_k^{(1)}$ and α_k, β_k, $E_k^{(2)}$. In our case of two nonequivalent sublattices the solution of these equations gives the following expressions for $E_k^{(1)}$ and $E_k^{(2)}$:

$$E_k^{(1)} = \frac{1}{2}\left\{A_k - D_k + \sqrt{(A_k + D_k)^2 - 4B_kC_k}\right\},$$
$$E_k^{(2)} = \frac{1}{2}\left\{D_k - A_k + \sqrt{(A_k + D_k)^2 - 4B_kC_k}\right\}, \tag{6}$$

where the following notation is used:

$$A_k = 2\sum_{(r')} I(r, r')\left[1 - e^{-ik(r'-r)}\right] - 2\sum_{(l)} I(r, l),$$
$$D_k = 2\sum_{(l')} I(l, l')\left[1 - e^{-ik(l'-l)}\right] - 2\sum_{(r)} I(r, l),$$
$$B_k = 2\sum_{(l)} I(r, l)\left[1 - e^{-ik(l-r)}\right[- 2\sum_{(l)} I(r, l),$$
$$C_k = 2\sum_{(r)} I(r, l)\left[1 - e^{-ik(r-l)}\right] - 2\sum_{(r)} I(r, l). \tag{7}$$

It is easily seen that the coefficients B_k and C_k are not equal to each other since the summation over l contains twice as many terms as the summation over r. $B_k = C_k$ only in the special case of equivalent sublattices which is characteristic of antiferromagnetics. Thus Equations (6), which characterize the energy spectrum for a ferromagnetic lattice of the considered type, are essentially different from the corresponding equations for an antiferromagnetic lattice in [7].

Passing now, as is customary, to the nearest neighbor approximation, expanding the coefficients A_k, B_k, C_k and D_k in series with respect to small values of the wave number k (low temperatures) and confining ourselves to second order terms in k, we obtain from (6):

$$E_k^{(1)} = \varepsilon_0 + \varepsilon_1 a^2 |k|^2, \quad E_k^{(2)} = \varepsilon_2 a^2 |k|^2, \tag{8}$$

where a is the separation of nearest neighbors, and ε_0, ε_1 and ε_2 are expressed in terms of the indirect exchange integrals between nearest neighboring ions.

Taking into consideration now the effect of an external magnetic field on the electron system of a ferrite and performing the usual statistico-thermodynamical calculations, we obtain for the temperature dependence of the spontaneous magnetization of a ferrite at low temperatures

$$M(T) = M_0\left\{1 - \frac{1.306}{2\pi^3}\left(\frac{kT}{\varepsilon_2}\right)^{3/2} + \frac{0.4431}{2\pi^3}\left(\frac{kT}{\varepsilon_1}\right)^{3/2} e^{-\varepsilon_0/kT}\right\}, \tag{9}$$

where $M_0 = {}^1/_3 N\mu_B$ is the magnetization of the ferrite at T = 0° K and μ_B is the Bohr magneton. If ϵ_0 has a value of the order of an exchange integral ($\sim 10^{-14}$ ergs) then at low temperatures the third term in (9) approaches zero considerably more rapidly than the second term and in this case (9) is practically transformed into a "three-halves law."

An analogous method can be used to calculate the temperature dependence of spontaneous magnetization for a ferrite whose lattice is a combination of three nonequivalent or, in a special case, equivalent sublattices. When the magnetization of sublattice A with sites $\bar{r}$ is antiparallel to the magnetization of sublattices B and C with sites $\ell^{(1)}$ and $\ell^{(2)}$, respectively, then for $I(\bar{r}_1, r_2) > 0$, $I(\ell_1^{(i)}, \ell_2^{(k)}) > 0$, $I(r, \ell^{(i)}) < 0$, i, k = 1, 2, the energy of the ground (lowest) level is

$$E_0 = G_0 - \frac{1}{2}\sum_{\substack{r_1,\ r_2 \\ r_1 \neq r_2}} I(r_1, r_2) - \frac{1}{2}\sum_{\substack{l_1^{(i)},\ l_2^{(i)} \\ l_1^{(i)} \neq l_2^{(i)} \\ i=1,\ 2}} I(l_1^{(i)}, l_2^{(i)}) + \\ + \sum_{\substack{r,\ l^{(i)} \\ i=1,2}} I(r, l^{(i)}) - \sum_{l^{(i)},\ l^{(k)}} I(l^{(i)}, l^{(k)}). \tag{10}$$

For the spontaneous magnetization M(T) in this case a calculation analogous to the above leads to

$$M(T) = \frac{1}{3} N\mu_B \left\{1 - \frac{1.306}{4\pi^2}\left(\frac{kT}{q_3}\right)^{3/2} - \frac{0.4431}{4\pi^2}\left(\frac{kT}{q_2}\right)^{3/2} e^{-p_2/kT} + \right. \\ \left. + \frac{0.4431}{4\pi^2}\left(\frac{kT}{q_1}\right)^{3/2} e^{-p_1/kT}\right\}, \tag{11}$$

where p_1, p_2, q_1, q_2, q_3 are functions of the indirect exchange integrals. When p_1 and p_2 have values of the order of the exchange integrals, at temperatures close to T = 0° K Equation (11) is transformed into a "three-halves law."

LITERATURE CITED

[1] L. Neel, Ann. Phys. 3, 137 (1948).

[2] C. G. Shull and J. S. Smart, Phys. Rev. 76, 1256 (1949).

[3] K. B. Vlasov and B. Kh. Ishmukhametov, J. Exptl.-Theoret. Phys. (U.S.S.R.) 27, 75 (1954).

[4] H. Kaplan, Phys. Rev. 86, 121 (1952).

[5] S. V. Vonsovskii and Iu. M. Seidov, Bull. Acad. Sci. U.S.S.R., Phys. Ser. 18, 319 (1954).

[6] N. N. Bogoliubov, Lectures on Quantum Statistics (Kiev, 1949) (In Ukrainian).

[7] N. N Bogoliubov and S. V. Tiablikov, J. Exptl.- Theoret. Phys. (U.S.S.R.) 19, 251, 256 (1949).

[8] E. I. Kondorskii and A. S. Pakhomov, Doklady Akad. Nauk SSSR 93, 431 (1953); 96, 1139 (1954).

[9] H. A. Kramers, Physica 1, 182 (1933); P. W. Anderson, Phys. Rev. 79, 350 (1950).

M. V. Lomonosov Moscow State University

Received March 13, 1956

SHORT-LIVED ISOMERS FROM PROTON BOMBARDMENT

O. I. Leipunskii, V. V. Miller, A. M. Morozov and P. A. Iampol'skii

(Presented by Academician N. N. Semenov March 7, 1956)

The present article is a continuation of work done under a general program for the detection of short-lived isomers produced in nuclear reactions. This program was set up because of a belief [1] that the absence of data concerning isomers with half lives from 0.01 to 10^{-6} sec is due to faulty techniques of measurement. For inelastic interactions with fast particles the proper method (impulsive radiation) can be expected to reveal new isomers with half lives in this range. The first isomer in this region (Bi^{208}) was discovered by us in 1953 through the bombardment of Bi with fast neutrons [1].

In the present work for the excitation of nuclei we used a pulsed beam of 20 Mev protons. The pulse duration was 300 μ sec. The pulse repetition rate was 1 or 2 per second so that all short-lived excited activity decayed between pulses. Targets of the investigated substances were placed in a vacuum with the surface of the target forming an angle of 45° with the direction of the beam. The targets were fastened to a rotatable disk; thus targets could be interchanged during the operation of the accelerator. In all cases the target thickness was 2 to 3 mean free paths of 20 Mev protons in the given substance. During the measurements it was possible to determine a beam intensity of $\sim 10^9$ protons per pulse. The targets were placed on a plexiglas backing and the charge accumulating on a target was measured with an SG-1M electrometer. For the purpose of excluding effects due to secondary electrons a positive voltage was applied to the targets.

For the study of short-period γ radiation we used a method which was essentially the same as that described in [1]. The γ radiation which resulted from proton bombardment was recorded with a scintillation counter (an FEU-19 photomultiplier with an NaI(Tl) crystal) placed close to the target. The efficiency of detection of γ radiation from the target as measured with a sample of Zn^{65}(E_γ = 1.118 Mev) was 1.5-2.5%. β radiation was recorded by a counter with a stilbene crystal covered with aluminum foil (of 0.1 mm thickness). The counter was placed on the side of the target that faced the proton beam. Counter pulses were amplified and then discriminated by an integral pulse-height analyzer. After shaping, the pulses appeared on the screen of a special cathode ray oscilloscope with driven sweep and were photographed. The sweep was started 0.7 msec after the start of the proton pulse; during this time the FEU-19 was cut out of the operating circuit. The oscilloscope had a set of sweeps with durations of 0.1, 0.05, 0.01 and 0.001 sec, each with its own time marking.

Pulses from more long-lived activity were recorded by an MPO-2 loop oscillograph. The β and γ channels of the apparatus were checked by measuring the half-lives of known isotopes. An analysis of the data obtained through proton bombardment of Fe, Ti and S revealed activities with $T_{1/2}$ = 0.18 ± 0.05 sec (Fe), 0.37 ± 0.05 sec (Ti), 3.4 ± 1.0 sec and 0.3 ± 1.15 sec (S). These half lives are in good agreement with the known half lives of Co^{54} (0.18 ± 0.01 sec), V^{46} (0.40 ± 0.01 sec), S^{31} (3.18 ± 0.4 sec), Cl^{32} (0.306 ± 0.004 sec) [2,3]. S^{31} apparently is produced through the reaction S^{32} (p, pn) S^{31}; we do not know of any data on this reaction in the literature.

It is of interest to note that the ratio of the yields of Cl^{32} (from a p, n reaction) and S^{31} (from a p, pn reaction) is $\sim$ 1 : 6.

When Be was irradiated considerable β activity was noted with $T_{1/2}$ = 0.85 ± 0.15 sec. This activity can be attributed to Li^8 ($T_{1/2}$ = 0.87 ± 0.02 sec) from the reaction Be^9 (p, 2p) Li^8 [4]. The threshold of this reaction (calculated from the masses) is 18.7 Mev (without consideration of the Coulomb barrier). The reaction Be^9 (p, 2n) leading to the formation of Be^8 with a half life close to the measured value (0.65 sec) is energetically impossible.

TABLE 1

Target	$T_{1/2}$, sec	E_γ, Mev	Relative yield
Ti, Metal	$(1.4 \pm 0.3) \cdot 10^{-3}$	~1.0	0.2
Cd "	0.04 ± 0.01		
Ta "	$(5.0 \pm 1.0) \cdot 10^{-3}$	~0.5	1
Tl "	$(6.5 \pm 0.5) \cdot 10^{-3}$	~0.9	0.3
Pb "	$(2.0 \pm 0.5) \cdot 10^{-3}$	~0.7	0.07
Bi "	$(3.0 \pm 1.0) \cdot 10^{-3}$		

In subsequent experiments we detected new γ activity which had not been observed earlier and belonging to new and previously unknown isomers. Table 1 gives the characteristics of this γ activity. Besides the half lives and relative yields the energies of these γ rays are given. The energy was estimated with an integral discriminator calibrated by γ radiation from Co^{60}. The relative yield was determined from the formula

$$K = \frac{N}{\epsilon \eta M},$$

where N is the number of active nuclei produced; M is the detector reading; ϵ is the efficiency for recording γ radiation with energy E_γ; η is a factor which allows for the attenuation of γ radiation with energy E_γ in the target sample.

The table gives the yields compared with the yield of γ radiation from Ta. In calculating the half lives we allowed for the background from a beam striking a neutral target (Au or Rh).

In addition to the activities listed in the table appreciable short-lived γ radiation (with $T_{1/2}$ ~ a few milliseconds) was observed from the bombardment of Cu, Mo, CaO. Irradiation of Co, Rh and Au revealed no short-lived activity. Long-lived activity was weak.

There is ground for believing that the detected short-lived γ radiation is associated with the excitation of isomeric states of the isotopes resulting from reactions with protons. Ground level decay of isotopes resulting from these reactions with the elements listed in the table is well known. After our measurements were completed, data was published [5] on isomeric activity excited through the bombardment of Ta with fast protons. The value $T_{1/2} = 5.5 \pm 0.3$ msec given there agrees within the limits of error with our measurements. According to the excitation curve obtained in this article the short-lived activity can be attributed to W^{180} (from the Ta^{181} (p, 2n) W^{180} reaction).

In the work of our laboratory reported in [1] we detected the excitation of short-lived γ radiation ($T_{1/2} \sim 2.5$ msec) from the bombardment of Bi with fast neutrons ($E_n = 14.5$ Mev). From the magnitude of the cross section of the reaction and other considerations the activity is assigned to an isomer of Bi^{208} resulting from the reaction Bi^{209} (n, 2n) Bi^{208}.*

The values of $T_{1/2}$ for the γ activity which we obtained through proton bombardment of Pb and Bi makes it possible to assume that in these cases Bi^{208m} results from the reactions Pb^{209} (p, n) and Bi^{209} (p, pn).

In the case of Tl, which has 2 isotopes, the isomeric activity can be associated with the isotopes Tl^{202} and Tl^{204} (p, pn reactions) or Pb^{203} and Pb^{205} (p, n reactions). Study of the excitation curve can show which type of reaction occurs. In [6] γ activity with a half life of ~ 10 sec is assigned to Pb^{203}; there is no reliable information concerning Pb^{205}. In the same work it was found that in the γ spectrum of Pb^{202m} ($T_{1/2} = 3.5$ hrs) a number of lines show conversion to Tl, so that it was suggested that there exists a K-capture branch from an isomeric state of Pb^{202} to a short-lived isomeric state of Tl^{202} with spin 8+. Tl^{202} emits photons with $E_\gamma = 460$ kev (E3 transition). It is possible that the measured activity excited by bombardment of Tl is associated with Tl^{202}. An estimate of $T_{1/2}$ for the 460 kev transition gives a value of the order of a few 10^{-4} sec, which is not very much different from our measurement.

The authors are grateful to K. D. Sinel'nikov, P. M. Zeidlits, A. P. Kliucharev and A. M. Smirnov for their interest and assistance in this work, and to O. B. Likin, who designed the electronic circuitry.

LITERATURE CITED

[1] P. A. Iampol'skii, M. Ia. Gen, O. I. Leipunskii and A. M. Tikhomirov, Bull. Acad. Sci. U.S.S.R., Phys. Ser. 19, 3,338 (1955).

---

* Bi^{208} was not detected in the ground state and is evidently long-lived.

[2] W. M. Martin and S. W. Breckton, Can. J. Phys. 30, 643 (1953).

[3] N. W. Glass, L. K. Jensenn and J. R. Richardson, Phys. Rev. 90, 320 (1953).

[4] L. W. Alvarez, Phys. Rev. 80, 519 (1950).

[5] S. D. Softky, UCRL-2754, Nucl. Sci. Abstr. 9, 2, 95 (1955).

[6] I. Bergström and A. H. Wapstra, Phil. Mag. 46, 372, 61 (1955).

Institute of Chemical Physics,
Academy of Sciences of the U.S.S.R.

Received February 26, 1956

REFLECTION AND TRANSMISSION OF 7-24 μ WAVES BY SILICA MODIFICATIONS

N. A. Sevchenko and V. A. Florinskaia

(Presented by Academician A. A. Lebedev April 5, 1956)

INTRODUCTION

The reflection and transmission spectra of α quartz and of fused quartz in the 1-15 μ region have been studied by many investigators [1-9], but information concerning these spectra for longer waves is very limited [10-12]. Other polymorphous forms of silica (cristobalite and tridymite) have begun to be studied very recently [13-16] and the published data concern mainly the 1-14 μ range [13-15]. This can be explained by the fact that natural cristobalite and tridymite are very rare and contain impurities, and that, moreover, the crystals of these modifications are very small. However, for study of the structure of silicates and silica glass it is very important to know the complete vibrational spectra of all forms of silica. The present article presents some of our results from an investigation of the reflection and transmission spectra of some modifications of silica in the 7-24 μ region.

EXPERIMENTAL

The reflection and transmission measurements were carried out with an IKS-11 spectrometer, which consists of a mirror monochromator and interchangeable prisms. In the 7-14 μ and 14-24 μ regions, respectively, we used sodium chloride and potassium bromide prisms with 60° refracting angles. The detector was a vacuum thermocouple with the amplifier of B. P. Kozyrev. Reflection was measured for unpolarized light close to an angle of 25°. Reflection from the investigated samples was compared with reflection from an aluminum mirror. The reflection and transmission measurements were repeated a few times both with automatic recording and visually.

We investigated the reflection spectra of the following samples of silica: α quartz cut perpendicular and parallel to the optic axis, Gereus Company quartz glass and α cristobalite. The last was a well polished plate of polycrystalline material provided by the museum of the Geological Institute of the Academy of Sciences of the USSR. It was tested electronographically and crystallographically; data obtained by the latter method showed 10-15% of impurities (magnetites and fayalites).

We also investigated the transmission spectra of the following powdered substances: α quartz, α cristobalite, α tridymite and quartz glass. The sample which served for transmission measurements was a sylvite plate bearing on one surface a uniform layer of powder with thickness of the order of 1 μ and grain size smaller than 1 μ.

Reflection Measurements

Fig. 1 shows the reflection from α quartz cut perpendicular and parallel to the optic axis, cristobalite and Gereus quartz glass. The accuracy in fixing the peaks up to 15 μ is 0.02 μ; in the longer wave region it was somewhat lower. As is known from earlier measurements the first fundamental reflection band in the 8-10 μ region is a doublet in the spectrum of quartz cut perpendicular and parallel to the optic axis. As can be seen from Fig. 1 other bands differ both in position and in structure. The second fundamental band, in the 12-13 μ region, for quartz cut perpendicular to the axis has one peak which agrees with the reflection peak for the ordinary beam; for quartz cut parallel to the axis two peaks are observed which coincide with the reflection peaks of the ordinary and extraordinary beams. The third fundamental band, which is in the 14-15 μ region, is observed for quartz cut perpendicular to the optic axis; its peak agrees with the reflection peak of the ordinary beam. In quartz cut

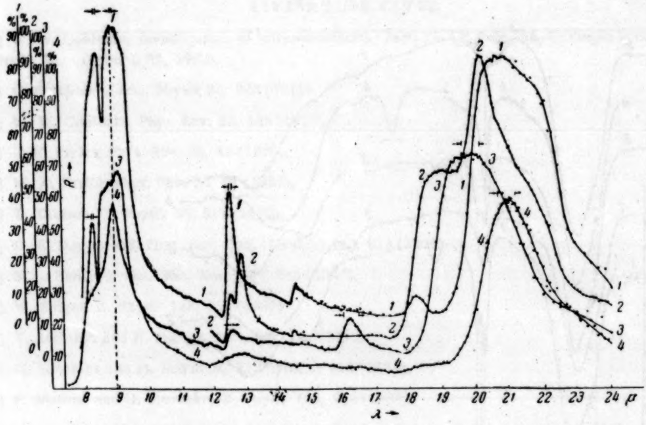

Fig. 1. Reflection spectra of silica.
1) α quartz cut perpendicular to the optic axis; 2) α quartz cut parallel to the optic axis;
3) α crystobalite; 4) Gereus fused quartz.

parallel to the optic axis only traces of this are detected. A fourth fundamental band, in the 20-21 μ region, for quartz cut perpendicular to the optic axis has a peak at 20.7-20.8 μ, which coincides with the reflection peak of the ordinary beam, whereas in quartz cut parallel to the axis the peak lies at 20.1 μ. In addition, in the spectrum of quartz cut perpendicular and parallel to the optical axis other bands are observed at 18.2 and 19 μ. A comparison of the reflection spectra of α quartz and α crystobalite shows that the bands at 8-10 μ, 12-13 μ and 20-21 μ, although common to both in the sense that they exist in both cases, differ considerably from each other in structure and position.

An especially marked difference is observed at 20-21 μ, the shift being approximately 1 μ. In addition, each of these crystals has its specific bands; such as the band at 14-15 μ for crystalline quartz and the crystobalite band at 16 μ. Thus comparison of the spectra indicates that although the same compound SiO_2 is found in both instances, the vibrational spectrum depends essentially on the lattice which couples the SiO_4 tetrahedrons. This fact provides us with a method which is not less powerful than x-ray analysis for discriminating according to their spectra the forms of silica in both minerals and crystallized glass. A comparison of the spectrum of Gereus quartz glass and of quartz and crystobalite shows that the first band coincides very accurately in position with the analogous band of α quartz. The band at 20-21 μ is closer in position to the ordinary beam of α quartz, i.e. the spectrum of the glass possesses more similarity to the spectrum of α quartz than to that of α crystobalite.

Transmission Measurements

Fig. 2 gives the transmission curves of different forms of silica. Table 1 contains a comparison of the reflection peaks and transmission minima of all silica modifications. Curves 1 and 3 belong to films of powder of different thicknesses of α quartz; Curves 2, 4 and 5 belong, respectively, to artificial tridymite, to crystobalite whose reflection spectrum is given in Fig. 1 and to Gereus quartz glass.

From a comparison of the transmission spectra it can be seen that, just as in the case of reflection, the bands at 8-10 μ, 12-13 μ and 20-21 μ are common to all, as they are observed in all spectra. But, in addition, the transmission of each crystalline form of silica reveals its specific bands. In quartz these are the bands at 14 and 19 μ,

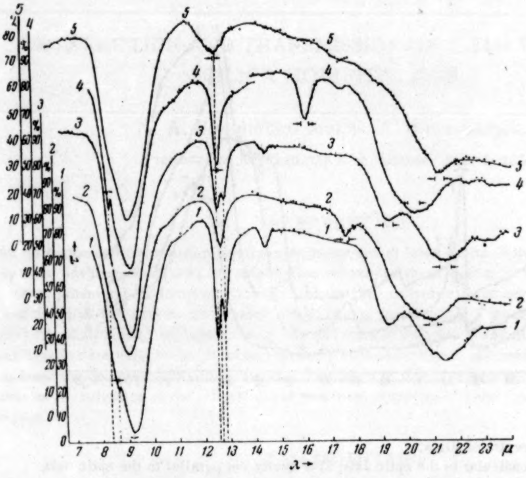

Fig. 2. Transmission spectra of silica.
1 and 3) Thin films of α quartz powder; 2) the same for α tridymite; 4) the same for α crystobalite; 5) the same for Gereus fused quartz.

TABLE 1

Test specimen	λ in μ
	Reflection
Quartz ⊥ axis	8.50; 8.95; 12.54; 14.54; 18.2; 20.7-20.8;
Quartz ∥ axis	12.55; 12.85; 14.5; 18.9-19.00; 20.1;
Crystobalite	8.30 ; 9.10 ; 12.60; 16.15-16.20; 19.8-19.9;
Quartz glass from the Gereus Company	8.95; 12.7-12.9; 20.9-21.0
	Transmission
α quartz	8.63; 9.15; 12.55; 12.85; 14.40-14.45; 19.2-19.3; 21.4-21.6;
α crystobalite	8.35; 9.12; 12.60; 16.10; 20.3;
α tridymite	9.05; 12.70; 17.6; 20.8-21.0 ;
Quartz glass from the Gereus Company	9.05-9.15; 12.50; 21.3

in crystobalite at 16 μ and in tridymite at 17.6 μ. A comparison of the transmission spectra of different samples of Gereus quartz glass with the spectra of crystalline forms of silica shows that the bands at 8-10 μ and 12-13 μ are broader than the corresponding bands of the crystals, also less intense- but in position they, for the larger part, coincide exactly with the analogous bands of α quartz. The 21 μ band is very sensitive to the lattice structure and lies closest to α quartz. Thus from the investigation of both reflection and transmission spectra it follows that the position of the fundamental bands in the spectra of Gereus quartz glass is closest to that of the analogous bands of α quartz. Since the position of the bands is related to the lattice structure it follows from this correspondence that the structure of Gereus quartz glass is closer to that of quartz than to that of crystobalite or tridymite.

LITERATURE CITED

[1] W. W. Coblentz, Investigation of Infrared Spectra, Parts III, IV, Publ. 65, Carnegie Inst., Washington, 1906; Parts V, VI, VII (Publ. 97, 1908).

[2] O. Reinkober, Ann. Physik 34, 343 (1911).

[3] W. W. Coblentz, Phys. Rev. 23, 125 (1916).

[4] E. K. Plyler, Phys. Rev. 33, 48 (1929).

[5] W. A. Paslin, Phys. Rev. 34, 81 (1929).

[6] T. Dreisch, Z. Physik 53, 317 (1929).

[7] D. E. Drummond, Proc. Roy. Soc. (London) 153, 318 (1936).

[8] R. L. Henry, J. Opt. Soc. Amer. 38, 745 (1948).

[9] W. Brügel, Z. Physik 128, 255 (1950).

[10] T. Liebisch and H. Rubens, Berl. Ber. 199 (1919).

[11] C. Schaefer and M. Schubert, Z. Physik 7, 313 (1931).

[12] F. Matossi and H. Bluschke, Z. Physik 108, 295 (1938).

[13] V. A. Florinskaia and R. S. Pechenkina, Doklady Akad. Nauk S.S.S.R. 85, 6 (1952).

[14] V. A. Florinskaia and R. S. Pechenkina, Trans. Conference on Glass Structure, Leningrad, 1953 (Academy of Sciences USSR Press, 1955).

[15] I. Simon and H. O. McMahon, J. Chem. Phys. 21, 23 (1953).

[16] M. Haccuria, Bull. Soc. Chim. Belg. 62, 428 (1953).

Received March 22, 1956

GAMMA RADIATION FROM THE COLLISIONS OF FAST CHARGED PIONS WITH NUCLEI

A. G. Sitenko

(Presented by Academician L. D. Landau February 27, 1956)

1. Because of the strong interaction between high energy pions and nuclei, a nucleus can be regarded as a blackbody (a sphere of radius R) with respect to such a pion. Under relativistic conditions the emission of gamma rays due to collisions of pions with nuclei takes place at large distances from the nuclei. Therefore knowledge of the pion wave function outside the nucleus as a sum of a plane and a spherical wave is sufficient for determining the gamma bremsstrahlung emitted in a direction which differs little from the direction of the incident particle. The diffraction mechanism of gamma emission by fast pions in collisions with nuclei was examined by L. D. Landau and I. Ia. Pomeranchuk [1]. In the present note we examine diffractive gamma emission by fast pions, taking into consideration the Coulomb interaction of the pions with the nuclear charge. It is especially important to consider this interaction in the case of semitransparent nuclei.

2. We first consider elastic diffractive scattering of fast charged pions by a perfect blackbody of radius R. The pion wave function in a plane perpendicular to the initial particle momentum **p** and passing through the nucleus can obviously be written as

$$\Omega_p(\rho) = \begin{cases} 0, & \rho \leqslant R, \\ e^{2i\eta(\rho)}, & \rho > R, \end{cases}$$

where ρ is the radius-vector of the particle in this plane: $\eta(\rho) = \arg\Gamma(p\rho + 1 + in)$; $n = Ze^2E/4\pi p$ and E is the energy of the pion. (We assume that $c = \hbar = 1$ and use Heaviside charge units). From the Huygens principle the wave function at any point beyond the nucleus becomes

$$\psi_p^+(\mathbf{r}) = \frac{p}{2\pi i}\int \frac{e^{ip|\mathbf{r}-\vec{\rho}|}}{|\mathbf{r}-\vec{\rho}|}\Omega_p(\rho)\,d\vec{\rho} = e^{i\mathbf{pr}} - \frac{p}{2\pi i}\int \frac{e^{ip|\mathbf{r}-\vec{\rho}|}}{|\mathbf{r}-\vec{\rho}|}\{1-\Omega_p(\rho)\}\,d\vec{\rho}. \tag{1}$$

At large distances from the nucleus the coefficient of the outgoing spherical wave is the elastic scattering amplitude

$$f(\vartheta) = -\frac{p}{2\pi i}\int e^{-i\mathbf{p}'\vec{\rho}}\{1-\Omega_p(\rho)\}\,d\vec{\rho}, \tag{2}$$

where $\mathbf{p}' = p\frac{\mathbf{r}}{r}$ and ϑ is the scattering angle. Since $pR \gg 1$ we can use in (2) an approximate expression for the scattering phase $\eta(\rho) \simeq n\ln p\rho$, so that the scattering amplitude becomes

$$f(\vartheta) = i\left\{\frac{RJ_1(pR\sin\vartheta)}{\sin\vartheta} + \frac{2in}{\sin\vartheta}\int\limits_R^\infty \left(\frac{\rho}{R}\right)^{2in} J_1(p\sin\vartheta\rho)\,d\rho\right\}(pR)^{2in}. \tag{3}$$

In the limiting case $n \ll 1$

$$f(\vartheta) = i\left\{\frac{RJ_1(pR\sin\vartheta)}{\sin\vartheta} + 2in\,\frac{J_0(pR\sin\vartheta)}{p\sin^2\vartheta}\right\}. \tag{4}$$

The differential cross section for elastic scattering of charged pions is then given by

$$d\sigma_e = \left\{\frac{R^2 J_1^2(pR\sin\vartheta)}{\sin^2\vartheta} + \frac{4n^2}{p^2}\,\frac{J_0^2(pR\sin\vartheta)}{\sin^4\vartheta}\right\} do. \tag{5}$$

The first term in (5) describes diffractive scattering of pions by a perfectly black nucleus. The second term describes the scattering of charged pions in the Coulomb field of the nucleus [2]. There is no interference in this approximation.

3. We shall now determine the cross section for diffractive scattering of a charged pion (a π^+ meson, for example) with the emission of a photon. The wave equation for a pion outside the nucleus is

$$\begin{gathered}\left\{\Delta + \left(i\frac{\partial}{\partial t} - \frac{\alpha}{r}\right)^2 - \mu^2\right\}\Psi = i2e\mathbf{A}\nabla\Psi, \quad \alpha = \frac{Ze^2}{4\pi}, \\ \mathbf{A} = \sum_{\mathbf{k}j}\sqrt{\frac{1}{2\omega}}\,\mathbf{j}\,(a_{kj}e^{i\mathbf{kr}-i\omega t} + a_{kj}^{+}e^{-i\mathbf{kr}+i\omega t}).\end{gathered} \tag{6}$$

Assuming the right-hand side of (6) to be small we seek a solution in the form of the series

$$\Psi = \psi_{\mathbf{p}}^{+}(\mathbf{r})\,e^{-iEt} + \sum_{\mathbf{p}'}\Phi_{\mathbf{p}'}e^{-iE't},$$

where

$$\left\{\Delta + \left(E' - \frac{\alpha}{r}\right)^2 - \mu^2\right\}\Phi_{\mathbf{p}'} = i2e\sqrt{\frac{1}{2\omega}}\sum \mathbf{j}\nabla\psi_{\mathbf{p}}^{+}\,e^{-i\mathbf{kr}}a_{kj}^{+}. \tag{7}$$

The amplitude $\varphi_{\mathbf{p}'}$, which corresponds to the emission of the photon, is

$$\Phi_{\mathbf{p}'}(\mathbf{r}) = \int G(\mathbf{r},\mathbf{r}')\,i2e\sqrt{\frac{1}{2\omega}}\,\mathbf{j}\nabla\psi_{p}^{+}\,e^{-i\mathbf{kr}'}\,d\tau', \quad p'^2 = (E-\omega)^2 - \mu^2. \tag{8}$$

$G(\mathbf{r},\mathbf{r}')$ is the Green's function of (7), with the following asymptotic form:

$$G(\mathbf{r},\mathbf{r}') = \frac{e^{ip'r}}{4\pi r}\,\psi_{p'}^{-*}(\mathbf{r}'), \quad r\to\infty, \tag{9}$$

where $\psi_{\mathbf{p}'}^{-}(\mathbf{r})$ is the sum of the plane wave and an ingoing spherical wave:

$$\psi_{\mathbf{p}'}^{-}(\mathbf{r}) = e^{i\mathbf{p}'\mathbf{r}} + \frac{p'}{2\pi i}\int\frac{e^{-ip'|\mathbf{r}-\vec{\rho}|}}{|\mathbf{r}-\vec{\rho}|}\{1 - \Omega_{-\mathbf{p}'}(\rho)\}\,d\vec{\rho}. \tag{10}$$

From (8) and (9) it is easy to obtain the following expression for the differential cross section of pion scattering within the solid angle do' accompanied by the emission of a photon of frequency ω and polarization $\mathbf{j}$ in the solid angle do:.

$$d\sigma_{\mathbf{j}} = \frac{e^2}{2\omega}\left|\int \psi_{\mathbf{p}'}^{-*}(\mathbf{r})\,(\mathbf{j}\nabla\psi_{\mathbf{p}}^{+}(\mathbf{r}))\,e^{-i\mathbf{kr}}\,d\tau\right|^2 \frac{p'}{p}\,\frac{\omega^2 d\omega}{(2\pi)^5}\,do\,do'. \tag{11}$$

We note that in (11) the integral of the product of the plane waves in $\psi_{\mathbf{p}}^{+}$ and $\psi_{\mathbf{p}'}^{-}$ vanishes according to the conservation laws, and the integral of the product of the diffracted waves vanishes because the shadows in the case of small angles ϑ and ϑ' between $\mathbf{k}$ and $\mathbf{p}$ and $\mathbf{p}'$ and $\mathbf{p}$, for which alone the diffraction picture has meaning, do not overlap.

Summing (11) over polarizations and assuming that $E, E' \gg \mu$, we obtain

$$\begin{aligned} d\sigma = \frac{e^2 p'}{4\pi^3 p}\Bigg| & \frac{RJ_1(\mu\,|\vec{\xi}+\vec{\eta}\,|R)}{|\vec{\xi}+\vec{\eta}\,|} + \\ & + \frac{2in}{|\vec{\xi}+\vec{\eta}\,|}\int\limits_R^\infty \left(\frac{\rho}{R}\right)^{2in} J_1(\mu\,|\vec{\xi}+\vec{\eta}\,|\rho)\,d\rho\Bigg|^2 \cdot \left(\frac{\vec{\xi}}{1+\xi^2}+\frac{\vec{\eta}}{1+\eta^2}\right)^2 \cdot \frac{d\omega}{\omega}\,d\vec{\xi}\,d\vec{\eta}, \end{aligned} \tag{12}$$

where $\vec{\xi} = \dfrac{E}{\mu}\,\vec{\vartheta}$ and $\vec{\eta} = \dfrac{E'}{\mu}(\vec{\vartheta}' - \vec{\vartheta})$ (μ is the mass of the meson).

The strong interaction of the pion with the nucleon background is associated with the spread of the pion charge over a certain region. Consideration of the finite size of a pion leads to the addition factor $|F|^2$ in (12), where F is a form factor which depends on the invariant frequency $\dfrac{E\omega - \mathbf{pk}}{\mu^2}$ [1].

Assuming in (12) that n = 0, we obtain the result of L. D. Landau and I. Ia. Pomeranchuk [1]. If we set R = 0, Equation (12) gives the differential cross section for bremsstrahlung by charged particles with spin zero in a Coulomb field [3].

4. Integrating (12) over the angles $\vec{\xi}$ and $\vec{\eta}$ we obtain the spectral distribution of the radiation:

$$d\sigma_\omega = \frac{e^2}{\pi}\,\frac{p'}{p}\,\frac{d\omega}{\omega}\int\left|\frac{RJ_1(2\mu Rq)}{q} + \frac{in}{\mu}\,\frac{(2\mu Rq)^{-2in}}{q^2}\int\limits_{2\mu Rq}^{\infty} J_1(\zeta)\,\zeta^{2in}d\zeta\right|^2 \varphi(q)\,q\,dq, \tag{13}$$

where $\varphi(q) = \left\{\dfrac{2q^2+1}{q\sqrt{1+q^2}}\ln\left(q+\sqrt{1+q^2}\right) - 1\right\}$. In the limiting case $n \ll 1$ the cross section (13) becomes the sum of two terms:

$$d\sigma_\omega = d\sigma_\omega^d + d\sigma_\omega^c, \tag{14}$$

where $d\sigma_\omega^d$ is the cross section for diffraction radiation and $d\sigma_\omega^c$ is the cross section for bremsstrahlung in the Coulomb field of the ultimate nucleus:

$$d\sigma_\omega^d = \frac{e^2R^2}{\pi}\,\frac{p'}{p}\,\frac{d\omega}{\omega}\int\limits_0^\infty \frac{J_1^2(2\mu Rq)}{q}\,\varphi(q)\,dq = \frac{e^2}{\pi}\,\frac{p'}{p}\,\frac{d\omega}{\omega}\,R^2 n^d(\mu R), \tag{15}$$

$$d\sigma_\omega^c = \frac{e^2n^2}{\pi\mu^2}\,\frac{p'}{p}\,\frac{d\omega}{\omega}\int\limits_{q_m}^\infty \frac{J_0^2(2\mu Rq)}{q^3}\,\varphi(q)\,dq = \frac{e^2}{\pi}\,\frac{p'}{p}\,\frac{d\omega}{\omega}\,\frac{n^2}{\mu^2}\,n^c(\mu R, q_m). \tag{16}$$

The integration over $\underline{q}$ in (16) must be carried out from a certain minimum value $q_m = \mu\omega/4EE'$, determined by the conservation laws. In case of complete screening of the Coulomb field the lower limit of integration over $\underline{q}$ will be $q_m \simeq z^{1/3}m/137\mu$ ($\underline{m}$ is the electron mass), where n^c will not depend on the frequency of the emitted photon. In this case the total energy loss associated with bremsstrahlung is given by

$$\int_0^E \omega\, d\sigma_\omega = \frac{e^2}{2\pi} ER^2\left(n^d + \frac{n^2}{\mu^2R^2}n^c\right). \tag{17}$$

The integral cross section of photon emission with frequencies above ω is given by

$$\int_\omega^E d\sigma_\omega = \frac{e^2R^2}{\pi}\left(n^d + \frac{n^2}{\mu^2R^2}n^c\right)\left(\ln\frac{E}{e\omega} + \frac{\omega}{E}\right). \tag{18}$$

5. In the limiting case $R\mu \gg 1$ (for heavy nuclei) (15) and (16) are considerably simplified:

$$d\sigma_\omega^d = \frac{e^2}{2\pi^2}\frac{R}{\mu}\frac{p'}{p}\frac{d\omega}{\omega}.\int_0^\infty \varphi(q)\frac{dq}{q^2} \simeq \frac{2{,}3}{4\pi}\frac{e^2R}{\mu}\frac{p'}{p}\frac{d\omega}{\omega}, \tag{19}$$

$$d\sigma_\omega^c = \frac{e^2n^2}{\pi\mu^2}\frac{p'}{p}\frac{d\omega}{\omega}(2\mu R)^2\int_{2\mu Rq_m}^\infty \frac{J_0^2(x)}{x^3}\varphi\left(\frac{x}{2\mu R}\right)dx \simeq \frac{4e^2n^2}{3\pi\mu^2}\frac{p'}{p}\frac{d\omega}{\omega}\int_{2\mu Rq_m}^\infty \frac{J_0^2(x)}{x}dx. \tag{20}$$

Inserting in (20) $q_m = \mu\omega/4EE'$ and assuming $2\mu Rq_m \ll 1$, after integration by parts we obtain

$$d\sigma_\omega^c = \frac{4e^2n^2}{3\pi\mu^2}\frac{p'}{p}\frac{d\omega}{\omega}\ln\frac{2EE'}{\mu^2R\omega} \tag{21}$$

This expression agrees with the cross section for bremsstrahlung by a particle with spin zero which was obtained in [3] with allowance for the finite size of the nucleus.

For complete screening of the Coulomb field the integral cross section of emission with frequencies above ω becomes

$$\int_\omega^E d\sigma_\omega \simeq \frac{2{,}3}{4\pi}\frac{e^2R}{\mu}\left(1 + 2{,}4\frac{n^2}{\mu R}\ln\frac{137}{2mRZ^{1/3}}\right)\left(\ln\frac{E}{e\omega} + \frac{\omega}{E}\right). \tag{22}$$

6. If the nucleus only partially absorbs mesons it is possible to use the optical model [4] in which the nucleus is characterized by a complex absorption coefficient $B = K - 2ik_1$. Then allowance for semitransparency of the nucleus requires only the replacement of $RJ_1(2\mu Rq)/q$ in (13) by the expression

$$\begin{aligned} &2\mu R^2\int_0^1 \left(1 - e^{-BR\sqrt{1-y^2}}\right) J_0(2\mu Rqy)\, y\, dy = \\ &= 2\mu R^2 \sum_{n=1}^\infty (-1)^{n-1}\frac{2^{n/2}\Gamma\left(\frac{n}{2}+1\right)}{n!}\left(\frac{(BR^2)}{2\mu Rq}\right)^{n/2}\frac{J_{n/2+1}(2\mu Rq)}{2\mu Rq}. \end{aligned} \tag{23}$$

For an almost transparent nucleus ($|B|^2 R^2 \ll 2\mu R q_m$) in (23) can be limited to only the first term of the expansion, in which case the cross-section for diffractive emission is obtained in the form

$$d\sigma_\omega^d = \frac{e^2 (K^2 + 4k_1^2) R^2}{4\mu} \frac{p'}{p} \frac{d\omega}{\omega} \int\limits_0^\infty \frac{J_{3/2}^2 (2\mu R q)}{q^3} \varphi(q)\, dq \simeq$$

$$\simeq \frac{e^2}{6\pi\mu^2} \frac{p'}{p} (K^2 + 4k_1^2) R^2 \ln 2\mu R \frac{d\omega}{\omega}. \qquad (24)$$

I am deeply grateful to L. D. Landau, A. I. Akhiezer and I. Ia. Pomeranchuk for discussions of this problem.

LITERATURE CITED

[1] L. D. Landau and I. Ia. Pomeranchuk, J. Exptl.-Theoret. Phys. (U.S.S.R.) 24, 505 (1953).

[2] H. Corben and J. Schwinger, Phys. Rev. 58, 953 (1940).

[3] R. Christy and S. Kusaka, Phys. Rev. 59, 414 (1941).

[4] S. Fernbach, R. Serber and T. B. Taylor, Phys. Rev. 75, 1352 (1949).

A. M. Gorkii Kharkov State University
and the
Physicotechnical Institute, Academy of
Sciences of the Ukrainian SSR

Received February 7, 1956

SOVIET PHYSICS – "DOKLADY" VOL. 1, NO. 4 APRIL, 1957

(Translation of all papers in the "Physics" Sections of the Proceedings of the Academy of Sciences of the USSR, Vol. 109, Nos. 1-6, July-August, 1956)

CONTENTS

		Russian	
	Page	Issue No.	Page
The Calculation of π-Electronic Polarizability of Polyenes and Benzene by the "Metallic" Molecular Model. M. N. Adamov and I. S. Milevskaia	399	1	57
On Nonionospheric Fluctuations of the Intensity of Radio Waves from Nebulae. V. L. Ginzburg	403	1	61
The Anomalous Scattering of Light in Glass. A. I. Koliadin	406	1	64
The Distortion and Interaction of Acoustic Waves of Finite Amplitude in a Viscous Medium. G. D. Mikhailov	409	1	68
A Gauge-Invariant Analogue of the Wigner Distribution. R. L. Stratonovich	414	1	72
The Nuclear Quadrupole Moment of U^{233}. A. G. Zimin and N. M. Iashin	419	2	283
Regrouping of the Latent Image in the Photographic Action of Ionizing Particles. A. L. Kartuzhanskii	421	2	285
Sublimation of a Crystal Lattice by a Strong Shock Wave. Iu. N. Riabinin	424	2	289
Duration of Fluorescence in Mesoderivatives of Anthracene. A. S. Cherkasov, V. A. Molchanov, T. M. Vember and K. G. Voldaikina	427	2	292
An Experimental Verification That the Velocity of Light is Independent of the Velocity of the Source with Respect to an Observer. A. M. Bonch-Bruevich	430	3	481
The Distortion of Ultrasonic Waves of Finite Amplitude in Liquids. L. K. Zarembo, V. A. Krasil'nikov and V. V. Shklovskaia-Kordi	434	3	485
Generalization of the Method of Supplementary Variables. D. N. Zubarev	437	3	489
The Elastic Properties of β-Quartz at High Temperatures. V. G. Zubov and M. M. Firsova	441	3	493
Electron Motion in Cyclical Accelerators as a Stochastic Process. A. N. Matveev	443	3	495
Magnetic Analysis of the Reactions (I) $pp \to np\pi^+$, (II) $pp \to pp\pi^0$ and (III) $pp \to d\pi^+$ at 660 Mev. M. G. Meshcheriakov	447	3	499
The Phosphorescence Spectra of Some Aromatic Acids at the Temperature of Liquid Air. B. A. Piatnitskii	451	3	503
A Dispersion Relation for Fermions. V. Fainberg and E. Fradkin	455	3	507
On the Theory of Alternating-Gradient Focusing. E. L. Burshtein and L.S. Solov'ev	459	4	721
Hyperfine Structure of Paramagnetic Resonant Lines in Supercooled Solutions of $^{51}V^{++}$, $^{53}Cr^{+++}$ and $^{55}Mn^{++}$. N. S. Garif'ianov	463	4	725
Electrical Phenomena in the Disruption Mechanism of Some Solids. B. V. Deriagin, N. A. Krotova and V. V. Karasev	466	4	728
The Absorption of Ultrasonic Waves of Finite Amplitude in Liquids. L. K. Zarembo, V. A. Krasil'nikov and V. V. Shklovskaia-Kordi	470	4	731
The Transverse Photomagnetic Effect in n- and p-type Germanium. I. K. Kikoin and Iu. A. Bykovskii	473	4	735

CONTENTS (Continued)

	Page	Russian Issue No.	Russian Page
A Study of the Reaction of He^3 with Deuterons. A. P. Kliucharev, B. N. Esel'son and A. K. Val'ter	475	4	737
The Spectral Representation and the Renormalization Group. A. A. Logunov	478	4	740
On Measuring the Resolving Power of an Optical Instrument. S. G. Rautian	481	4	743
On the Possibility of a Transition Between Two Types of Concentration Quenching of Fluorescence. B. Ia. Sveshnikov, L. A. Kuznetsova and V. A. Molchanov	484	4	746
Magnetoresistance and Hole Conduction in Tellurium. S. S. Shalyt	488	4	750
Redistribution of Electron Density and Change of Electrical Conductivity in Cadmium Sulfide Crystals. Iu. N. Shuvalov	490	4	753
Measurement of the Dynamical Modulus of Elasticity of Rubber for Very Small Deformations by an Optical Modulation-Interference Method. N. M. Borovitskaia	493	5	923
Determination of the Orientation Relaxation Time of Some Liquids by the Widths of Scattered Lines. M. F. Vuks and A. K. Atakhodzhaev	496	5	926
A New Method of Measuring the Velocity of Light. K. S. Vul'fson	499	5	929
On the Theory of the Spontaneous Magnetization of Ferromagnetic Semiconductors at Low Temperatures. E. I. Kondorskii, A.S. Pakhomov and T. Shiklosh	501	5	931
Short-lived Isomers from Proton Bombardment. O. I. Leipunskii, V. V. Miller, A. M. Morozov and P. A. Iampol'skii	505	5	935
Reflection and Transmission of 7-24μ Waves by Silica Modifications. N. A. Sevchenko and V. A. Florinskaia	508	6	1115
Gamma Radiation from the Collisions of Fast Charged Pions with Nuclei. A. G. Sitenko	512	6	1119

The expanded program of the American Institute of Physics comprises translation of four leading Soviet physics journals, as listed below. These translations, by competent, qualified scientists, will provide all research laboratories and libraries with accurate and up-to-date information of the results of research in the U.S.S.R.

Soviet Physics — Technical Physics

A translation of the "Journal of Technical Physics" of the Academy of Sciences of the U.S.S.R. The 1956 volume, which was originally announced as containing eighteen issues, is instead being issued monthly, in expanded issues. All issues of the original Russian journal for 1956 will be translated. Approximately 4,000 Russian pages. Annually, $90.00 domestic, $95.00 foreign.

Soviet Physics — Acoustics

A translation of the "Journal of Acoustics" of the Academy of Sciences of the U.S.S.R. Four issues per year, approximately 500 Russian pages. Annually, $20.00 domestic, $22.00 foreign. The 1955 issues of "Journal of Acoustics" U.S.S.R. will also be published. Will consist of two volumes, approximately 500 pages, and the subscription price will be $20.00 for the set.

Soviet Physics "Doklady"

A translation of the "Physics Section" of the Proceedings of the Academy of Sciences of the U.S.S.R. Six issues per year, approximately 900 Russian pages. Annually $25.00 domestic, $27.50 foreign.

Soviet Physics — JETP

A translation of the "Journal of Experimental and Theoretical Physics" of the Academy of Sciences of the U.S.S.R. Twelve issues per year, approximately 2,600 Russian pages. Annually $60.00 domestic, $64.00 foreign. Back issues of Volume 1 and 2 are available at a special price of $30.00 for both to subscribers to Volume 3.

Subscriptions should be addressed to the American Institute of Physics, 57 East 55th Street, New York 22, N.Y.